BRCA2 SUPPRESSES REPLICATION STRESS THROUGH HOMOLOGOUS RECOMBINATION

by

Weiran Feng

A Dissertation

Presented to the Faculty of the Louis V. Gerstner, Jr.

Graduate School of Biomedical Sciences,

Memorial Sloan-Kettering Cancer Center

in Partial Fulfillment of the Requirements for the Degree of

Doctor of Philosophy

New York, NY

September, 2018

Maria Jasin, PhD	Date
Dissertation Mentor	

DEDICATION

I dedicate this thesis to my wife Hanzhi Luo, and my parents Wei Feng and Xuyang Xie.

ABSTRACT

The long-term goal of my thesis project is to elucidate the fundamental question about the seemingly conflicting consequences of genome instability, a hallmark of cancer. While genome instability fuels cancer growth, it also paradoxically compromises cell fitness and even causes lethality. Resolving this question can provide insight into tumor-forming as well as therapy resistance mechanisms and potentially benefit cancer therapy. To decipher this conundrum, I decided to use BRCA2 deficiency as a model. As a tumor suppressor, BRCA2 functions to protect genome integrity. Interestingly, while BRCA2 loss confers breast and ovarian cancer susceptibility, it can also trigger lethality, thus recapitulating both aspects of the paradox. However, the underlying mechanism remains poorly defined.

Given the tissue tropism of BRCA2-mutated cancers, key to resolving the question is to model BRCA2 deficiency in a relatively normal and disease-relevant background. To this end, using orthogonal approaches, I generated two conditional loss-of-function models of BRCA2 in a non-transformed human mammary epithelial cell line (MCF10A) using CRISPR-Cas9 tools. I found that BRCA2 deficiency triggers cell lethality. I then employed single molecule DNA fiber analysis, high-resolution microscopy and automated high-content imaging to study the underlying mechanisms. I uncovered the “DNA under replication-mitotic abnormality-53BP1 nuclear body formation-G1 arrest” axis as the trigger of the cell lethality.

Another topic that is currently under heated debate is as to the relative contribution of two BRCA2-centered processes, homologous recombination (HR) and replication fork protection (FP), to genome integrity. An HR defect in BRCA2-mutated cancers was initially leveraged to develop synthetic-lethality-based therapeutic

strategies, while subsequent restoration of HR and/or possibly FP in tumors confers resistance. The relative contribution of HR and FP to genome integrity maintenance and thereby therapy resistance remains somewhat controversial. Thus, the BRCA2 conditional models I generated afford the opportunity to dissect the functions of the two pathways in a clean way and from a disease-relevant background.

To this end, I established multiple, complementary separation-of-function systems to individually perturb either pathway while keeping the other intact. These approaches came together to reveal that it is HR, but not FP, that plays a critical role to suppress replication stress and support cell viability. These results, unanticipated from previous studies using other systems, converge to a model that HR and FP are differentially required in diverse biological contexts and highlight the importance of generating genetic models in a relevant cellular background (Feng and Jasin, Nature Communications, 2017).

For the long term, the genetic tools and the above results I obtained now open the door to exploring a series of unresolved questions in the field. First, my study has made an unanticipated discovery that the timing of DNA replication completion dictates the outcome of BRCA2 perturbation. Could the under-replicated DNA and its sequelae add to the Achilles heel of BRCA2-mutated cancers and thereby open novel therapeutic avenues? Conversely, could tumor cells acquire chemoresistance by manipulating the timing to their advantage? Moreover, could DNA under replication contribute to forming the mutational signatures observed in BRCA2-deficient cancers? Finally, what is the mechanism that allows for survival of BRCA2-deficient cells and ultimately tumor formation? I am currently focusing on elucidating these questions.

In sum, I have generated *BRCA2* conditional human cell models, delineated the downstream processes leading to cell lethality in the absence of BRCA2 and dissected the contributions of HR and FP in genome integrity maintenance, which together provide

insights into our understanding of genome instability and cancer with implications in therapies.

BIOGRAPHICAL SKETCH

Weiran Feng was born in Chengdu, Sichuan Province in China. He received education from Zhengfujie primary school, Chengdu No. 7 Yucai middle school (East section) before graduating from Chengdu No. 7 high school in 2007. In the same year, he entered Peking University for college education in Beijing. Weiran performed his undergraduate research studying ubiquitin-proteasome degradation mediated by tumor suppressor VHL, under the mentorship of Dr. Jianguo Chen. In 2010, he was enrolled in a summer research program where he contributed to identifying novel binding partners of ASPP2, co-mentored by Dr. John Christianson and Dr. Xin Lu. He graduated with a Bachelor in Science (B.S.) degree in Biological Sciences in 2011 with honors. On July 25th 2011, Weiran moved to New York and started his pursuit of a Ph.D degree at the Louis V. Gerstner, Jr. Graduate School of Biomedical Sciences at Memorial Sloan Kettering Cancer Center. Subsequently, he joined Dr. Maria Jasin's laboratory in 2012 and started his thesis research aimed at elucidating the roles of tumor suppressor BRCA2 in preventing genome instability, a hallmark of cancer.

ACKNOWLEDGMENTS

I would like to express my sincere gratitude to my mentor, Dr. Maria Jasin, for the guidance, motivation, support and care. Maria is an extraordinary scientist with passion and vision. The breadth of her horizon and depth of her scientific thinking continuously inspires me to keep learning and improving myself. Her warmth and kindness further makes the journey of my PhD training such a joyful experience. What I harvest from her lab is not only a solid training in science, but also tremendous support in every aspect of life, from the series of encouraging toasts for progress, to critical advice for my career development.

I would also like to thank my committee members, Drs. Scott Keeney and Prasad Jallepalli for their advice and support. Every meeting with them is a fruitful experience from which I not only harvested useful feedback on the projects, but also learned from their rigorousness, insightfulness, and persistent pursuit of truth. Of course their support is way beyond the committee meeting per se. Their office door is always open. They are there whenever I ask for advice, both in science and career development. It is also through them that I know a bunch of great scientists from their lab, many of whom helped me a lot over the past years. I am grateful to my external exam member Dr. Ashok Venkitaraman for agreeing to come all the way from England to advice on defense. I also would like to thank Dr. Xiaolan Zhao for chairing my thesis defense.

I would like to thank my rotation mentors Drs. Eric Holland and Prasad Jallepalli, and my first year mentor Dr. Jayanta Chaudhuri for advice and sharing their knowledge and expertise. I also benefit a lot from daily conversations with Drs. Danwei Huangfu, Liang Deng, Xuejun Jiang and Zhirong Bao, whom I am very grateful to. I

would like to thank my future postdoc mentor, Dr. Charles Sawyers, for offering me a position in the lab and opening a whole new world of research in front of me.

I would like to thank my undergraduate mentors at Peking University, Drs Jianguo Chen and Junlin Teng, and Wenyuan Cao, the PhD student whom I worked with. It was their training that sparked my interest in research and laid the foundation of my scientific thinking. I would like to thank my mentors during my summer internship training at University of Oxford, Drs. Xin Lu and John Christianson, for their insightful advice.

My PhD life would have not been possible without the help from my friends and colleagues. I would like to thank previous and current members of the Jasin lab, Drs. Mary Moynahan, Travis White, Fabio Vanoli, Darpan Medhi, Agnieszka Lukaszewicz, Elisabeth Kass, Pei Xin Lim, Chun-chin Chen, Carla De Castro Abreu, Shaun Peterson, Francesca Cavalo, Francesca Cole, Rohit Prakash, Yu Zhang, Patricia Sung, Shuhei Ito, Katharina Schlacher, Maria Barbara, Lianne Vriend, Prezemyslaw Matt Krawczyyk and Raymond Wang, for all the inspiring discussions. I owe much to Drs. Mathew Jones and John Maciejowski, for sharing their expertise. I would like to thank Natalia Bonilla for administrative support and Paige Arnold for assistance. I would like to thank my friends, Lei Wei, Zhen Cao, Qiao Wang, Yuchen Qi, Leili Ran, Yilong Zou, Xi Wang, Xiaochun Li, Kai Liu, Di Yao, Wenyan Jiang, Bingbing Wan, Xiangzhou Meng, Zhengrong Zhu, Zhongdong Shi, Yige Guo, Jingjing Wang, Jie Su, Tao Xue, Rui An, Xiangyu Wang, Jiwei Li, Wulin Yang, Baili Zhu, Chao Zhang, Wang Xu for insightful comments, as well as the wonderful time we spend together.

I would like to thank my graduate school, our Dean Dr. Kenneth Marians, Associate Dean Linda Burnley, previous staff Maria J. Torres, Iwona Abramek, and Ivan R. Gerena, and current staff Julia, Stacy De La Cruz, and David L. McDonagh. It is their tremendous efforts to foster such a warm and supportive training environment. I would

like to thank my fellow graduate students for their friendship and companion through the years.

I would like to thank my parents for raising me up in a warm, supportive and inspiring family environment. It is their unconditional love that shapes my personality and motivates me to pursue my dream. My mother passed away right before I came to this land. How I wish she could be there with me during my graduate study. I wish she could see my defense and be proud of her son.

I am very grateful to have my wife Hanzhi Luo by me all over the years. All the joy and tears we share, the support and relief we get from each other, become a precious memory that I will treasure for the rest of my life. I look forward to walking along the journey ahead with her, hand in hand.

TABLE OF CONTENTS

LIST OF FIGURES **XV**

LIST OF ABBREVIATIONS **XVII**

CHAPTER 1 INTRODUCTION **1**

1.1 GENOME INSTABILITY AND DNA REPLICATION STRESS AS HALLMARKS OF CANCER **1**

1.1.1 GENOME INSTABILITY, A PERVASIVE CHARACTERISTIC OF CANCER 1

1.1.2 GENOME INSTABILITY, A DOUBLE-EDGED SWORD FOR CANCER 2

1.1.3 DNA REPLICATION STRESS, A HALLMARK OF PRE-CANCEROUS LESIONS 6

1.1.4 SOURCES OF GENOME INSTABILITY IN CANCER 12

1.2 BRCA2, GENOME INTEGRITY MAINTENANCE, AND CANCER **17**

1.2.1 BRCA2 IS A MAJOR HR PLAYER 18

1.2.2 FP, AN HR-RELATED AND YET –INDEPENDENT PROCESS 20

1.2.3 HR AND FP IN CANCER THERAPY 21

1.3 NASCENT STRAND DEGRADATION AND FP: A CLOSER LOOK **22**

1.3.1 FORK REVERSAL AND NASCENT STRAND DEGRADATION 22

1.3.2 NUCLEASES INVOLVED IN NASCENT STRAND DEGRADATION 24

1.4 BRCA2 DOMAINS AND BINDING PARTNERS **26**

1.4.1 PALB2 27

1.4.2 RAD51: BRC REPEATS AND C-TERMINUS 28

1.4.3 DNA AND DSS1 31

1.5 THESIS OBJECTIVE AND OVERVIEW **32**

CHAPTER 2 METHODS AND MATERIALS **38**

2.1 MCF10A CELL CULTURE AND DRUG TREATMENT **38**

2.2 PLASMID CONSTRUCTION **38**

2.3 LENTIVIRAL TRANSDUCTION **40**

2.4 *BRCA2* GENE TARGETING AND COMPLEMENTATION **40**

2.5 GENE KNOCKOUT **43**

2.6 RNA INTERFERENCE **44**

2.7 CELL PROLIFERATION AND CLONOGENIC SURVIVAL ASSAYS **45**

2.8 CELL SENESCENCE AND APOPTOSIS ASSAYS **45**

2.9 CELL CYCLE ANALYSIS **45**

2.10 DNA FIBER ASSAY **46**

2.12 HR ASSAY **46**

2.13 IMMUNOFLUORESCENCE AND MICROSCOPY **47**

2.14 SERUM STARVATION AND MITOTIC CELL ANALYSIS **48**

2.15 SUBCELLULAR FRACTIONATION AND IMMUNOPRECIPITATION **49**

2.16 WESTERN BLOTTING **49**

2.17 STATISTICAL ANALYSIS **50**

CHAPTER 3 MODELING BRCA2 LOSS IN NON-TRANSFORMED HUMAN MAMMARY CELLS **51**

3.1 INTRODUCTION **51**

3.2 RESULTS **52**

3.2.1 BRCA2 IS ESSENTIAL FOR HUMAN MAMMARY MCF10A CELL VIABILITY 52

3.2.2 BRCA2 ABLATION CAUSES SPONTANEOUS DNA DAMAGE AND G1 ARREST 53

3.2.3 BRCA2 SUPPRESSES G1 53BP1 NUCLEAR BODY FORMATION 54

3.2.4 BRCA2 PREVENTS UNDER REPLICATION AND MITOTIC ABNORMALITIES 56

3.2.5 BRCA2 SUPPRESSES SINGLE-STRANDED DNA LESIONS IN G2 57

3.3 DISCUSSION **59**

3.3.1 BRCA2 SUPPRESSES REPLICATION STRESS 60

3.3.2 BRCA2 DEFICIENCY AND MITOTIC ABNORMALITIES 61

3.3.3 INVOLVEMENT OF P53 AFTER BRCA2 LOSS 61

3.3.4 IMPLICATIONS FOR CANCER BIOLOGY 63

CHAPTER 4 DISSECTING THE CONTRIBUTION OF HOMOLOGOUS RECOMBINATION AND REPLICATION FORK PROTECTION PATHWAYS **81**

4.1 INTRODUCTION **81**

4.2 RESULTS **82**

4.2.1 FP IS A MINOR SURVIVAL AND REPAIR PATHWAY 82

4.2.2 REPLICATION STRESS SUPPRESSION PRIMARILY ASSOCIATES WITH HR 85

4.3 DISCUSSION **88**

4.3.1 SEPARATION-OF-FUNCTION SYSTEMS TO DISSECT ROLES OF HR AND FP 89

4.3.2 CONTEXT-DEPENDENT PATHWAY REQUIREMENT FOR CELL SURVIVAL 90

CHAPTER 5 53BP1 NUCLEAR BODY-MARKED REPLICATION STRESS IN A HUMAN MAMMARY CELL MODEL OF BRCA2 DEFICIENCY **108**

5.1 INTRODUCTION **108**

5.2 RESULTS AND DISCUSSION **109**

5.2.1 ALLELE-SPECIFIC EDITING OF THE *BRCA2* LOCUS 109

5.2.2 REPLICATION STRESS-VULNERABLE SITES IN BRCA2-DEFICIENT CELLS 111

5.2.3 LINK BETWEEN 53BP1 NBS AND P53 ACTIVATION 113

5.2.4 FUNCTIONAL INTERPLAY BETWEEN SMARCAL1 AND BRCA2 114

5.3 CONCLUDING REMARKS **116**

CHAPTER 6 CONCLUSIONS AND PERSPECTIVE **124**

6.1 CONSEQUENCES OF BRCA2 DEFICIENCY IN MCF10A CELLS 124

6.2 GENETIC BACKGROUND OF MCF10A CELLS 125

6.3 CONTRIBUTIONS OF HR AND FP TO GENOME INTEGRITY AND CELL FITNESS 127

6.4 REPLICATION STRESS AS A GENERAL BARRIER AGAINST TUMOR FORMATION 129

6.5 POSSIBLE MECHANISMS TO FORM TUMORS WITH *BRCA2* MUTATIONS 130

6.6 IMPLICATIONS FOR CANCER THERAPY 134

BIBLIOGRAPHY 136

LIST OF FIGURES

FIGURE 1-1. UNDER-REPLICATED DNA IN MITOSIS. 34

FIGURE 1-2. HR AND FP FUNCTIONS OF BRCA2 TO PROTECT GENOME INTEGRITY. 35

FIGURE 1-3. MECHANISMS OF FORK DEGRADATION AND PROTECTION. 36

FIGURE 1-4. BRCA2 BINDING PARTNERS REQUIRED FOR A FUNCTIONAL HR PATHWAY..... 37

FIGURE 3-1. BRCA2 IS ESSENTIAL FOR NON-TRANSFORMED HUMAN MAMMARY MCF10A CELL VIABILITY 64

FIGURE 3-2. GENERATION OF *BRCA2*$^{FL/-}$ AND *BRCA2*$^{\Delta Ex3\text{-}4/-}$ CELLS 65

FIGURE 3-3. GENERATION AND CHARACTERIZATION OF *BRCA2*$^{-/-}$*AAVS1*^{FL} CELLS 66

FIGURE 3-4. BRCA2 DEFICIENCY TRIGGERS SPONTANEOUS DNA DAMAGE AND G1 ARREST 68

FIGURE 3-5. BRCA2 INACTIVATION CAUSES INCREASED DNA DAMAGE 69

FIGURE 3-6. BRCA2-DEFICIENT CELLS SHOW P53-DEPENDENT G1 ARREST 70

FIGURE 3-7. VALIDATED *BRCA2*$^{\Delta Ex3\text{-}4/-}$ CLONES FORM IN THE ABSENCE OF P53 71

FIGURE 3-8. BRCA2 SUPPRESSES REPLICATION STRESS ASSOCIATED WITH G1 53BP1 NUCLEAR BODIES 72

FIGURE 3-9. S/G2-ASSOCIATED DNA DAMAGE INDUCTION UPON BRCA2 DEFICIENCY..... 73

FIGURE 3-10. BRCA2 DEFICIENCY CAUSES DNA UNDER REPLICATION THAT RESULTS IN ABNORMAL MITOSES..... 74

FIGURE 3-11. BRCA2 DEFICIENCY CAUSES UNDER REPLICATION AND MITOTIC ABNORMALITIES 76

FIGURE 3-12. BRCA2-DEFICIENT CELLS ACCUMULATE SINGLE-STRANDED DNA LESIONS IN G2 77

FIGURE 3-13. VALIDATION OF PROTEIN DEPLETION BY WESTERN BLOT 78

FIGURE 3-14. MODEL FOR REPLICATION STRESS AND ITS AFTERMATH IN THE ABSENCE OF BRCA2 79
FIGURE 4-1. BRCA2 INACTIVATION CAUSES HR DEFICIENCY 93
FIGURE 4-2. FP PLAYS A MINOR ROLE IN CELL VIABILITY AND DNA REPAIR 94
FIGURE 4-3. PARP1 MEDIATES MRE11 CHROMATIN RECRUITMENT UPON REPLICATION STRESS 96
FIGURE 4-4. FP IS NOT SUFFICIENT TO SUPPORT CELL VIABILITY 97
FIGURE 4-5. FP IS NOT ESSENTIAL FOR CELL VIABILITY OR DNA REPAIR 98
FIGURE 4-6. FP IS A MINOR REPLICATION STRESS SUPPRESSION PATHWAY 99
FIGURE 4-7. HR PROFICIENCY IS ASSOCIATED WITH REPLICATION STRESS SUPPRESSION AND CELL VIABILITY 101
FIGURE 4-8. HR IS CRITICAL FOR CELL VIABILITY AND LIMITING G2 DNA DAMAGE 102
FIGURE 4-9. EFFECTS OF RAD51 DEPLETION ON BRCA2-DEFICIENT CELLS 104
FIGURE 4-10. SEPARATION-OF-FUNCTION SYSTEMS TO STUDY HR AND FP FUNCTIONS. 105
FIGURE 4-11. CONTEXT-DEPENDENT REQUIREMENT FOR HR VERSUS FP FOR CELL SURVIVAL. 106
FIGURE 4-12. ΓH2AX INTENSITY REPLICATES FOR THE INDICATED FIGURES 107
FIGURE 5-1. GENE TARGETING AT THE *WT* ALLELE OF *BRCA2*$^{FL/+}$ CELLS. 118
FIGURE 5-2. PRESENCE OF A SNP AT THE BRCA2 SGRNA SITE FACILITATES ALLELE-SPECIFIC GENE EDITING. 119
FIGURE 5-3. BRCA2 SUPPRESSES REPLICATION STRESS INDUCED BY BOTH LOW-DOSE APH, WHICH SELECTIVELY TRIGGERS CFS EXPRESSION, AND HU, A MORE GLOBAL INDUCER OF REPLICATION STRESS. 121
FIGURE 5-4. 53BP1 NB FORMATION IS ASSOCIATED WITH P53 ACTIVATION 122
FIGURE 5-5. SMARCAL1 DISRUPTION IN BRCA2-DEFICIENT CELLS RESTORES FP BUT CELLS STILL MAINTAIN HIGH 53BP1 NB LEVELS 123

LIST OF ABBREVIATIONS

53BP1 NB: 53BP1 nuclear body

APC/C: Anaphase-promoting complex/cyclosome

APH: Aphidicolin

BER: Base excision repair

CFS: Common fragile site

cGAS: Cyclic GMP-AMP synthase

CIN: Chromosomal instability

CRISPR: Clustered regularly interspaced short palindromic repeats

DAPI: 4′,6-diamidino-2-phenylindole

DDR: DNA damage response

DSB: DNA double-strand break

dsDNA: double-stranded DNA

ERFS: Early-replicating fragile sites

FACS: Fluorescence-activated cell sorting

FP: Replication fork protection

HR: Homologous recombination

HU: Hydroxyurea

ICL: Interstrand crosslinks

MMR: Mismatch repair

NER: Nucleotide excision repair

NHEJ: Nonhomoulogous end joining

SAC: Spindle assembly checkpoint

ssDNA: single-stranded DNA

STING: Stimulator of interferon genes

UFB: Ultrafine DNA bridge

Chapter 1 Introduction

1.1 Genome instability and DNA replication stress as hallmarks of cancer

1.1.1 Genome instability, a pervasive characteristic of cancer

Although human cancers vary profoundly across different types, they do share some key properties, collectively named hallmarks of cancer (Hanahan and Weinberg 2000; Hanahan and Weinberg 2011). Genome instability represents one of these defining features (Hanahan and Weinberg 2011). Genome instability comes in different forms contingent upon the cancer types. It can be characterized as alterations at the DNA sequence level, manifesting as base-pair mutations, or microsatellite instability, which features changes in the number of short nucleotide repeats called microsatellites (Vilar and Gruber 2010). Abnormal chromosome structures and numbers represent another form of genome instability, referred to as chromosomal instability (CIN). CIN manifests as chromosomal fusions/translocations, gains or losses of chromosomal regions, changes in copy number of a whole chromosomes (aneuploidy), or changes in the whole genome copy number (Sansregret et al. 2018).

Advances in next-generation DNA sequencing now enable systematic characterization of mutation levels and uncover tumor heterogeneity in enormous numbers of cancer genomes across different types (Yates and Campbell 2012; Burrell et al. 2013b; Kass et al. 2016b). The more recent advent of single-cell DNA sequencing technologies further allows for deciphering the genetic intratumor heterogeneity at unprecedented resolution (Navin 2015). A comprehensive landscape of the cancer

genome is now emerging and will continue to shape our understanding of underlying features of cancer.

1.1.2 Genome instability, a double-edged sword for cancer

Despite a clear association with cancer, genome instability impacts the behaviors of cells and cancer in a complex manner. How the cancer cells harness genome instability to their advantage while minimizing its downside is not fully understood and remains a topic of interest. In this section, the benefits and costs of genome instability and its potential clinical value are discussed.

1.1.2.1 Positive effects of genome instability on cancer development

Cancer formation is considered as a multistep process during which a series of mutations are progressively acquired by chance, ultimately leading to clonal outgrowth (Nowell 1976; Vogelstein and Kinzler 1993; Greaves and Maley 2012). Under this framework, it is conceivable that with the mutation-prone nature, genome instability provides a basis that fosters cancer evolution (Cahill et al. 1999), although whether an increase in mutation rate (i.e., a mutator phenotype) is necessarily a requirement for tumorigenesis is still under debate (Fox et al. 2013). Not only is the genetic diversity advantageous during disease progression under micro-environmental pressure, it may also fuel evolution of chemoresistance under therapeutic pressure. In the latter case, the resistance mutations could be pre-existing before the treatment (Ding et al. 2012; Kim et al. 2015; Patch et al. 2015; Kim et al. 2018), or acquired during the course of treatment (Ding et al. 2012; Kurtova et al. 2015). In addition to genome instability, other functional (i.e., not necessarily genetic) diversity likely also contributes to tumor heterogeneity, such as a hierarchy of tumorigenic cells and their non-tumorigenic progeny (Meacham and Morrison 2013).

Besides an elevated mutation rate, genome instability, especially through chromosomal rearrangements and copy number changes, can promote tumor formation by altering gene expression. Chromosomal translocations can cause gene fusions that result in ectopic oncogene expression. As a result of somatic copy number alterations, gain of oncogene copy numbers or loss of tumor suppressor genes can also contribute to tumor formation. Strikingly, a recent study provides evidence that the whole-arm or whole-chromosome (i.e. aneuploidy) gain or loss patterns in cancer can be explained by the balance between tumor suppressor genes and oncogenes present in the altered regions (Davoli et al. 2013).

Genome instability also affects tumor formation in an apparently non-gene-specific manner. Aneuploidy is correlated with an increase in expression of cell proliferation genes and a decrease of immune infiltrate (Davoli et al. 2017; Taylor et al. 2018). This observation is not likely to be caused by changes of a particular gene or gene set, since it is a general feature of aneuploidy per se across many cancer types with various types and regions of copy number alterations. Recent work also shows compelling evidence in yeast that aneuploidy increases phenotypic variation (Beach et al. 2017). Importantly, the observed heterogeneity is to some extent independent of genetic or epigenetic changes and is instead attributed to stochastic DNA damage. Since an increased phenotypic variability is also observed in aneuploid mouse embryos, presumably it can contribute to heterogeneity seen in cancer (Beach et al. 2017). Finally, aberrations due to genome instability can also activate immune pathways, which can exhibit both positive and negative impacts on cancer (discussed below).

1.1.2.2 Negative effects of genome instability on cell fitness: a price to be paid to play!

Genome instability as much a hallmark of cancer as it is, is not purely a favorable event for cancer and more generally cell survival. Intuitively speaking, this notion is not entirely unexpected: it would be much more likely to develop deleterious alterations than beneficial ones from a stochastically mutagenic process. Indeed, mutations of numerous DNA repair and DNA damage response genes turn out to be detrimental at organismal and/or cellular levels, even if many of these genes are canonical tumor suppressors in the meantime. As an example, tumor suppressor genes demonstrating this paradoxical property include, but not restricted to, *BRCA1*, *BRCA2* (the topic of the thesis), *PALB2* and *RAD51C* (Prakash et al. 2015). Presumably the endogenous DNA damage reaches an intolerable level in the absence of these repair/response pathways (further discussed below).

CIN can also exert negative impacts on cell fitness. Aneuploidy impedes cell proliferation, largely irrespective of the approaches to achieve it, whether by genetically engineered single-chromosome gains or by perturbing chromosome segregation (Santaguida and Amon 2015). Aneuploidy also demonstrates tumor suppressive effects on mouse cells (Sheltzer et al. 2017). Multiple mechanisms may contribute to compromising cell fitness, including gene expression alterations, p53 activation (as a result of chromosome mis-segregation), and aneuploidy-associated stresses etc. (Santaguida and Amon 2015). Tetraploidy, a result of whole-genome doubling, another frequently occurring event in cancer (Zack et al. 2013), also induces a p53-dependent cell cycle arrest (Andreassen et al. 2001; Ganem and Pellman 2007; Kuffer et al. 2013; Ganem et al. 2014b).

1.1.2.3 Aberrant exposure of genomic DNA to cytosol elicits immune pathway activation

In additional to those discussed above, another recently uncovered, non-gene-specific effects of genome instability lies in the exposure of DNA to cytosol, which in turn activates the cytosolic nucleic acid sensor cGAS (cyclic GMP-AMP synthase) and the downstream STING (stimulator of interferon genes)-mediated transcriptional responses. A natural function of cGAS is to respond to foreign DNA that is present in the cytosol (e.g., that from a virus) and activates a downstream innate immune response (Chen et al. 2016). It is now known from multiple studies that the genomic DNA of a cell on its own, once becoming accessible to cGAS, can also elicit similar downstream responses (Chen et al. 2017; Dou et al. 2017; Gluck et al. 2017; Harding et al. 2017; Mackenzie et al. 2017; Bakhoum et al. 2018; Coquel et al. 2018). For example, one trigger of this axis is a micronucleus, a byproduct of CIN due to chromosome mis-segregation. The nuclear envelope of the micronucleus undergoes extensive rupture (Hatch et al. 2013). As a consequence, the encompassed DNA is recognized by cGAS, which then activates an interferon or pro-inflammatory response (Harding et al. 2017; Mackenzie et al. 2017; Bakhoum et al. 2018).

Notably, an ever-expanding list of other sources of cytosol-accessible DNA can also lead to cGAS activation, including cytosolic chromatin fragments (a byproduct of senescence) (Dou et al. 2017; Gluck et al. 2017), extrachromosomal telomere repeat (Chen et al. 2017) and replication stress (Coquel et al. 2018). Complexity also exists among the various outcomes of cGAS-STING activation, ranging from growth-inhibitory or anti-tumor effects such as anti-proliferation (Chen et al. 2017; Gluck et al. 2017), senescence (Dou et al. 2017; Gluck et al. 2017; Yang et al. 2017) and immunesurveillance (Harding et al. 2017; Mackenzie et al. 2017) to pro-cancer effects such as inflammation and metastasis (Bakhoum et al. 2018). The diverse consequences can in part be explained by various genetic backgrounds, cellular contexts, and microenvironments that may activate distinct downstream transcription programs. It

would be of importance and clinical relevance for future studies to dissect the mechanisms that dictate the outcome of cGAS-STING pathway.

Overall, it emerges that although genome instability is nearly a universal feature of cancer and clearly benefits tumor formation and progression at multiple levels, it does come at a cost, such that the immediate consequences of genome instability are almost invariably detrimental to cell fitness and are thus tumor suppressive. As a consequence, it is likely that cancer cells have evolved ways to bypass these growth-inhibitory effects to ultimately balance the outcome of genome instability towards their advantage. Needless to say, it is undoubtedly critical to understand how this is achieved, which is a major underlying big question of my thesis project.

1.1.3 DNA replication stress, a hallmark of pre-cancerous lesions

DNA replication represents one of the most fundamental processes that occur in a proliferating cell. A direct consequence of aberrant DNA replication is alterations to the genome, including mutations as well as rearrangements. Not surprisingly then, disruption of the DNA replication program constitutes a significant source of genome instability in cancer and particularly precancerous lesions (Halazonetis et al. 2008; Macheret and Halazonetis 2015). In fact, multiple processes that cause genome instability are indeed related to compromising DNA replication, as discussed below.

Replication stress is generally defined as any perturbation that challenges DNA replication fork progression (Branzei and Foiani 2010). Replication stress causes either transient slowing, stalling or permanent collapse of replication forks (Berti and Vindigni 2016). Failing to restart the forks, or improperly processing the intermediates results in DNA lesions (Cortez 2015) or generates substrates for APOBEC3B-deaminase-mediated mutagenesis (Kanu et al. 2016), thereby hampering genome integrity. Various causes and consequences of replication stress are comprehensively reviewed

elsewhere (Branzei and Foiani 2010; Cortez 2015; Berti and Vindigni 2016). One specific type of stressed fork processing, nascent strand degradation, will be discussed in detail below. In this section, the discussion is specifically focused on replication stress in the context of cancer.

1.1.3.1 Oncogene-induced replication stress

Like everything that has been discussed so far, an oncogene is not always oncogenic, but also paradoxically induces tumor-suppressive responses. Oncogene activation by a variety of means all leads to cellular senescence in precancerous lesions (Serrano et al. 1997; Braig et al. 2005; Chen et al. 2005; Collado et al. 2005; Michaloglou et al. 2005). This phenomenon, named oncogene-induced senescence, serves as a barrier against malignancy. The underlying cause is an induction of DNA damage checkpoint signaling due to replication stress (Bartkova et al. 2005; Gorgoulis et al. 2005; Bartkova et al. 2006; Di Micco et al. 2006).

1.1.3.2 Possible causes of oncogene-induced replication stress

Multiple non-mutually exclusive processes may contribute to oncogene-induced replication stress. It is possible that different oncogenes induce replication stress by different mechanisms, or a single oncogene may act via multiple mechanisms. Oncogene activation perturbs DNA replication dynamics, resulting in fork stalling and/or collapse (Bartkova et al. 2006; Di Micco et al. 2006; Bester et al. 2011). In cases of oncoprotein E6-E7 or Cyclin E overexpression, this effect could be a reflection of nucleotide pool depletion (Bester et al. 2011), a condition known to impede replication (Anglana et al. 2003).

Aberrant replication origin firing forms a second cause of replication stress. Proto-oncogene *c-MYC* encodes a protein that directly promotes DNA replication

initiation (Dominguez-Sola et al. 2007), independently from its function as a master transcription regulator (Dang et al. 2006). *c-MYC* overexpression causes excessive origin firing, which in turn stalls replication forks (Dominguez-Sola et al. 2007; Srinivasan et al. 2013). Aberrant origin firing could also be a consequence of premature S phase entry upon oncogene activation (Macheret and Halazonetis 2018).

Conflicts between replication and transcription, which are sources of replication stress in general (Garcia-Muse and Aguilera 2016), also underlie oncogene-induced replication stress. For example, transcription inhibition was shown to partially alleviate Cyclin E overexpression-mediated fork slowing (Jones et al. 2013). A recent study provides more insight into the interaction between transcription and replication under oncogene activation. A genome-wide map of replication initiation sites revealed a set of replication origins ectopically fired from highly transcribed genes due to oncogene activation (Cyclin E or c-Myc overexpression). These origins, normally suppressed by transcription in G1, are thought to be aberrantly fired due to a short G1 as a result of oncogene-induced precocious S phase entry. Fork collapse is in turn triggered by the resulting conflict between replication and transcription (Macheret and Halazonetis 2018).

Common fragile sites (CFSs) and early-replicating fragile sites (ERFSs) are two types of genomic regions that are prone to breakage under replication stress, including that induced by oncogene activation, and are hotpots for rearrangements in cancer (Macheret and Halazonetis 2015) (further reviewed below). CFSs generally reside in large genes (Le Tallec et al. 2013). Transcription of large genes can take longer than the whole S phase, making replication-transcription interference more likely, which has been implicated as one cause of CFS fragility of particularly long genes among others (Helmrich et al. 2011). ERFSs are also associated with highly-transcribed region with fragility being correlated with the expression status of the underlying genes (Barlow et al. 2013).

1.1.3.3 Beyond S phase - late manifestation of replication stress

Replication stress stems from S phase, but it also exerts an impact beyond S phase, into subsequent cell cycle stages. One possible outcome of replication stress is an incomplete duplication of the genome, referred to as DNA under replication. The resulting incompletely replicated sister chromatids remain connected at the under-replicated region. Importantly, unlike severe replication problems or DNA lesions that typically trigger DNA damage response and cell cycle arrest, under-replicated DNA on its own (i.e., without excessive DNA damage) seems insufficient to activate the checkpoint such that cells still continue to enter mitosis with their presence (Mankouri et al. 2013). The possible reasons for their tolerance are not very clear, but these structures, if not properly resolved, can in turn be subject to breakage or perturb chromosome segregation, leading to mitotic and post-mitotic problems (Mankouri et al. 2013).

One source of under-replicated DNA is CFSs. As briefly introduced above, these sites are some genomic regions that are particularly fragile under replication stress and have been implicated as rearrangement hotspots in cancer (Glover et al. 2017). One defining feature of CFSs is a propensity to form breaks or gaps on metaphase chromosomes following partial inhibition of DNA replication (Glover et al. 1984). A typical way to induce CFS breakage (i.e. CFS expression) is by a low dose of aphidicolin (APH), a DNA polymerase inhibitor that induces a mild replication stress without causing cell cycle arrest (Glover et al. 1984). Multiple non-exclusive mechanisms have been proposed to explain the fragility property of CFSs, including the aforementioned replication-transcription interference (Helmrich et al. 2011), presence of difficult-to-replicate DNA sequences (Schwartz et al. 2006) and a paucity of replication origins (Letessier et al. 2011). Notably, CFSs are generally late replicating (Glover et al. 2017),

which together with the above features make CFSs particularly prone to DNA under replication and then manifest as gaps and breaks during mitosis.

The carry-over of under-replicated DNA through mitosis is consequential in multiple respects, ranging from compensatory to deleterious ones. First, DNA continues to replicate in mitosis (**Fig. 1-1**): Although originally identified as a pathological outcome, formation of gaps and breaks at CFSs is now appreciated as a programmed breakage event mediated by the DNA structure-specific nuclease MUS81 (Naim et al. 2013; Ying et al. 2013). The purpose is to prevent chromosome non-disjunction and further catastrophe by triggering mitotic DNA synthesis, a compensatory process to finish DNA synthesis during early mitosis. Mitotic DNA synthesis requires POLD3, a non-catalytic subunit of DNA Polymerase δ, downstream of MUS81, and is proposed to occur by break-induced replication, a specialized form of DNA repair synthesis (Minocherhomji et al. 2015). The strand-annealing enzyme RAD52 was additionally found to recruit MUS81 during mitotic DNA synthesis (Bhowmick et al. 2016). Thus, a break-induced repair synthesis pathway is emerging to complete the unfinished DNA replication at CFSs during mitosis and prevent otherwise more detrimental outcomes.

Ultrafine DNA bridges (UFBs) represent a second type of mitotic products generated from CFSs (**Fig. 1-1**). These structures are characterized as DAPI-negative DNA ‘threads’ that connect sister chromatids during anaphase (Baumann et al. 2007; Chan et al. 2007). In fact, the sources of UFBs are more general: not only do they arise from CFSs, but also from centromeres, telomeres (Mankouri et al. 2013) and, as more recently described, unresolved recombination intermediates (Chan et al. 2018; Tiwari et al. 2018). All UFBs are commonly bound by helicases PICH and BLM, which are implicated in bridge resolution (Mankouri et al. 2013). UFBs from replication stress, including CFSs, are specifically marked by a Fanconi anaemia protein FANCD2 at the two bridge ends (**Fig. 1-1**) (Chan et al. 2009; Naim and Rosselli 2009). In fact, upon

replication stress, FANCD2 binds to CFSs from as early as G2 phase and remains bound throughout early mitosis as a very defined, paired foci structure with one on each sister chromatid (**Fig. 1-1**) (Chan et al. 2009). Mitotic DNA synthesis occurs at these FANCD2 twin foci, while perturbing this process further increases FANCD2-labelled UFBs in the subsequent anaphase (Minocherhomji et al. 2015). A failure to resolve UFBs in BLM deficient cells is associated with anaphase bridge formation and chromosome mis-segregation (Chan et al. 2007; Chan et al. 2009; Naim and Rosselli 2009). Thus, although the precise role of the CFS-derived UFBs remains to be clearly defined, it appears these structures serve as a fail-safe mechanism to assist in chromosome segregation when mitotic DNA synthesis is absent or overwhelmed.

The consequences from DNA under replication even extend beyond mitosis to the daughter cells. Specifically, a DNA double-strand break (DSB) repair protein 53BP1 forms prominent, large foci, termed 53BP1 nuclear bodies (53BP1 NBs) in the subsequent G1 phase (Harrigan et al. 2011; Lukas et al. 2011). These large nuclear compartments follow a remarkably symmetrical pattern in the two daughter cells (Lukas et al. 2011). 53BP1 NBs arise spontaneously but are greatly increased under replication stress (low-dose APH) and are associated with CFSs (Harrigan et al. 2011; Lukas et al. 2011). A recent study using genetic manipulation of replication origin numbers demonstrates an inverse correlation between the levels of 53BP1 NBs and active origins (Moreno et al. 2016). These observations together support a model that these nuclear bodies mark under-replicated DNA from the previous cell cycle.

Two aspects of 53BP1 NBs remain incompletely understood: how do they arise and what roles do they play? Regarding the first point, the occurrence of 53BP1 NBs is associated with unresolved UFB levels in anaphase, suggesting that these persistent sister-chromatid linkages in the preceding mitosis might be the source for the later formation of nuclear bodies (Mankouri et al. 2013). There also exist some clues for their

possible functions. A plethora of DNA damage response proteins are found in the nuclear bodies (Harrigan et al. 2011; Lukas et al. 2011), suggesting 53BP1 NBs could serve as a signaling center with a high local concentration of functionally related proteins. In addition, 53BP1 was shown to shield lesions at the under-replicated DNA loci (Lukas et al. 2011). Together with the observation that 53BP1 NBs disappear in the ensuing S phase (Harrigan et al. 2011), it is possible that 53BP1 protects the lesions through the G1 phase for them to be properly repaired in S phase, for example, via high-fidelity replication or recombination-related mechanisms.

1.1.4 Sources of genome instability in cancer

It is now clear that aberrations of many processes, including replication stress discussed above, lead to genome instability. The sources of genome instability can be broadly categorized as two types: DNA damage and mitotic abnormalities. Crosstalk often exists among the multiple types of aberrations, which together threaten the integrity of the genome.

1.1.4.1 DNA damage, DNA damage response and repair

DNA is the building block of the genome. Naturally, DNA damage represents a significant source of genome instability. DNA damage is derived both exogenously and endogenously (Ciccia and Elledge 2010). Common exogenous DNA damage include sunlight, which results in pyrimidine dimers, cigarette smoke, which generates DNA adduct and radiation from various sources which can lead to DSB formation (Ciccia and Elledge 2010). Endogenous DNA damage arises from spontaneous DNA alterations or agents that are often generated as byproducts from normal cellular processes. Spontaneous DNA alterations include cytosine deamination, depurination and base alkylation etc. (Lindahl and Barnes 2000). One common DNA damaging metabolite is

reactive oxygen species, which modify DNA bases and cause DNA strand breaks (Cadet and Wagner 2013). It is recently revealed that aldehydes, derived from endogenous cellular metabolism or alcohol, also display genotoxic effects (Langevin et al. 2011; Pontel et al. 2015; Garaycoechea et al. 2018). In addition to DNA modification per se, endogenous challenges against processes of DNA metabolism also form a source of DNA damage, including, for example, the aforementioned replication stress.

Various repair mechanisms have been evolved to tackle different types of DNA damage. Single-stranded DNA damage is mainly repaired by three pathways, all taking advantage of the intact DNA strand as the repair template. Mismatch repair (MMR) corrects base-to-base mispairings (Jiricny 2006), while the base excision repair (BER) and nucleotide excision repair (NER) pathways repair small or bulky lesions at DNA bases, respectively (Barnes and Lindahl 2004; Marteijn et al. 2014). Lesions across both DNA strands are considered particularly dangerous since the repair template is not as easily accessible. DSBs can be repaired through nonhomologous end joining (NHEJ), which directly ligates the break ends without the need for a homologous DNA template. NHEJ is considered error-prone because it often involves a potentially mutagenic break end processing step before ligation (Lieber 2010). Alternatively, DSBs can also be processed through homologous recombination (HR), a focus of the thesis. HR is a more accurate DSB repair pathway that uses homologous DNA template to guide the repair. HR occurs in S and G2 phases, which is when the sister chromatid, the typical repair template, is present (Jasin and Rothstein 2013). In addition to broken DNA strands, repairing covalent links between the two DNA strands (interstrand crosslinks, ICLs) also requires HR in the context of the Fanconi anaemia pathway (Ceccaldi et al. 2016).

Each repair pathway involves actions of multiple proteins that are both temporally and spatially regulated, which also needs to be coordinated with cell cycle status and other cellular events. The sensing of DNA damage, execution of repair and transduction

of signals to downstream cellular responses are achieved by a signaling network named the DNA damage response (DDR) (Ciccia and Elledge 2010). At the core of the cascade are primarily two DDR master regulators, ATM and ATR. Both kinases are members of the phosphatidylinositol 3-kinase-like protein kinase family, activated in the face of genotoxic stresses and trigger signaling cascades by phosphorylating a multitude of substrates. The outcome of their various downstream pathways is to facilitate effective repair and arrest cell cycle progression until repair is finished. In a simplistic view, ATM mainly responds to DSB induction and regulates DSB repair, while ATR is activated in upon replication stress and promotes replication fork restart while blocking origin firing (Shiloh and Ziv 2013; Saldivar et al. 2017). Despite differing at mechanism of activation and substrate preference, ATM and ATR pathways are not entirely independent, but rather crosstalk with each other at multiple levels (Marechal and Zou 2013).

Defects in various components of DDR and DNA repair processes are implicated in cancer formation. This notion is supported by the fact that germline mutations of DDR or DNA repair genes causes a variety of cancer-prone genetic syndromes. For example, a defective MMR underlies hereditary non-polyposis colon cancer (Fishel et al. 1993; Leach et al. 1993). Hereditary mutations of HR genes *BRCA1* and *BRCA2* results in breast and ovarian cancer susceptibility (Prakash et al. 2015). Germline inactivation of multiple ICL genes causes Fanconi anaemia syndrome, which is associated with cancer predisposition (Ceccaldi et al. 2016). Ataxia telangiectasia (A-T) syndrome, caused by *ATM* mutations, displays increased risk of malignancy (Shiloh and Ziv 2013). Beyond hereditary cancers, even in cases of pan-cancer analysis, germline mutations of a series of DDR or DNA repair genes, including *BRCA1, BRCA2, ATM*, are still significantly enriched, as revealed by a recent, large-scale investigation (Huang et al. 2018). Mutations of DDR and DNA repair genes are also enriched in metastatic cancers. Strikingly, in a cohort of 500 patients with metastatic cancers from a variety of tissues,

mutations in this category accounted for 75% of the total amount of putative pathogenic germline mutations that were uncovered (Robinson et al. 2017). In addition to germline mutations, evidence is also emerging that reveals the presence of somatic mutations of these genes in sporadic cancers (Pennington et al. 2014; Robinson et al. 2015a).

1.1.4.2 Abnormal mitosis underlies chromosomal aberrations

Various forms of mitotic abnormalities exist, manifesting aberrations of different processes (Bizard and Hickson 2018). Chromatin bridges represent one form of non-disjunction between sister chromatids that manifest during anaphase. Depending on whether they can be detected with a conventional DNA dye such as DAPI, they are classified as either DAPI-positive anaphase bridges (hereafter called anaphase bridges), or DAPI-negative UFBs (reviewed above). While UFBs are prevalent even under unperturbed conditions and therefore considered as a physiological structure, anaphase bridges are generally considered as pathological outcomes. Anaphase bridges are typically products of pre-mitotic DNA lesions, including DSBs (Gisselsson 2008), those from replication stress (Burrell et al. 2013a) (also discussed above) or telomere fusions (Maciejowski and de Lange 2017). One consequence of these chromatin bridges is an interference with cytokinesis, which potentially results in binucleation and tetraploidy (Shi and King 2005). Dicentric anaphase bridges arising from telomere fusion are also shown to be resolved and processed by cytoplasmic nucleases and can cause gross genome rearrangements including chromothripsis and kataegis, single-step processes that generate complex chromosomal rearrangements or localized mutagenesis (Maciejowski et al. 2015).

Lagging chromosomes are another type of segregation defect, which are detected as chromatin bodies or whole chromosomes that are left behind other segregated chromosomes during anaphase. Some of these structures originate from

acentric chromatin fragments, which are formed by DNA breakage. These fragments lag behind because they cannot attach to the spindle (Gisselsson 2008). Another type of lagging chromosome is centromere-positive, and manifests as mitotic defects, typically caused by merotelic microtubule attachment. These chromosomes lag behind due to pulling forces from opposite spindle poles (Cimini et al. 2001). Segregating lagging chromosomes to the same daughter cell as its corresponding sister chromatid directly results in aneuploidy. Another fate of lagging chromosomes is the reassembly of their own nuclear envelopes, forming micronuclei (Ganem and Pellman 2012). In contrast with the primary nucleus, a micronucleus is profoundly compromised in DNA integrity: the DNA inside carries extensive damage and its reincorporation into the genome underlies gross genomic rearrangements characterized as chromothripsis (Crasta et al. 2012; Zhang et al. 2015; Ly et al. 2017).

A defective spindle assembly checkpoint (SAC) also causes chromosome mis-segregation, CIN and aneuploidy. SAC is a surveillance pathway that ensures the proper segregation of chromosomes during mitosis. SAC delays separation of chromosomes (i.e. anaphase onset) until all sister chromatid pairs are attached to spindle microtubules from both poles. At the molecular level, unattached kinetochores recruit SAC proteins including MAD1, MAD2, BUB1, BUBR1, BUB3 and MPS1, which then inhibit the anaphase-promoting complex/cyclosome (APC/C)-CDC20 complex, an E3 ubiquitin ligase that initiates anaphase onset (Cheeseman 2014; Musacchio 2015; Funk et al. 2016).

1.1.4.3 Crosstalk between non-mitotic DNA damage and mitotic abnormalities

Pre/post-mitotic DNA damage and aberrations during mitosis are not isolated events, but rather, are closely linked to each other. Pre-mitotic DNA damage can serve as the cause of subsequent mitotic defects. This notion has already been exemplified in multiple

scenarios discussed above, such as replication stress and DSBs, both leading to formation of anaphase bridges and lagging chromosomes (specifically lagging chromatin fragments) during mitosis (Bizard and Hickson 2018).

Conversely, mitotic abnormalities can lead to post-mitotic DNA damage as well (Ganem and Pellman 2012). As discussed, persistent anaphase bridges are subject to processing by cytoplasmic nucleases (Maciejowski et al. 2015). Micronuclei, products of lagging chromosomes during mitosis, undergo extensive DNA damage (Crasta et al. 2012; Zhang et al. 2015; Ly et al. 2017). In both cases, a disrupted nuclear envelope surrounding these mitotic products is thought to play a role in DNA damage (Hatch et al. 2013; Maciejowski et al. 2015). In addition, cytokinesis can directly induce DNA damage on lagging chromosomes that are trapped at the cleavage furrow, which is associated with chromosomal aberrations in the next cell cycle (Janssen et al. 2011).

1.2 BRCA2, genome integrity maintenance, and cancer [*]

BRCA2 is a well-known tumor suppressor that was identified more than two decades ago (Wooster et al. 1995) yet interest in this protein continues to grow. Monoallelic inheritance of a deleterious *BRCA2* mutation confers up to a 70% risk for breast cancer and a 40% risk for ovarian cancer before age 70 (Antoniou et al. 2003), and a lower risk for other tumor types. Although emerging to be retained some cases (Maxwell et al. 2017; Huang et al. 2018), the wild-type allele is lost in tumor cells from majority of *BRCA2* mutation carriers. Therefore, tumor formation is typically associated with a

[*] Section 1.2 is adapted from Prakash R, Zhang Y, Feng W, Jasin M. 2015. Homologous recombination and human health: the roles of BRCA1, BRCA2, and associated proteins. *Cold Spring Harb Perspect Biol* **7**: a016600, Copyright 2015, with permission from Cold Spring Harbor Laboratory Press.
Chen C-C, Feng W, Lim PX, Kass EM, Jasin M. 2018. Homology-Directed Repair and the Role of BRCA1, BRCA2, and Related Proteins in Genome Integrity and Cancer. *Annual Review of Cancer Biology* **2**: 313-336. (With permission from the Annual Review of Cancer Biology, Volume 2 © 2018 by Annual Reviews, http://www.annualreviews.org/.)

severe disruption in BRCA2 function. Somatic *BRCA2* mutations have also been identified more recently in several tumor types, including of the ovary (Pennington et al. 2014) and prostate (Robinson et al. 2015b). Biallelic *BRCA2* germline mutations predispose to Fanconi anaemia, a syndrome characterized by developmental defects and tumor susceptibility (D'Andrea 2010). In these cases, at least one of the *BRCA2* alleles is expected to be hypomorphic, since complete loss of BRCA2 function causes embryonic lethality in mice (Evers and Jonkers 2006).

It is widely accepted that BRCA2 suppresses tumor formation by preventing genome instability, a hallmark of cancer (Hanahan and Weinberg 2011). Nevertheless, it is not fully understood how BRCA2 loss, or genome instability in general, promotes tumor formation. There is a paradox in that BRCA2 deficiency leads to cell lethality in mouse models (Patel et al. 1998; Evers and Jonkers 2006; Kuznetsov et al. 2008; Badie et al. 2010), rather than unrestrained proliferation as might be expected by loss of a tumor suppressor gene. BRCA2 has a well-established function in maintaining the integrity of the genome through its role in homologous recombination (HR) (Moynahan et al. 2001). More recently, a related but separable function, replication fork protection (FP), has been discovered (Schlacher et al. 2011), and the relative contribution of these two pathways to genome integrity maintenance and cell viability is under active investigation.

1.2.1 BRCA2 is a major HR player

The role of BRCA2 in HR has been a subject of active investigation for many years (Prakash et al. 2015). HR repairs DNA lesions including DNA double-strand breaks (DSBs) using a homologous DNA sequence, typically the sister chromatid in mitotic cells. One critical step of HR is strand invasion, which primes subsequent DNA synthesis using the homologous sequence as a template, thereby ensuring an error-free repair outcome (**Fig. 1-2**). BRCA2 plays an essential role in this process by loading RAD51

recombinase onto single-stranded DNA formed at DSBs; the RAD51 nucleoprotein filaments then catalyze the subsequent strand invasion reaction (Prakash et al. 2015).

The earliest clues about the importance of BRCA2 in maintaining genome integrity came from observations that *Brca2* mutant mice and mouse cells they derive exhibit early embryonic lethality and DNA repair defects (Connor et al. 1997; Ludwig et al. 1997; Sharan et al. 1997; Suzuki et al. 1997; Patel et al. 1998) similar to *Rad51* mutant mice (Lim and Hasty 1996; Tsuzuki et al. 1996). Of note, BRCA2 was found to directly interact with RAD51 (Sharan et al. 1997; Wong et al. 1997) and to colocalize with RAD51 in damage-induced nuclear foci (Chen et al. 1998a). Reporter-based HR analyses directly demonstrated the importance of BRCA2 in HR (Moynahan et al. 2001). More recent work has further demonstrated the requirement for BRCA2 in interstrand crosslink-induced HR (Nakanishi et al. 2011) and suppressing error-prone long-tract gene conversion induced by either a DSB or replication fork stalling (Willis et al. 2014).

The critical biochemical function of BRCA2 in HR is to promote RAD51 filament assembly onto single-stranded DNA (ssDNA) that arises from end resection. The RAD51 nucleoprotein filaments then catalyze the subsequent strand invasion reaction (Jensen et al. 2010; Liu et al. 2010; Thorslund et al. 2010). BRCA2 directly interacts with RAD51 at multiple sites to facilitate RAD51 filament assembly at two levels. First, BRCA2 helps RAD51 overcome the inhibitory effect of the high affinity ssDNA-binding protein RPA, which normally coats the ssDNA to prevent RAD51 loading. Second, by preferentially binding to ssDNA over double-stranded DNA (dsDNA), BRCA2 specifically promotes the productive assembly of RAD51 filaments onto ssDNA, which is critical for strand invasion of a homologous DNA, while preventing the non-productive formation of RAD51 filaments onto dsDNA (Jensen et al. 2010; Liu et al. 2010; Thorslund et al. 2010). Full-length BRCA2 protein may function as an oligomer, as indicated by structural and imaging studies (Reuter et al. 2014; Shahid et al. 2014; Sanchez et al. 2017). In cells,

BRCA2 is responsible for recruiting RAD51 to DNA damage sites (Yuan et al. 1999; Tarsounas et al. 2003). A recent study using super resolution microscopy reveals that BRCA2 forms local clusters that progressively overlap with the more elongated RAD51 foci, suggesting dynamic interactions during the repair process (Sanchez et al. 2017).

In addition to HR, BRCA2 has also been implicated in G2/M checkpoint maintenance (Menzel et al. 2011), R-loop processing (Bhatia et al. 2014; Shivji et al. 2018), the spindle assembly checkpoint (Choi et al. 2012), and cytokinesis (Daniels et al. 2004; Mondal et al. 2012), all having an impact on genome or chromosomal stability. Some of these processes are not correlated with HR proficiency, suggesting they may be distinguishable from HR (Menzel et al. 2011; Mondal et al. 2012; Bhatia et al. 2014), but additional studies are required to fully understand the role of BRCA2 in these processes.

1.2.2 FP, an HR-related and yet –independent process

FP is an additional BRCA2-mediated process that helps safeguard genomic integrity (Schlacher et al. 2011). Under replication stress, nascent DNA strands at stalled forks are susceptible to degradation by nucleases such as MRE11. BRCA2 prevents such nascent strand degradation thereby protecting stalled forks (**Fig. 1-2**). In addition to BRCA2, other HR proteins, such as RAD51 itself, the breast and ovarian cancer suppressor BRCA1, and Fanconi anaemia proteins also play important roles in the FP pathway (Schlacher et al. 2011; Schlacher et al. 2012). However, FP and HR are functionally separable, as evidenced by multiple approaches that specifically manipulate one process without affecting the other (Schlacher et al. 2011; Ding et al. 2016; Ray Chaudhuri et al. 2016; Dungrawala et al. 2017; Feng and Jasin 2017; Taglialatela et al. 2017). Of note, the role of RAD51 in FP seems to be more complicated than BRCA2: disruption of its function compromises FP in some studies (Schlacher et al. 2011;

Kolinjivadi et al. 2017), but does not affect FP activity under other circumstances (Thangavel et al. 2015; Feng and Jasin 2017; Lemacon et al. 2017; Mijic et al. 2017). The seeming discrepancy can be attributed to an additional function of RAD51, that of fork reversal (Zellweger et al. 2015), which seems to be required for nascent strand degradation, a subject that is currently a focus of the field (discussed in detail below).

Since the initial identification of BRCA1 and BRCA2, a series of other HR factors, in particular PALB2, which bridges BRCA1 and BRCA2 (discussed below), and RAD51 paralogs RAD51C and RAD51D have been identified as tumor suppressors (Erkko et al. 2007; Rahman et al. 2007a; Tischkowitz et al. 2007b; Meindl et al. 2010; Loveday et al. 2011). Where tested, these proteins also have roles in FP (Somyajit et al. 2015) (**Fig. 1-3**). Similar to BRCA1 and BRCA2 deficiency, disruption of these proteins also causes sensitivity to cross-linking agents and PARP inhibitors (Prakash et al. 2015). *BRCA1/2* mutant cancers exhibit a particular pattern of base substitutions and genome rearrangements, i.e., “mutational signatures” (Nik-Zainal et al. 2016; Polak et al. 2017). A computational model based on these mutational signatures has been used to predict additional patient tumors with HR-deficiency beyond those containing mutations in known HR genes, thus expanding the pool of cancers that may respond to platinum or PARP inhibitor therapy (Davies et al. 2017).

1.2.3 HR and FP in cancer therapy

Due to the HR deficiency, cells with impaired BRCA2 function are hypersensitive to DNA damaging agents that lead to lesions normally repaired by HR, including cross-linking agents, such as cisplatin, and to poly(ADP-ribose) polymerase (PARP) inhibitors, which are being extensively explored as cancer therapeutics (Bryant et al. 2005; Farmer et al. 2005).

Despite encouraging success in the clinic, resistance to platinum drugs and PARP inhibitor therapy can eventually be acquired by tumors. Secondary mutations in the mutated HR genes are frequently observed that reestablish the reading frame and, when checked, restore protein function (Edwards et al. 2008; Sakai et al. 2008; Norquist et al. 2011; Kondrashova et al. 2017a; Chen et al. 2018). Remarkably, in a recent study of circulating tumor DNA from prostate cancer patients, 34 secondary mutations were identified in a single patient that restored the BRCA2 reading frame to confer therapy resistance (Quigley et al. 2017). HR restoration is usually considered to be the underlying mechanism, although FP is likely to be restored as well in most instances.

Restoration of FP has also been proposed as a mechanism leading to PARPi and cisplatin resistance in BRCA1/2-deficient cells. In this scenario, nascent strand degradation is prevented by precluding the recruitment of MRE11 nuclease to stalled replication forks, achieved by ablation of PTIP, MLL3/4, CHD4, and even PARP1 itself among others (Guillemette et al. 2015; Ding et al. 2016; Ray Chaudhuri et al. 2016) (discussed in detail below). Interestingly, HR activity is not restored in these cases, indicating that FP alone is sufficient to confer chemoresistance. It remains to be determined whether restoration of FP is an important resistance mechanism in patients. However, it has been noted that in BRCA2-deficient ovarian tumors treated with platinum drugs, high PTIP expression is associated with longer progression-free survival (Ray Chaudhuri et al. 2016).

1.3 Nascent strand degradation and FP: a closer look

1.3.1 Fork Reversal and nascent strand degradation

Unlike other canonical HR factors such as BRCA2, RAD51 plays a more complex role during FP. Manipulating RAD51 filament stability itself clearly impacts FP: Disrupting

RAD51 filaments in wild-type cells, by overexpressing a BRC repeat from BRCA2, impairs FP, while stabilizing the filament, by expressing RAD51 K133R, can restore FP in deficient cells (Schlacher et al. 2011; Schlacher et al. 2012). Paradoxically, depletion of RAD51 itself, however, does not affect FP (Thangavel et al. 2015; Feng and Jasin 2017). Emerging evidence suggests that the resolution of this conundrum lies in the process of fork reversal that precedes nascent strand degradation (**Fig. 1-3a**). Fork reversal refers to the remodeling of replication forks into a four-way junction structure, a process that ensures proper resumption of replication observed in a variety of species/cell types including mammalian cells (Neelsen and Lopes 2015; Berti and Vindigni 2016; Quinet et al. 2017). Surprisingly, RAD51 is critical for reversing forks, but BRCA2 does not seem to play a role in this process (Zellweger et al. 2015; Mijic et al. 2017). Therefore, the fork reversal activity of RAD51 is distinguishable from its strand invasion function during the canonical HR process.

Reversed forks have emerged as the entry point for subsequent nascent strand degradation (Kolinjivadi et al. 2017; Lemacon et al. 2017; Mijic et al. 2017; Taglialatela et al. 2017). Indeed, RAD51 depletion in BRCA2-deficient cells precludes nascent strand degradation (Lemacon et al. 2017; Mijic et al. 2017), which we also observe in our system (Feng and Jasin 2017). Moreover, disruption of DNA translocases that have established fork reversal activity, such as SMARCAL1 (Betous et al. 2012; Betous et al. 2013), ZRANB3 (Ciccia et al. 2012), and HLTF (Kile et al. 2015), also restores FP to BRCA2-deficient cells or BRCA2-depleted *Xenopus* egg extracts (Kolinjivadi et al. 2017; Lemacon et al. 2017; Mijic et al. 2017; Taglialatela et al. 2017). Together, these recent studies converge on a two-step model in which stalled replication forks are first reversed by RAD51 and DNA translocases, which are then vulnerable to nascent strand degradation, a step antagonized by the FP process mediated by BRCA2-dependent RAD51 filament formation/stabilization (**Fig. 1-3a**).

The fork reversal and protection activities of RAD51 prove to be functionally separable, as evidenced by the RAD51 T131P mutant expressed in a patient-derived cell line (Wang et al. 2015) which is proficient at fork reversal, but impaired in FP (Mijic et al. 2017). The FP defect in these cells is presumably due to a failure to form stable RAD51 filaments (Wang et al. 2015), consistent with the previous findings using a BRCA2 separation of function mutant (Schlacher et al. 2011). Whether RAD51 has intrinsic fork reversal activity or promotes the activity of a translocase is not clear. Taken together, the ability of RAD51 to act at distinct biochemical steps may explain the diverse outcomes when RAD51 is perturbed in different ways.

1.3.2 Nucleases involved in nascent strand degradation

Along with requiring a reversed fork as a substrate, nascent strand degradation involves multiple nucleases and epigenetic control. MRE11 was the first nuclease characterized to be involved in the resection of stalled forks in BRCA/Fanconi anemia-deficient backgrounds and remains the gold standard for analyzing FP pathways (Schlacher et al. 2011; Schlacher et al. 2012). MRE11 recruitment to stalled replication forks is mediated by histone H3 lysine 4 methyltransferases MLL3 and MLL4 (MLL3/4) and interacting protein PTIP (Ray Chaudhuri et al. 2016) and also relies on a continuously expanding list of proteins, such as PARP1 (Ding et al. 2016), CHD4 (Ray Chaudhuri et al. 2016) and RAD52 (Mijic et al. 2017) (**Fig. 1-3a**). Either directly inhibiting MRE11 activity with small molecules or disrupting its recruitment by depleting any of these proteins restores FP to BRCA2- (and where tested BRCA1-) deficient cells (**Fig. 1-3b**), underscoring the critical role of MRE11 in nascent strand degradation.

In addition to MRE11, resection enzymes EXO1 and CTIP also independently mediate nascent strand degradation in BRCA1- and BRCA2-deficient cells (Lemacon et al. 2017) (**Fig. 1-3**). By contrast, another resection nuclease DNA2 does not play a major

role in these mutants (Thangavel et al. 2015; Ray Chaudhuri et al. 2016), although it has been shown to play a role in other contexts (i.e., with deficiencies of the FP factors BOD1L and ABRO1 (**Fig. 1-3**)). ABRO1 protects stalled forks independent of RAD51 (Xu et al. 2017a); while BOD1L promotes RAD51 chromatin loading (Higgs et al. 2015), whether stabilized RAD51 filaments are required in the absence of BOD1L remains to be tested. DNA2 also degrades stalled forks even in wild-type U2OS cells under prolonged replication stress resulting from hydroxyurea treatment, while MRE11, EXO1 and CTIP are not involved in this process (Thangavel et al. 2015). Therefore, multiple nucleolytic pathways are differentially activated in response to varying stresses and genetic perturbations.

The structure-specific nuclease MUS81 has a more complex involvement in the FP pathway. Parallel to the MLL3/4-PTIP recruitment path for MRE11 is the recently described EZH2-MUS81 axis (**Fig. 1-3a**), which provides one context in considering the role of MUS81. EZH2 is recruited to stalled forks and mediates methylation of histone H3 at lysine 27, and MUS81 is able to interact with this histone modification. Perturbation of either EZH2 or MUS81 restores FP to BRCA2-defective cells (Rondinelli et al. 2017). This discovery further extends the scope of nucleases and epigenetic alterations at the fork that promote nascent strand degradation, although it remains to be determined whether MUS81 nuclease activity is directly involved. Interestingly, the EZH2-MUS81 axis only operates in BRCA2-, but not BRCA1-, deficient backgrounds (Rondinelli et al. 2017) (**Fig. 1-3b**), indicating that the FP functions of BRCA1 and BRCA2 are separable. Accordingly, MUS81 chromatin recruitment is induced upon loss of BRCA2 (Bhowmick et al. 2016; Lai et al. 2017; Lemacon et al. 2017; Rondinelli et al. 2017), but not BRCA1 (Lemacon et al. 2017; Xu et al. 2017b). It is well appreciated that BRCA1 acts at a distinct step of HR, upstream of BRCA2 (Chen et al. 2018), but thus far, the biology behind their different roles in FP remains unclear and warrants future investigation.

While providing a risk to genome integrity, one potentially positive role for nascent strand degradation is to promote fork restart. BRCA2-deficient cells undergo extensive fork degradation but maintain normal fork restart activity, at least in some contexts (Schlacher et al. 2011). Two recent studies reported that MUS81 nuclease supports fork restart in the absence of BRCA2 (Lemacon et al. 2017; Rondinelli et al. 2017). MUS81 acts by cleaving degraded forks to mediate fork restart, a conclusion that is supported by the observation that MUS81 depletion in BRCA2-deficient cells leads to fewer DSBs and a concomitant increase of reversed forks, especially those with a single-stranded arm, indicative of extensive fork resection (Lemacon et al. 2017). Consistent with this, MUS81 depletion did not rescue FP in the BRCA2-deficient U2OS cells and in fact the cells are sensitized to hydroxyurea (Lemacon et al. 2017), in line with a synthetic lethal interaction between the two genes observed in another study (Lai et al. 2017).

However, Rondinelli et al, using a panel of other cell lines, has argued for a synthetic viable, rather than synthetic lethal interaction: MUS81 disruption restores FP upon BRCA2 deficiency to confer resistance to PARP inhibition (Rondinelli et al. 2017), although this was not observed by Lemacon et al (2017). The discrepant roles of MUS81 in fork degradation could be related to its ability to process diverse types of substrates (Dehe and Gaillard 2017).

1.4 BRCA2 domains and binding partners

Human BRCA2 is a 3418 amino acid protein which consists of multiple domains (**Fig. 1-4**). Deleterious *BRCA2* mutations have been reported throughout the length of the protein, mostly truncating mutations but also point mutations, some of which are in conserved domains (Breast Cancer Information Core; http://research.nhgri.nih.gov/bic/).

Mutations of uncertain clinical significance have also been identified, such that several approaches have been devised to evaluate their functional significance (Hucl et al. 2008; Kuznetsov et al. 2008; Chang et al. 2009; Biswas et al. 2011; Biswas et al. 2012; Bouwman et al. 2013). These and other approaches have also been used to evaluate the importance of rationally designed mutations.

1.4.1 PALB2

The N terminus of BRCA2 binds to the C-terminal WD40 β-propeller domain of PALB2 (**Fig. 1-4**) (Xia et al. 2006; Oliver et al. 2009; Sy et al. 2009; Zhang et al. 2009a; Zhang et al. 2009b). Emphasizing the importance of the PALB2 interaction for BRCA2 function, disruption of this interaction results in severe HR defects (Xia et al. 2006; Siaud et al. 2011). Furthermore, human *BRCA2* mutations that abrogate PALB2 interaction fail to support viability of *Brca2*-null mouse embryonic stem cells (Biswas et al. 2012), although paradoxically *Palb2*-null embryonic stem cells have been reported to be viable (Bowman-Colin et al. 2013).

The significance of PALB2 is further manifested by the fact that, like *BRCA2*, monoallelic *PALB2* mutation is associated with breast cancer susceptibility (Erkko et al. 2007; Rahman et al. 2007b; Tischkowitz et al. 2007a). Although mutations are rare compared with *BRCA1* and *BRCA2*, in the Finnish population ~1% of unselected breast cancers are associated with a founder *PALB2* mutation (Erkko et al. 2007). Interestingly, the clinical phenotype of PALB2 breast cancers is intermediate between BRCA1 and BRCA2 in that a substantial fraction (~40%) is triple negative (i.e., negative for estrogen and progesterone receptors and human epidermal growth factor receptor 2 (*HER2*) amplification) (Tischkowitz and Xia 2010). Monoallelic *PALB2* mutation has also been associated with pancreatic and ovarian cancer susceptibility (Jones et al. 2009; Walsh et al. 2011). Biallelic *PALB2* mutation leads to a Fanconi anemia subtype (FA-N) which

shares a similar tumor spectrum with the FA-D1 subtype arising from *BRCA2* mutation: patients are predisposed to developing early childhood cancers such as Wilms' tumor and medulloblastoma (Reid et al. 2007; Xia et al. 2007). Further, homozygous germline deletion of *Palb2* in mice leads to early embryonic lethality (Bouwman et al. 2011; Bowman-Colin et al. 2013), while conditional deletion of *Palb2* causes mammary tumors with long latency accelerated by p53 loss (Bowman-Colin et al. 2013; Huo et al. 2013).

1.4.2 RAD51: BRC repeats and C-terminus

BRCA2 binds RAD51 at motifs repeated in the middle of the protein (BRC repeats) and at the C terminus (Sharan et al. 1997; Wong et al. 1997) (**Fig. 1-4**). Mammalian BRCA2 has eight BRC motifs that are conserved amongst vertebrates in both sequence and spacing, but not in the intervening sequences (Bignell et al. 1997). DMC1, the meiotic specific RAD51 homolog, has been shown to have a distinct binding site (a PheProPro motif) (Thorslund et al. 2007), however, disrupting the motif in the mouse does not have a discernible effect on DMC1 function and meiosis (Biswas et al. 2012), suggesting that DMC1 binds elsewhere, perhaps to sites also bound by RAD51.

BRC repeats regulate RAD51 filament formation in a complex manner. An individual BRC peptide, when present in excess, disrupts RAD51 filament formation *in vitro* (Davies et al. 2001) and interferes with damage-induced RAD51 foci formation and HR *in vivo* (Chen et al. 1999; Xia et al. 2001b; Stark et al. 2002; Saeki et al. 2006), presumably by mimicking the interface between RAD51 monomers within the RAD51 filament (Pellegrini et al. 2002). Evidence from *Rad51* mutant chicken cells indicates that Rad51 is sequestered under normal conditions by interacting with BRC repeats, but in response to damage, this sequestered fraction undergoes mobilization, suggesting dynamic regulation of Rad51 through interaction with BRC repeat region (Yu et al. 2003). In contrast, the full-length BRCA2 protein or the peptide containing all the eight BRC

repeats promotes RAD51-mediated strand exchange by stimulating assembly of RAD51 onto ssDNA, while preventing nucleation of RAD51 on dsDNA (Carreira et al. 2009; Jensen et al. 2010; Liu et al. 2010; Thorslund et al. 2010). Even a single BRC4 motif exhibits these activities under the appropriate experimental conditions (Carreira et al. 2009). The underlying mechanism is thought to be through blocking ATP hydrolysis and thus stabilizing the active ATP-bound RAD51-ssDNA filament.

Genetic studies further established the importance of BRC repeats for BRCA2 function. Mice deleted for the BRC-encoding exon 11 in the germline are inviable, while somatic exon 11 deletion causes tumor development (Jonkers et al. 2001). Conversely, a mouse mutant that maintains the N terminus of BRCA2 including just three BRC repeats can survive embryogenesis, albeit at low frequency (Friedman et al. 1998). On the cellular level, the essentiality of BRC repeats for BRCA2 function is supported by proliferation defects observed in Δexon 11 embryonic fibroblasts (Bouwman et al. 2010) and the failure to rescue defects in BRCA2-deficient cells with constructs devoid of BRC repeats (Chen et al. 1998b). Remarkably, HR activity, chromosome stability, and crosslink repair are restored to BRCA2-deficient hamster cells by fusing a single BRC motif to the ssDNA-binding protein RPA (Saeki et al. 2006), demonstrating the key role of the BRC repeats in HR. Not surprisingly, point mutations in BRC repeats that impair RAD51 interaction are found in breast cancer patients (Pellegrini et al. 2002), although functional studies are required to determine the effects of these mutations in full-length BRCA2.

Both functional redundancy and divergence may exist among BRC repeats in the context of full-length BRCA2 protein. Redundancy amongst BRC repeats is supported by the sufficiency of an individual BRC repeat for HR function within the BRC-RPA fusion protein (Saeki et al. 2006). A divergence of function is suggested by the poor sequence identity between BRC repeats within a species, in contrast to high inter-species

conservation of individual repeats (Bignell et al. 1997). Consistent with this notion, electron microscopy shows that different BRC repeats bind to different regions of RAD51 filament (Galkin et al. 2005) and biochemical studies proposed the existence of two classes of BRC repeats: BRC1, 2, 3, 4, bind to RAD51 monomers at high affinity and reduce the ATPase activity of RAD51, effectively targeting RAD51 onto ssDNA over dsDNA and stimulating RAD51 strand exchange, whereas BRC5, 6, 7, 8 bind to the RAD51-ssDNA filament at high affinity (Carreira and Kowalczykowski 2011). These results have led to a model whereby the first class of repeats facilitate nucleation of RAD51 on ssDNA and the second class stabilizes the nascent RAD51 nucleoprotein filament (Carreira and Kowalczykowski 2011).

The C-terminal RAD51 binding site of BRCA2 shares no homology with the BRC repeats (Mizuta et al. 1997; Sharan et al. 1997). RAD51 binding to this region is regulated: it is abrogated by CDK phosphorylation at S3291 at G2/M, leading to the hypothesis that it coordinates BRCA2 activity with cell cycle progression (Esashi et al. 2005). BRCA2 S3291 is a key site for RAD51 binding, as both phospho-mimic (S3291E) and phospho-defective (S3291A) mutations block RAD51 interaction (Esashi et al. 2005). Unlike the BRC repeats, a BRCA2 C-terminal peptide selectively binds RAD51 filaments at the interface region between two RAD51 protomers, such that C-terminal binding functions to stabilize RAD51-ssDNA filaments (Davies and Pellegrini 2007; Esashi et al. 2007). The in vitro property of BRCA2 C-terminus in stabilizing RAD51 filaments is now confirmed in cells by a recent super resolution microscopy study (Haas et al. 2018). Surprisingly, however, S3291 mutation confers little or no DNA damage sensitivity and does not compromise HR in the context of full-length protein (Hucl et al. 2008; Ayoub et al. 2009; Schlacher et al. 2011), although the mutation does compromise HR in crippled BRCA2 peptides that have defects in other functional domains (Siaud et al. 2011), implying that C-terminal RAD51 binding is not essential for HR but can promote HR

under some circumstances. However, RAD51 binding by the BRCA2 C terminus has been implicated in the protection of nascent DNA strands at stalled replication forks (Schlacher et al. 2011).

1.4.3 DNA and DSS1

Structural studies revealed that BRCA2 is a DNA binding protein (Yang et al. 2002). The DNA binding domain (DBD) is in the C-terminal half of the protein and consists of five components: a helical domain, three oligonucleotide-binding (OB) folds that bind ssDNA, and a tower domain with a three-helix bundle (3HB) at its end (**Fig. 1-4**). The 3HB is similar to the DNA binding domain of Hin recombinase, suggesting dsDNA-binding activity. The helical domain, OB1 and OB2 interact with the small, highly conserved DSS1 protein (Marston et al. 1999; Yang et al. 2002), which has been shown to promote HR in human cells (Gudmundsdottir et al. 2004; Li et al. 2006; Kristensen et al. 2010).

BRCA2 peptide mutants abrogated for DSS1 binding have impaired HR (Siaud et al. 2011), indicating that at least part of the HR function of DSS1 is through interaction with BRCA2. Biochemical studies have demonstrated that DSS1 promotes the RAD51-loading activity of BRCA2 (Liu et al. 2010). The enhancement of RAD51 loading has been attributed to an interaction with RPA and attenuation of its binding to ssDNA (Zhao et al. 2015). DSS1 also promotes nuclear localization of BRCA2 by masking its nuclear export signal, which in turn ensures nuclear localization of RAD51 (Jeyasekharan et al. 2013). This observation explains an earlier finding that mutations in DSS1 interaction residues of BRCA2 peptides per se are paradoxically more detrimental to HR than deletion of the whole DBD region where the DSS1 binding sites reside (Siaud et al. 2011). DSS1 also appears to maintain the stability of BRCA2 protein in cells (Li et al. 2006), although this effect is not always reproducible (Gudmundsdottir et al. 2004). In *U. maydis*, the ortholog of DSS1 is also required for HR and functions by regulating HR

activity of Brh2 (Kojic et al. 2003; Kojic et al. 2005). In budding yeast, which does not have a BRCA2 homolog, the DSS1 homolog localizes to DSB break sites and promotes HR- and NHEJ-mediated DSB repair, suggesting a BRCA2-independent function of DSS1 in DSB repair (Krogan et al. 2004). DSS1 is also found to interact with the 19S proteasome, the relevance of which to BRCA2 function remains to be clarified.

Patient missense mutations are found throughout DBD domain (Yang et al. 2002). Mutations predicted to compromise either the structural integrity of DBD domain and/or DSS1/DNA binding affect function (Kuznetsov et al. 2008; Biswas et al. 2011; Siaud et al. 2011; Biswas et al. 2012). Moreover, mutation of ssDNA contact residues or deletion of the 3HB has detrimental effects on HR in reporter-based assays of BRCA2 peptide activity (Siaud et al. 2011). Surprisingly, a BRCA2 peptide deleted for the entire DBD is still functional in HR (Siaud et al. 2011); in fact, deletion of the DBD is one type of reversion mutation identified for BRCA2 (Edwards et al. 2008). These findings emphasize the plasticity of BRCA2 function in HR: an intact DBD is required if it is present, but loss of the entire DBD can be tolerated for substantial HR function (Siaud et al. 2011).

1.5 Thesis objective and overview

My thesis aims at studying BRCA2 functions in a relatively normal and disease-related background with the goal of shedding light on the early, acute consequences of genome instability and in turn revealing how they can be linked to late, tumorigenic effects. Specifically, the project focuses on addressing two questions. First, what are the consequences of BRCA2 deficiency? Second, what are the relative contributions of HR and FP in protecting genome integrity?

To this end, I first generated two orthogonal *BRCA2* conditional loss-of-function systems in MCF10A cells, a karyotypically stable, non-transformed human mammary epithelial cell line. I found that BRCA2 deficiency triggers a replication stress that causes abnormalities in subsequent cell cycle stages, leading to a p53-dependent G1 arrest and cell lethality (chapter 2). I also established multiple separation-of-function systems to dissect the contributions of HR and FP. I showed that HR, but not FP, plays a major role in suppressing replication stress and supporting viability of these non-transformed human mammary cells, an unexpected finding based on previous results using other systems (chapter 3). Building on these results, I then further explored the possible causes and consequences of replication stress seen in *BRCA2* mutant cells and investigated the possible involvement of replication fork reversal, another critical process that emerges to impact replication stress and FP (chapter 4).

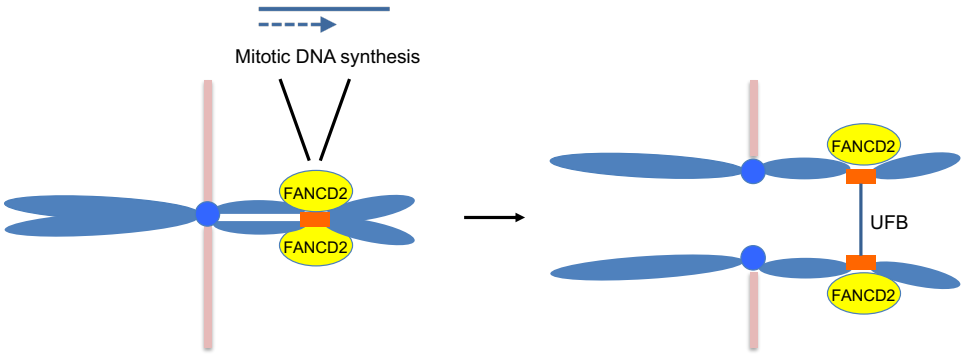

Figure 1-1. Under-replicated DNA in mitosis.
Under-replicated DNA are marked by FAND2 foci pairs. Mitotic DNA synthesis occurs at sites with DNA under replication as a compensatory pathway to finish DNA replication (left). Carry-over of under-replicated DNA into anaphase can lead to UFB formation between the two sister chromatids (right).

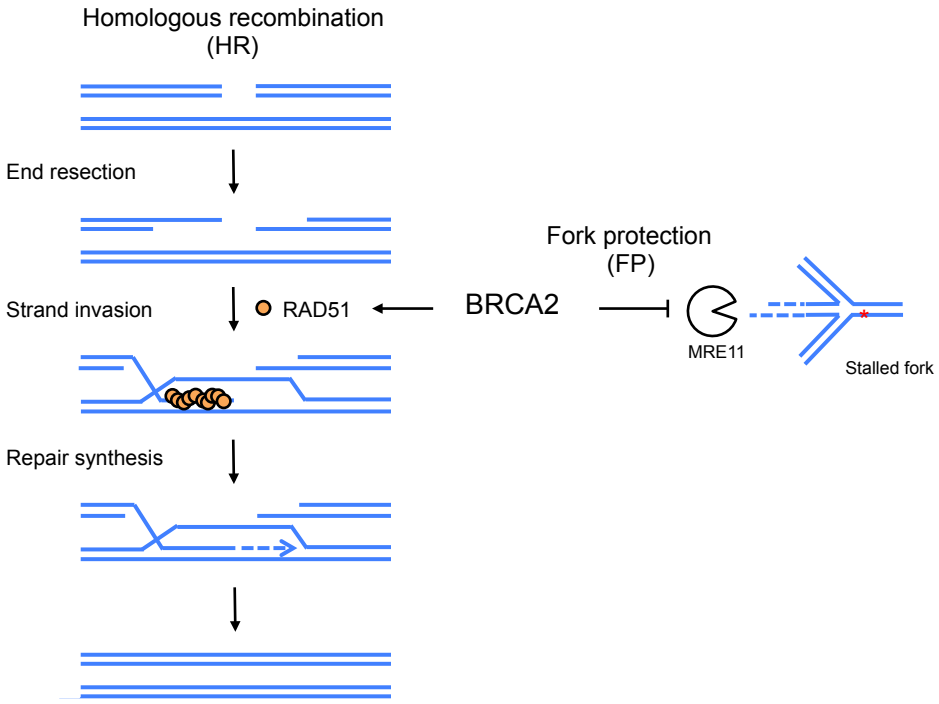

Figure 1-2. HR and FP functions of BRCA2 to protect genome integrity.
(Left) HR repair of a DSB is initiated by resection of the break ends to generate 3' single-stranded DNA overhangs. Subsequent strand invasion into a homologous DNA is critical for repair DNA synthesis, which ultimately promotes an error-free repair outcome. While RAD51 is crucial for strand invasion, BRCA2 plays an essential role by recruiting RAD51 onto the resected DNA. (Right) In the FP process, BRCA2 prevents the nascent strands of a stalled replication fork from being degraded by nucleases such as MRE11.

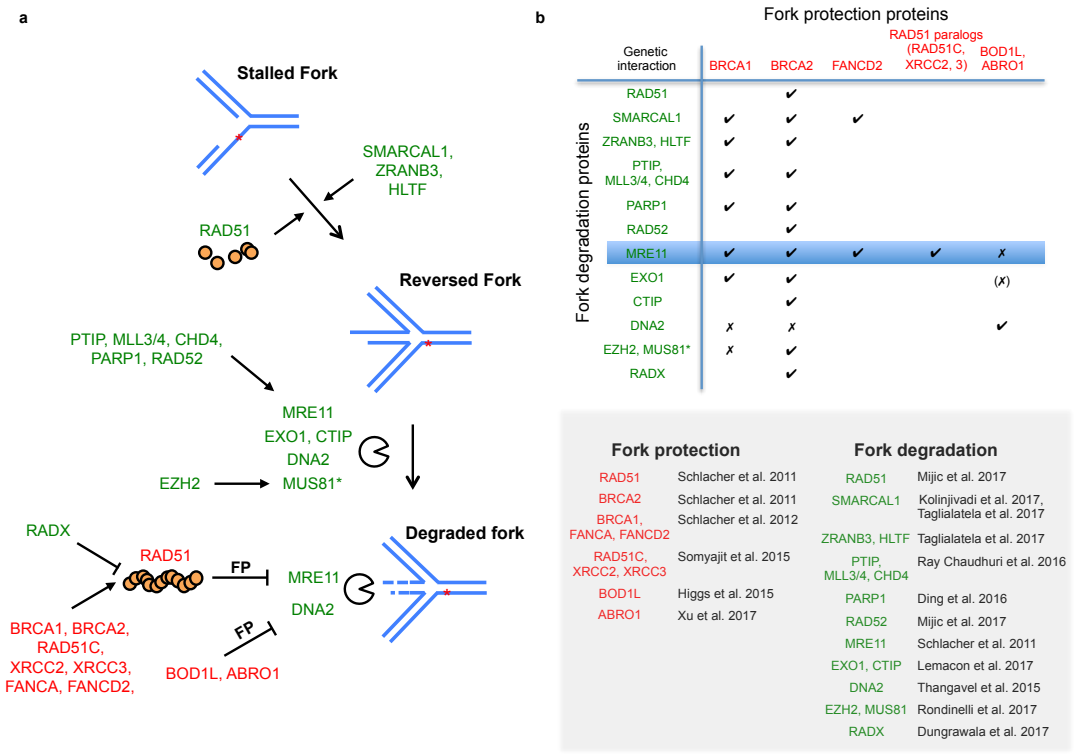

Figure 1-3. Mechanisms of fork degradation and protection.
a. Fork degradation occurs on a reversed fork. Reversal of stalled replication forks is promoted by RAD51 recombinase and DNA translocases (SMARCAL1, ZRANB3, HLTF). In the absence of FP factors like BRCA2, MRE11 and other nucleases can lead to fork degradation. Different pathways regulate MRE11 and MUS81 recruitment to stalled forks. MRE11 recruitment is promoted by a number of proteins, including PARP1 and the PTIP-MLL3/4 axis, while MUS81 recruitment relies on chromatin modifier EZH2. Prevention of MRE11-mediated fork degradation requires RAD51, which is facilitated by HR-Fanconi anemia proteins but antagonized by RADX. Thus, RAD51 both promotes and prevents fork degradation, in particular, at the steps of fork reversal and through the formation of stabilized filaments, respectively. Prevention of DNA2-mediated fork degradation involves BOD1L and ABRO1. Proteins that contribute to FP and degradation are labeled with a red and green color, respectively. Asterisk, MUS81's role in fork degradation is not always observed (discussed in the text).
b. Summary of the reported genetic interactions between FP proteins and proteins that directly or indirectly promote fork degradation, simplified here as "fork degradation proteins". A checkmark indicates that the absence of a FP protein leads to nascent strand degradation involving the corresponding fork degradation protein. An x indicates that evidence exists that a given fork degradation protein is not responsible for fork degradation in the absence of the corresponding FP protein. (x) indicates that EXO1 was not tested for BOD1L. Citations of proteins involved in FP and degradation are listed.

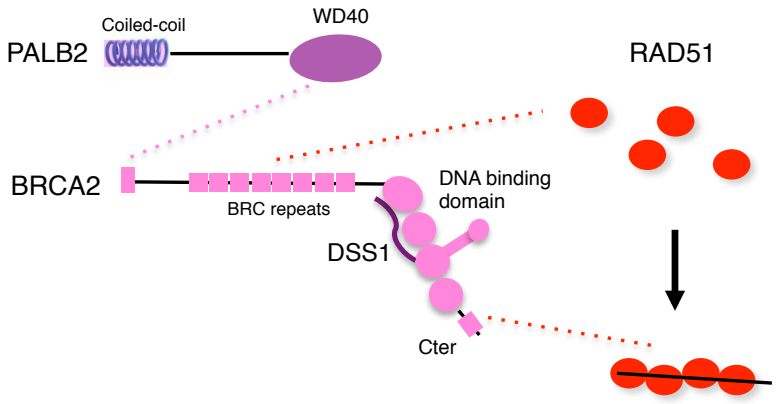

Figure 1-4. BRCA2 binding partners required for a functional HR pathway. PALB2 through its WD40 repeats binds BRCA2. BRCA2 also has important domains that are required for its mediator activity for loading RAD51 onto the RPA coated ssDNA and for the stabilization of RAD51 presynaptic filament. BRC repeats binds RAD51 monomers and help them load on the resected ssDNA. BRCA2 carboxyl terminus (C-ter) is required for stabilizing the RAD51 presynaptic filament.

Chapter 2 Methods and Materials*

2.1 MCF10A cell culture and drug treatment

MCF10A cells, obtained from ATCC through B. H. Park (Johns Hopkins University School of Medicine) (Vitolo et al. 2009) and tested negative for mycoplasma contamination, were grown in DME-HG/F-12 supplemented with 5% horse serum, 20 ng ml^{-1} epidermal growth factor, 0.5 mg ml^{-1} hydrocortisone, 100 ng ml^{-1} cholera toxin, 10 µg ml^{-1} insulin, and 1% penicillin–streptomycin. IdU (50 µM; I7125, Sigma), CldU (50 µM; C6891, Sigma), Aphidicolin (0.1 µg ml^{-1}; A4487, Sigma), hydroxyurea (4 mM; H8627, Sigma), cisplatin (5 µM; 479306, Sigma), olaparib (5 µM, MSKCC Organic Chemistry Core Facility), mirin (50 µM, MSKCC Organic Chemistry Core Facility), RO-3306 (10 µM; SML0569, Sigma) and nocodazole (100 ng ml^{-1}; M1404, Sigma) were used at the indicated concentrations.

2.2 Plasmid construction

For *BRCA2* Ex3-4flox donor plasmid (Ex3-4 fl-Hyg) construction, sequences containing loxP, FRT sites, and the SA-2A module were synthesized and cloned together with a hygromycin-resistance gene between SpeI/SalI sites of the pBluescript II SK+ backbone. The *BRCA2* left homology arm, right homology arm, and exon 3 and 4 region were amplified from genomic DNA from MCF10A cells and sequentially cloned into the above vector with the PAM sequence of the sgRNA recognition site removed. The *BRCA2* "–"

* Chapter 2 is adapted from Feng W, Jasin M. 2017. BRCA2 suppresses replication stress-induced mitotic and G1 abnormalities through homologous recombination. *Nat Commun* **8**: 525.(Under a Creative Commons license http://creativecommons.org/licenses/by/4.0/). Unpublished methods are added.

allele donor plasmid was constructed by replacing the left and right homology arms in an existing hygromycin targeting plasmid (Zhang et al. 2014); a blasticidin-resistance cassette replaced the hygromycin cassette where indicated. The TrBRC5-Cter DNA sequence was amplified in two parts from a previously described plasmid (Siaud et al. 2011) and stepwise cloned between EcoRI/SalI sites of the *AAVS1* donor plasmid (a gift from Dr. Dirk Hockemeyer). Homology arms for all targeting vector are designed to be 700-900 bp in length.

BRCA2 expression vectors were generated by cloning the full-length *BRCA2* sequence from pcDNA3-BRCA2 (Xia et al. 2001a) between XhoI/NotI sites of the PiggyBac transposon plasmid (a gift from Drs. David Allis and Ping Chi) together with a 3XFLAG tag fused to the N terminus. The *BRCA2* S3291E mutation was introduced by replacing the DNA fragment between AgeI/NotI sties in wild-type *BRCA2* with the corresponding region from the FE-BRCA2-TR2 plasmid (Yata et al. 2014).

The lentiviral vector that expresses I-SceI endonuclease for the HR assay was generated by replacing the fragment between SpeI/SalI sites of the pCDH-CMV-MCS-EF1-copGFP vector (CD511B-1, System Biosciences) with the CAGGS-I-SceI fragment from the pCBASce plasmid (Siaud et al. 2011). DNA sequences of all constructs were confirmed by Sanger sequencing. The *BRCA2* Ex3-4flox donor plasmid contained a few polymorphisms in the 6-kb intron 3 that did not affect *BRCA2* expression.

sgRNAs were cloned into a non-viral backbone (Addgene plasmid # 41824) (Mali et al. 2013) or a lentiGuide-puro backbone (Addgene plasmid # 52963) (Sanjana et al. 2014), as described. shRNA expression vectors were generated by cloning the target sequences between AgeI/EcoRI sites of the pLKO.1-NeoR backbone, which was modified from the original pLKO.1 vector (Addgene plasmid # 1864) (Sarbassov et al. 2005) by swapping the puromycin-resistance gene with the neomycin-resistance gene.

2.3 Lentiviral transduction

Lentivirus was produced by standard methods. Briefly, HEK293T cells at 80% confluence were co-transfected with a lentiviral vector, VSV-G expression plasmid and psPAX2 by Lipofectamine 2000 (11668027, Thermo Fisher Scientific) following the manufacturer's instructions. The envelope and packaging vectors were gifts from Dr. Ping Chi. Supernatants containing virus were collected and 0.45-μm filtered 48 h and 72 h after transfection. Infections of MCF10A cells were performed in the presence of 8 μg ml^{-1} polybrene (TR-1003-G, EMD Millipore).

2.4 *BRCA2* gene targeting and complementation

To achieve gene targeting, cells were co-transfected with a donor plasmid and vectors expressing either AAVS1 TALENs (for AAVS1 targeting) (Hockemeyer et al. 2011) or Cas9-sgRNA (for other targeting purposes). Wild-type Cas9 (Addgene plasmid # 41815) (Mali et al. 2013) or paired nickases (Cas9 H840A) (Ran et al. 2013; Vriend et al. 2014) were used. Transfections were performed either by electroporation (Gene Pulser II, Bio-Rad; 350 V, 1000 μF) or nucleofection (Amaxa® Nucleofector® II, Lonza; program X-005). Cells were treated with drugs for selection 2 or 3 days post transfection depending on the selectable marker: hygromycin (100 μg ml^{-1}), G418 (0.2 mg ml^{-1}) or blasticidin (5.0 μg ml^{-1}). The hygromycin-resistance gene cassette from *BRCA2*$^{fl\text{-}Hyg/+}$ cells was removed by transfection of the Flpo plasmid (a gift from Dr. Prasad Jallepalli); colonies were analyzed to identify *BRCA2*$^{fl/+}$ clones. *BRCA2*$^{fl/–}$ cells were subsequently generated by introducing the *BRCA2* "–" allele donor plasmid into *BRCA2*$^{fl/+}$ cells.

sgRNA target sequences:

For *BRCA2* exon 2 G allele targeting:

G allele-specific sgRNA: AGACTTATTTACCAAGCAT

For *BRCA2* exon 2 A allele targeting:

A allele-specific sgRNA: AGACTTATTTACCAAACAT

Another *BRCA2* exon 2 sgRNA (not allele specific, used together with the A allele-specific sgRNA for paired nickase strategy (Ran et al. 2013)): GCCTCTCTTTGGATCCAAT

Gene targeting was confirmed by Southern blotting. Genomic DNA was digested with the indicated restriction enzymes overnight at 37°C and then electrophoresed on a 0.8% agarose gel and transferred to a charged nylon membrane (NEF987001PK, PerkinElmer). Probes were radiolabeled with [α-^{32}P]-dATP using a random primer labeling kit (Agilent) and hybridized with the membrane overnight at 67°C. The membrane was then washed three times with saline-sodium citrate (SSC) buffer containing 0.1% SDS and developed.

For genotyping PCR, trypsinized cell suspensions were mixed with PCR grade water and heated at 100 °C for 5 min before PCR analysis. Oligos 1 (forward) and 2 (reverse) were used to detect the Hyg-targeted allele. Oligos 1 (forward) and 3 (reverse) were used to detect the allele that had not been targeted by the Hyg cassette (i.e., the untargeted allele). Oligo 4 was used to characterize the untargeted allele by Sanger sequencing.

DNA oligo sequences:

Oligo 1: GCTTCTGAAACTAGGCGGCAG

Oligo 2: ATATCCACGCCCTCCTACATCG

Oligo 3: AATGTTGGCCTCTCTTTGGATC

Oligo 4: TCACTGGTTAGCGTGATTGAAAC

For stable *BRCA2* complementation, the PiggyBac plasmid was co-transfected with a transposase expression plasmid (a gift from Drs. David Allis and Ping Chi) into cells by nucleofection and G418 (0.2 mg ml^{-1}) selection was applied 48 h later to obtain G418-resistant cell pools. For BRCA2 expression in *BRCA2*$^{-/-}$*AAVS1*$^{\Delta}$ cells, the neomycin-resistance gene at the targeted *AAVS1* locus was first inactivated by CRPSPR-Cas9 followed by screening for G418-sensitive clones. sgRNA target in Neo: GCTGACAGCCGGAACACGG

For *BRCA2* conditional deletion, cells were infected with purified adeno-Cre (Ad5-CMV-Cre, Baylor College of Medicine Vector Development Laboratory) and applied at a multiplicity of infection of 1000 in the presence of 1.2% Genejammer (204130, Agilent). Alternatively, cells were infected with a lentivirus that expresses a self-deleting Cre (Pfeifer et al. 2001). Both methods generated similar results. Downstream assays were performed using cell pools at least 72 h after infection, except the S/G2 entry experiments (**Fig. 3-8a, Fig. 3-9**), which were performed 2 days after infection as indicated in the figures.

Genotyping PCRs to distinguish the Cre-excised (∆) from the unexcised (fl) allele were performed using genomic DNA prepared with the PureLink™ Genomic DNA Kit (K182002, Thermo Fisher Scientific) following manufacture's instructions. Alternatively, cell pellets were resuspended in PCR grade water and heated at 100°C for 5 min. The resulting extract was directly used for PCR. Oligo 5 (forward) and 6 (reverse) were used to detect the excised ∆*Ex3-4* allele in *BRCA2*$^{\Delta Ex3\text{-}4/-}$. Oligos 5 (forward) and 7 (reverse) were used to detect the wild-type (+) or unexcised *fl* allele in *BRCA2*$^{fl/+}$ and *BRCA2*$^{fl/-}$ cells. Oligo 8 (forward) and 9 (reverse) were used to detect the excised ∆ allele (yielding a 400 bp product) in *BRCA2*$^{-/-}$*AAVS1*$^{\Delta}$ cells. Unexcised allele would yield a product that is too long (6.5 kb) to be amplified. Oligo 10 (forward) and 11 (reverse) were used to detect the unexcised *fl* allele (yielding a 460 bp product) in *BRCA2*$^{-/-}$*AAVS1*^{fl} cells. This

PCR from excised allele is not productive due to removal of the Oligo 10 binding site by Cre.

Oligo 5: ACTTTTGTGAACTCTTGTTACACC

Oligo 6: GGTGTATGAAACAAACTCCCAC

Oligo 7: CTAAGATTTTAACACAGGTTTGCC

Oligo 8: ATTGTGCTGTCTCATCATTTTGGC

Oligo 9: CAGGAAATGGGGGTGTGTCAC

Oligo 10: TGTGGCACCAAATACGAAACACC

Oligo 11: ACAAATGTGGTATGGCTGATTATG

For RT-PCR, RNA was prepared using RNeasy Plus Mini Kit (74134, Qiagen) following manufacture's instructions. cDNA was then synthesized from RNA using SuperScript® III First-Strand Synthesis Kit (18080051, Thermo Fisher Scientific) following manufacture's instructions. Oligo 12 (forward) and 13 (reverse) were used to amplify ex1-10 region from BRCA2 transcript.

Oligo 12: GAAGCGTGAGGGGACAGATTTG

Oligo 13: TACTTCATCTTCTAGGACATTTGG

2.5 Gene knockout

p53 knockout cells were generated by co-transfection of vectors expressing Cas9 and an sgRNA for *TP53* (a gift from Dr. Prasad Jallepalli) by nucleofection. Single colonies were picked and screened by Western blotting. To knock out PARP1, a *BRCA2*$^{fl/-}$ clone that stably expresses Cas9 was first generated from viral infection of lentiCas9-Blast (Addgene plasmid # 52962) (Sanjana et al. 2014). (Note these cells also stably express Cre-ERT2 from the pQCXIN backbone, a gift from Dr. Prasad Jallepalli, although Cre remains inactive in all experiments in this study.) Cells were next nucleofected with a

vector for an sgRNA for *PARP1* in a lentiGuide-puro backbone (Addgene plasmid # 52963) (Sanjana et al. 2014). One day after transfection, cells were transiently selected with puromycin (1 μg ml^{-1}) for 2 days before drug removal and being plated for growth as single colonies. Clones were screened based on restriction site loss at the Cas9 cleavage site and knockouts were confirmed by Western blotting.

sgRNA target sequences:

p53: GGCAGCTACGGTTTCCGTC

PARP1: AACGTCAGGGTGCCGGA

2.6 RNA interference

Stable knockdown cell lines were generated by infecting cells with viruses expressing the target shRNA, followed by continuous G418 (0.2 mg ml^{-1}) selection.

shRNA target sequences:

MRE11 (Olson et al. 2007): GATGAGAACTCTTGGTTTAAC

PARP1-1 (TRCN0000356475): GGAGACCCAATAGGCTTAATC

PARP1-2 (TRCN0000338407): CTGATCCTTCAGCTAACATTA

Transient knockdown with siRNAs by Lipofectamine RNAiMax (13778075, Thermo Fisher Scientific), according to the manufacturer's instructions, was performed 24 or 48 h after Cre infection. siRNAs were purchased as follows: RAD51 (Qiagen, siRAD51#6, SI02629837; #8, SI03061338), SMARCAL1 (SMARTpool, Dharmacon, M-013058-01-0005), EXO1 (Qiagen, siEXO1#7, SI02665138; #8, SI02665145), DNA2 (SMARTpool, Dharmacon, M-026431-01-0005). Cells were analyzed 48 h after transfection. A scrambled shRNA (Sarbassov et al. 2005) and a non-target siRNA (1027281, Qiagen) were used as negative controls.

2.7 Cell proliferation and clonogenic survival assays

For proliferation assays, cells were counted, diluted and plated 3 days after Cre infection (passage 0). Two further rounds of cell counting and re-plating were performed (passage 1 and 2) at 3-day intervals. Cell numbers were normalized to the number of *BRCA2*$^{\Delta Ex3\text{-}4/+}$ cells at passage 0.

For clonogenic survival assays, 1000-2000 cells were seeded in a 10 cm plate and stained by Giemsa (620G-75, EMD Millipore) after methanol fixation 11 days later. Plating efficiency was calculated as the ratio of the amount of colonies formed to the total number of cells plated. All clonogenic assays from this study were performed in an unchallenged condition (i.e. no exogenous DNA damage applied).

2.8 Cell senescence and apoptosis assays

Senescence-associated β-galactosidase staining was performed following manufacture's instructions (9860S, Cell Signaling Technology). The fraction of β-galactosidase+ cells was quantitated using ImageJ software. Apoptotic cells were labeled using a FITC Annexin V kit (640905, BioLegend) according to the manufacturer's instructions, followed by flow cytometry (Becton Dickinson FACScan) and quantification by FlowJo software.

2.9 Cell cycle analysis

Cells were fixed in ice-cold 70% ethanol overnight, before being pelleted, resuspended, and then incubated in propidium iodide (PI) staining buffer (20 ug ml^{-1} PI, 0.2 mg ml^{-1}

RNase A, 0.1% Triton-X, PBS) for 30min at room temperature. Where indicated, cells were incubated with EdU for 30 min before harvest. In this case, EdU was detected using Click-iT® Plus EdU Alexa Fluor® 488 Flow Cytometry Assay Kit (C10632, Thermo Fisher Scientific) following manufacture's instructions and 7-AAD (420403, BioLegend) was used in place of PI for DNA staining. Cell cycle distribution was analyzed by flow cytometry (Becton Dickinson FACScan) and FlowJo software.

2.10 DNA fiber assay

DNA fiber assays were performed as previously described (Schlacher et al. 2011). Briefly, cells were pulse labeled with 50 μM IdU and 50 μM CldU, untreated or treated with 4 mM HU, as indicated. 2000-4000 cells were lysed in lysis buffer (0.5% SDS, 200 mM Tris-HCl pH 7.4, 50 mM EDTA). DNA fibers were spread on microscope slides and fixed in methanol/acetic acid (3:1 by volume). DNA was denatured in 2.5 M HCl for 30 min, followed by 1 h blocking buffer (10% goat serum and 0.1% Triton-X in PBS). Slides were incubated with primary antibodies, anti-CldU (1:75; MA1-82088, Thermo Fisher Scientific) and anti-IdU (1:75; 347580, BD Biosciences) followed by secondary antibodies, anti-rat Alexa Fluor® 488 and anti-mouse Alexa Fluor® 594 (1:250, Thermo Fisher Scientific), for 1h each in blocking buffer at room temperature. Slides were mounted in Prolong with DAPI (P36935, Thermo Fisher Scientific) before image acquisition under Axio2 microscope (Zeiss). Images were analyzed with FIJI (ImageJ) software.

2.12 HR assay

All cell lines used are derived from an MCF10A cell clone that contains the DR-GFP reporter (Pierce et al. 1999) stably integrated as a single copy in the genome (a gift of Dr. Elizabeth Kass). Cells were infected with I-SceI-expressing lentivirus and HR was measured by quantifying the fraction of GFP+ cells by flow cytometry (Becton Dickinson FACScan) 48 h after infection using FlowJo software.

2.13 Immunofluorescence and microscopy

Cells were cultured on Nunc™ Lab-Tek™ II CC2™ Chamber Slides (12-565-1, Thermo Fisher Scientific) and fixed with 2% paraformaldehyde (PFA) for 15 min and permeabilized in blocking buffer (0.1% Triton-X and 1% BSA in PBS) for 30 min at room temperature. To stain chromatin-bound RPA and MRE11, cells were pre-extracted (0.5% Triton-X, 1 mM EDTA, 30 mM sucrose in PBS) on ice for 5 min before fixation. Where indicated, EdU was detected using Click-iT® Plus EdU Alexa Fluor® 647 Imaging Kit (C10640, Thermo Fisher Scientific) following manufacture's instructions, except that $CuSO_4$, Alexa Fluor® azide and reaction buffer additive were used at half of the instructed final concentrations. Cells were then incubated with primary antibodies followed by secondary antibodies diluted in blocking buffer for 1 h each with three PBS washes in between. Slides were mounted in Prolong with DAPI (P36935, Thermo Fisher Scientific) before image acquisition under Axio2 microscope (Zeiss). Where indicated, deconvolution was carried out with z stacks acquired with 0.2 μm spacing using enhanced ratio method, and projected based on maximum intensity on a DeltaVision Image Restoration System (GE Healthcare). Quantification of fluorescence signal intensity per nucleus with was performed with high content image-based cytometry methods essentially as described (Toledo et al. 2013) using FIJI (ImageJ) and analyzed using Excel (Microsoft) softwares. Briefly, nucleus regions were segmented based on

total DAPI intensity, and mean fluorescence intensities of other channels within each nucleus were quantified in FIJI and exported to Excel where data analysis was performed. Replicate experiments for γH2AX intensity quantification are shown in **Fig. 4-12**.

Primary antibodies used were γH2AX (1:1000; 05-636, EMD Millipore; 1:500; 2577S, Cell Signaling Technology), 53BP1 (1:1000; 612522, BD Biosciences), 53BP1 (1:1000; NB100-304, Novus), cyclin A (1:1000; sc-751, Santa Cruz Biotechnology), FANCD2 (1:500; NB 100-182, Novus Biologicals), MRE11 (1:1000; a gift from Dr. John Petrini), p53 (1:1000; Santa Cruz, sc-98), p53-pS15 (1:1000; CST, 9284), PICH (1:500; H00054821-M01, Novus Biologicals), pATM-S1981 (1:1000; 200-301-400, Rockland), pCHK2-T68 (1:1000; 2661S, Cell Signaling Technology), RPA (1:1000; ab2175, Abcam; 1: 1000, 2208S, Cell Signaling Technology). Secondary antibodies used were anti-mouse Alexa Fluor® 488, anti-rat Alexa Fluor® 488, anti-mouse Alexa Fluor® 594, anti-mouse Alexa Fluor® 647, anti-rabbit Alexa Fluor® 568, and anti-rabbit Alexa Fluor® 594 (1:1000; Thermo Fisher Scientific).

2.14 Serum starvation and mitotic cell analysis

For serum starvation, cells were cultured for 24 h in DME-HG/F-12 with 1% penicillin–streptomycin but no other additive. Cells were then released into regular culture media at the indicated time interval. To detect mitotic DNA synthesis, EdU was added to the media for another 1 h incubation before fixation and permeabilization as described in the immunofluorescence section. EdU was detected using Click-iT® Plus EdU Alexa Fluor® 488 Imaging Kit (C10637, Thermo Fisher Scientific) following manufacture's instructions, except that $CuSO_4$, Alexa Fluor® azide and reaction buffer additive were used at half of the instructed final concentrations. Slides were mounted in Prolong with DAPI (P36935,

Thermo Fisher Scientific). Mitotic cells were detected by microscopy. More than 80 mitotic cells from at least three independent experiments were scored.

2.15 Subcellular fractionation and immunoprecipitation

Subcellular fractionation was performed using the Subcellular Protein Fractionation Kit (78840, Thermo Fisher Scientific) following manufacture's instructions. For protein lysate preparation, cells were trypsinized and lysed with NETN lysis buffer (150 mM NaCl, 1 mM EDTA, 20 mM Tris pH 8.0, 0.5% NP40, 10% Glycerol) containing protease inhibitor (11836153001, Roche). For FLAG-IPs, EZview™ Red ANTI-FLAG M2 Affinity Gel (F2426, Sigma) was added to 0.5-2.0 mg protein lysate and incubated overnight at 4°C. After extensive washes with 0.05% Tween 20 in PBS, proteins were eluted with SDS-PAGE sample buffer (B7703S, NEB).

2.16 Western blotting

Equal amounts of protein samples (whole cell lysate, subcellular fractions, or IP samples) were heated at 70 or 100°C for 10 min, run on a precast Tris-acetate (for BRCA2 blots; EA03752BOX, Thermo Fisher Scientific) or Mini-PROTEAN® TGX™ protein gel (Bio-Rad) and then transferred to a nitrocellulose membrane (162-0145, Bio-Rad). The membrane was blocked in 5% non-fat dry milk in PBST and incubated overnight with primary antibodies at 4°C, followed by incubation with secondary antibodies for 1 h at room temperature.

Primary antibodies used were BRCA2 (1:300; OP95, EMD Millipore), clathrin (1:3000; 610499, BD Biosciences), DNA2 (1:500; ab96488, Abcam), EXO1 (1:1000;

A302-640A-T, Bethyl Laboratories), FLAG (1:1000; A8592, Sigma), MRE11 (1:5000; a gift from Dr. John Petrini), PARP1 (1:1000; sc-7150, Santa Cruz Biotechnology), p53 (1:1000; sc-98, Santa Cruz Biotechnology), p21 (1:1000; sc-6246, Santa Cruz Biotechnology), HDAC2 (1:2000; 2540S, Cell Signaling Technology), SMARCAL1 (1:500; sc-376377, Santa Cruz Biotechnology), tubulin (1:10,000; T9026, Sigma), RAD51 (1:2000; PC130, EMD Millipore), histone H3 (1:2000; 9715, Cell Signaling Technology). Secondary antibodies used were peroxidase-linked anti-mouse or anti-rabbit IgG (1:10,000; GE Healthcare).

2.17 Statistical analysis

Statistical analysis was performed using Prism software. p values for FP, γ H2AX, MRE11 nuclear intensity and FANCD2 foci pair quantification were determined using a two-tailed Mann-Whitney test. The remaining data were analyzed by an unpaired two-tailed t test. Statistical tests were justified appropriate for every figure (see legends) and the variance between groups was usually similar. No statistical methods or criteria were used to estimate sample size or to include or exclude samples. For DNA fiber analysis, investigators were blinded in most experiments to the group allocation; for other experiments, investigators were not blinded. P values of <0.05 are considered statistically significant and are indicated with asterisks as follows: *, $p<0.05$; **, $p<0.01$; ***, $p<0.001$; ****, $p<0.0001$.

Chapter 3 Modeling BRCA2 loss in non-transformed human mammary cells*

3.1 Introduction

Breast and ovarian tumor suppressor BRCA2 suppresses genome instability, a hallmark of cancer, by playing a central role in two processes: homologous recombination (HR) for the repair of DNA lesions and protection of nascent strands at stalled replication forks from degradation (FP) (Prakash et al. 2015).

Loss of the wild-type *BRCA2* allele, indicative of functional inactivation of BRCA2, is common in breast and ovarian cancers arising in *BRCA2* mutation carriers. Conditional knockout of BRCA2 in mouse models also results in tumorigenesis (Jonkers et al. 2001; Ludwig et al. 2001). However, rather than providing a growth advantage as in cancers, BRCA2 deficiency causes inviability of mouse embryos and normal mouse cells (Patel et al. 1998; Evers and Jonkers 2006; Kuznetsov et al. 2008; Badie et al. 2010). It is not fully understood how the lethality program is induced in the absence of BRCA2 in otherwise normal cells. Elucidating the underlying mechanisms of how BRCA2 maintains genome integrity and supports cell viability will provide insight into how tumor cells emerge and survive the crisis when BRCA2 is lost, which may also potentially impact therapeutic approaches.

To dissect the mechanisms by which relatively normal, non-cancerous mammary cells respond to BRCA2 deficiency, we developed conditional cell lines to examine the acute response to BRCA2 loss. We demonstrate that BRCA2 deficiency triggers

---

* Chapter 3 is mainly adapted from Feng W, Jasin M. 2017. BRCA2 suppresses replication stress-induced mitotic and G1 abnormalities through homologous recombination. Nat Commun 8: 525. (Under a Creative Commons license http://creativecommons.org/licenses/by/4.0/).

replication stress that is transmitted to the next cell cycle through DNA under replication and chromosomal missegregation, forming 53BP1 nuclear bodies at G1. p53-dependent G1 arrest and senescence are activated, ultimately leading to cell inviability. Thus, our work reveals G1 abnormalities as an unanticipated mechanism to trigger cell lethality upon BRCA2 deficiency.

3.2 Results

3.2.1 BRCA2 is essential for human mammary MCF10A cell viability

To better understand BRCA2's role in a tumor-relevant cell type, We generated a *BRCA2* conditional system in MCF10A cells, a non-transformed human mammary epithelial cell line with a relatively stable genome (Soule et al. 1990). Through CRISPR-Cas9-mediated gene targeting, we knocked in loxP sites to flank exons 3 and 4 of one *BRCA2* allele, and knocked out the other allele by targeting a selectable marker immediately downstream of the start codon (**Fig. 3-1a, Fig. 3-2a-d**). Deletion of exons 3 and 4 is expected to cause a frameshift mutation that generates a premature stop codon to prevent further protein translation. Moreover, exons 3 and 4 encode residues that are essential for PALB2 binding (Xia et al. 2006), which is required for mouse embryonic stem cell viability (Biswas et al. 2011). An exon 3 skipping mutation is associated with familial breast cancer (Nordling et al. 1998), further supporting the notion that loss of PALB2 binding disrupts BRCA2 function.

BRCA2 inactivation in these conditional cells was achieved by infecting $BRCA2^{fl/-}$ cells with either adeno-Cre or a lentivirus that expresses a self-deleting Cre (Pfeifer et al. 2001). We detected the expression of a peptide smaller than full-length BRCA2 in the resulting $BRCA2^{\Delta Ex3\text{-}4/-}$ cells as well as in control $BRCA2^{\Delta Ex3\text{-}4/+}$ cells (**Fig. 3-1b**). Transcript analysis indicated aberrant splicing that presumably promotes translation from

a downstream, in-frame start codon (**Fig. 3-2e**). PALB2 binding mediates BRCA2 chromatin localization; indeed, the truncated ΔEx3-4 peptide was found to be deficient in chromatin binding (**Fig. 3-2f,g**). To test whether exon3-4 deletion affected viability of MCF10A cells, we performed clonogenic survival assays after Cre expression. Unlike *BRCA2*$^{\Delta Ex3\text{-}4/+}$ cells, *BRCA2*$^{\Delta Ex3\text{-}4/-}$ cells did not form colonies (**Fig. 3-1c**), indicating that intact BRCA2 is essential for the viability of these non-transformed human mammary epithelial cells.

We also generated a second *BRCA2* conditional system in which BRCA2 is completely lost upon Cre expression by targeting a floxed *BRCA2* transgene (*TrBRC5-Cter*) (Siaud et al. 2011) into the safe-harbor *AAVS1* locus. The endogenous *BRCA2* alleles were then knocked out by targeting selectable markers downstream of the start codon to generate *BRCA2*$^{-/-}$*AAVS1*^{fl} cells **(Fig. 3-1d, Fig. 3-3)**. The TrBRC5-Cter peptide restores some BRCA2 function (Siaud et al. 2011), although it is expressed at low levels in the *BRCA2*$^{-/-}$*AAVS1*^{fl} cells **(Fig. 3-3c)** and so the cells grow slowly. The requirement for BRCA2 was studied by introducing a vector that expresses full-length, FLAG-tagged BRCA2 (WT) or an empty vector (EV). Unlike the WT-complemented cells, the EV-transfected *BRCA2*$^{-/-}$*AAVS1*^{fl} cells were devoid of full-length BRCA2 **(Fig. 3-1e).** Only the WT-complemented cells formed viable clones upon Cre expression **(Fig. 3-1f).** Thus, the AAVS1 system recapitulated our observations from the ΔEx3-4 system.

Consistent with cell inviability, BRCA2 deficiency led to an acute proliferation defect within the first few passages after Cre infection **(Fig. 3-1g)** associated with **c**ellular senescence and apoptosis **(Fig. 3-1h,i)**. Because no viable BRCA2-deficient clones were obtained from either system, unless otherwise noted, we performed our analysis of BRCA2-deficient cells shortly after Cre expression.

3.2.2 BRCA2 ablation causes spontaneous DNA damage and G1 arrest

To gain more insight into how cell lethality is triggered in these non-transformed, human mammary epithelial cells, we analyzed the consequences of BRCA2 deficiency at the cellular level. As expected, γH2AX staining under unchallenged conditions revealed a higher level of spontaneous DNA damage in *BRCA2*$^{\Delta Ex3\text{-}4/-}$ cells **(Fig. 3-4a, Fig. 3-5)**. DNA damage activates checkpoints to pause cell cycle progression until DNA repair is complete (Ciccia and Elledge 2010). Given its roles in FP and DNA repair during the S and G2 phases, BRCA2-deficient cells would be expected to be arrested in these cell cycle phases (Patel et al. 1998). Surprisingly, however, cell cycle analysis demonstrated that *BRCA2*$^{\Delta Ex3\text{-}4/-}$ cells were enriched in G1 instead **(Fig. 3-4b, Fig. 3-6)**.

To test whether p53 is responsible for G1 arrest and inviability of BRCA2-deficient cells, we generated *p53* knock out cells in the *BRCA2*$^{fl/-}$ background using CRISPR-Cas9 **(Fig. 3-4c)**. *BRCA2*$^{\Delta Ex3\text{-}4/-}$ cells exhibited an increase in p53 levels and p53-dependent p21 induction compared to *BRCA2*$^{\Delta Ex3\text{-}4/+}$ cells **(Fig. 3-4d)**, indicating p53 pathway activation. Importantly, the *BRCA2*$^{\Delta Ex3\text{-}4/-}$ G1 cell population was diminished upon p53 loss **(Fig. 3-4e, Fig. 3-6)**. p53 loss also abrogated cellular senescence induced by BRCA2 deficiency **(Fig. 3-4f)**, in agreement with a previous study using mouse cells (Carlos et al. 2013). Remarkably, PCR-validated *BRCA2*$^{\Delta Ex3\text{-}4/-}$ colonies were formed only in the absence of p53 **(Fig. 3-4g, Fig. 3-7).** These colonies were smaller and fewer compared to the *BRCA2*$^{\Delta Ex3\text{-}4/+}$ control and grew very slowly upon expansion, indicating only a partial rescue of cell viability by p53 loss. Interestingly, the high apoptotic fraction of *BRCA2*$^{\Delta Ex3\text{-}4/-}$ cells was not affected by p53 loss **(Fig. 3-4h)**, thus explaining the partial rescue. Collectively, our results suggest that p53 pathway activation, likely in response to spontaneous DNA damage, leads to G1 arrest and cellular senescence and contributes to cell lethality upon BRCA2 deficiency.

3.2.3 BRCA2 suppresses G1 53BP1 nuclear body formation

To investigate why BRCA2 deficiency caused G1 cell cycle arrest, we first sought to determine the cell cycle stage at which spontaneous DNA damage arose. Cells were first arrested in G1 before Cre expression, which was then followed by a release to reinitiate the cell cycle. γH2AX induction was associated with S and G2 entry of the BRCA2-deficient cells after release from arrest and was also enriched within the S/G2 population specifically marked by cyclin A **(Fig. 3-8a, Fig. 3-9)**, indicating that spontaneous DNA damage primarily originates in these cell cycle phases.

53BP1 NBs mark DNA lesions in G1 as a consequence of replication stress in the previous cell cycle (Harrigan et al. 2011; Lukas et al. 2011). We hypothesized that the G1 arrest arising from BRCA2 deficiency may be associated with 53BP1 NB formation arising from lesions generated in the previous S/G2 phases. Indeed, spontaneously arising 53BP1 NBs were dramatically induced in number in G1 phase *BRCA2*$^{\Delta Ex3\text{-}4/-}$ cells (i.e., cyclin A– cells, **Fig. 3-8b)**. The majority of G1 *BRCA2*$^{\Delta Ex3\text{-}4/-}$ cells had 53BP1 NBs, with ~20% showing three or more, whereas 53BP1 NBs were rare in control G1 cells.

We next determined the impact of replication stress on BRCA2-deficient cells. While HU treatment greatly increased the amount of damage, it did not have a specific impact on overall DNA damage induction or recovery in BRCA2-deficient cells during S phase **(Fig. 3-8c)**. By contrast, however, HU treatment led to a remarkable induction of 53BP1 NB formation in the next G1 phase, as revealed by high content image cytometry **(Fig. 3-8d)**. Thus, in BRCA2-deficient cells, HU-generated replication stress does not induce a more profound DNA damage response in S phase, but rather in the subsequent G1 phase. Because 53BP1 interacts with p53 and 53BP1 NBs mark DNA lesions and contain classical DNA damage signaling proteins (Iwabuchi et al. 1994; Lukas et al. 2011; Cuella-Martin et al. 2016), 53BP1 NBs can conceivably trigger the aforementioned p53-dependent G1 arrest.

3.2.4 BRCA2 prevents under replication and mitotic abnormalities

One possible reason for 53BP1 NB formation is that it serves as a response to replication stress that interferes with the timely completion of replication: The resulting under-replicated DNA forms unresolved structures, which cause aberrations during mitosis and ultimately generate 53BP1 NBs in the daughter cells (Mankouri et al. 2013). To delineate the impact of BRCA2 inactivation on these processes, we first analyzed DNA under replication using mitotic DNA synthesis as a surrogate, a pathway activated during early stages of mitosis as a compensatory attempt to finish replication of unduplicated DNA (Minocherhomji et al. 2015). Foci of DNA synthesis, labeled as sites with EdU incorporation, were evident in a majority of M-phase BRCA2-deficient cells (>70%) and were substantially elevated in number, while they were rarely present in control cells **(Fig. 3-10a,b, Fig. 3-11a).** Notably, mitotic DNA synthesis occurred almost exclusively at sites marked by FANCD2 foci pairs **(Fig. 3-10a)**, an indicator of incompletely replicated DNA in the preceding S phase (Chan et al. 2009; Naim and Rosselli 2009). Overall, the total number of FANCD2 foci pairs was greatly elevated with BRCA2 deficiency, and a substantial fraction of these were sites of DNA synthesis **(Fig. 3-10c,d)**. These results imply that BRCA2 suppresses DNA under replication. Moreover, that BRCA2-deficient cells also exhibited a concomitant elevation in the number of FANCD2 foci pairs in which DNA synthesis did not occur **(Fig. 3-10a,c)** suggests that incompletely replicated DNA may not be fully duplicated during early mitosis and is therefore likely carried over to later mitotic stages.

Unresolved DNA structures such as persistent under-replicated DNA can cause chromosome non-disjunction manifested as ultra-fine bridges (UFBs), a DNA linkage that stains negative for conventional DNA dyes (e.g., DAPI) but can be visualized by staining with bound proteins such as PICH (Baumann et al. 2007; Chan et al. 2007).

These DNA linkages can in turn cause chromosome missegregation, forming DAPI+ anaphase bridges and lagging chromosomes, ultimately generating micronuclei (Chan et al. 2009; Naim and Rosselli 2009; Naim et al. 2013; Ying et al. 2013). Consistent with this, UFBs, anaphase bridges, and lagging chromosomes were all significantly more common in the BRCA2-deficient cells **(Fig. 3-10e,f, Fig. 3-11b)**. Importantly, these anaphase structures were associated with FANCD2 foci in most cases **(Fig. 3-10e,f, 3-11b)**, suggesting that they form as a consequence of DNA under replication. To test this hypothesis, cells were allowed more time to finish replication before entering mitosis by treatment with the CDK1 inhibitor RO-3306, which arrests cells at G2/M phase (Vassilev et al. 2006). As expected, FANCD2 foci pairs in early mitotic BRCA2-deficient cells were diminished to control levels upon release from RO-3306 treatment **(Fig. 3-10d)**. Moreover, formation of both anaphase DAPI bridges and lagging chromosomes in these cells were also abrogated **(Fig. 3-10g,h)**. BRCA2 deficiency also led to a concomitant increase of micronuclei **(3-11c)**. These results strongly suggest that DNA under replication leads to mitotic abnormalities upon BRCA2 deficiency.

Next, we examined if DNA under replication is also the cause of the observed 53BP1 NBs, using a pulse of EdU to mark S-phase cells before RO-3306 treatment **(Fig. 3-10i)**. 53BP1 NB formation in EdU+ *BRCA2*$^{\Delta Ex3\text{-}4/-}$ cells was diminished to control levels upon release into the next G1 phase. Similarly, nocodazole, which leads to a prolonged prometaphase during which the compensatory mitotic DNA synthesis occurs (Minocherhomji et al. 2015), also abolished the subsequent 53BP1 NB formation **(Fig. 3-10j)**. Taken together, our data strongly suggest that BRCA2 suppresses DNA under replication, which, if unrestrained, causes mitotic abnormalities that lead to 53BP1 NB formation in the subsequent G1 phase.

3.2.5 BRCA2 suppresses single-stranded DNA lesions in G2

To further explore the mechanisms by which BRCA2 prevents DNA under replication, we tested the hypothesis that unrepaired DNA damage in HR-deficient cells impedes timely replication completion. Early mitotic *BRCA2*$^{\Delta Ex3\text{-}4/-}$ cells displayed a dramatically increased level of γH2AX, with ~80% of cells containing ≥8 γH2AX foci **(Fig. 3-12a)**. Sites of under-replicated DNA, marked by FANCD2 foci pairs, typically co-occurred with these γH2AX foci, although not all γH2AX foci were marked by FANCD2**.** Importantly, these early mitotic DNA damage sites were diminished by delaying mitotic entry**,** implying that pre-mitotic DNA damage impedes replication completion.

We therefore assayed for possible lesions prior to mitosis in G2 phase. γH2AX foci were substantially induced in BRCA2-deficient cells in G2 and, remarkably, single-stranded DNA (ssDNA), as indicated by RPA foci, was particularly enriched in these lesions **(Fig. 3-12b,c)**. The ssDNA lesions were prevalent, although not all γH2AX-marked sites contained RPA foci **(Fig. 3-12b)**.

Next, we investigated the mechanisms by which G2 DNA damage is generated. Replication fork reversal is considered to be a general response to different types of replication stress (Zellweger et al. 2015) and reversed forks are susceptible to breakage (Couch et al. 2013; Neelsen et al. 2013). Indeed, depleting the fork remodeling protein SMARCAL1 (Betous et al. 2012; Betous et al. 2013; Couch et al. 2013) markedly reduced both overall and RPA+ G2 γH2AX foci produced in *BRCA2*$^{\Delta Ex3\text{-}4/-}$ cells **(Fig. 3-12d, Fig. 3-13a)**. Thus, although it remains to be directly tested whether BRCA2 loss itself affects fork reversal, our observations raise the possibility that fork reversal contributes to the formation of G2 lesions that arise in BRCA2-deficient cells. Reversed forks are subject to direct processing, a DNA2-specific function that is not shared by MRE11 or EXO1 (Thangavel et al. 2015). These four-way structures can also be cleaved by structure-specific endonucleases to produce DSBs (Couch et al. 2013; Neelsen et al. 2013), which can then undergo classical DNA end resection by nucleases, including

MRE11, EXO1 and DNA2. Given the residual RPA+ γH2AX foci from SMARCAL1-depleted cells, it is also possible that lesions can arise independently of fork remodeling. To test the involvement of the resection enzymes in ssDNA formation, we transiently depleted DNA2 or EXO1 (**Fig. 3-13b,c)** or inhibited MRE11 by mirin. Disruption of each individual resection enzyme in BRCA2-deficient cells led to a considerable reduction of RPA foci without markedly affecting the overall γH2AX level in G2 phase **(Fig. 3-12e,f)**. Thus, although direct processing of reversed forks may play some role, the contribution of MRE11 and EXO1, in addition to DNA2, in producing ssDNA is consistent with end resection of DNA breaks. Indeed, we detected ATM pathway activation, manifested by foci of phosphorylated ATM and CHK2 at the damage sites **(Fig. 3-12g,h)**, indicating break formation. Together, our results suggest that fork reversal, DNA breakage, and hyper-resection contribute substantially to the lesions that accumulate in G2 phase upon BRCA2 deficiency and that these persistent intermediates compromise the timely completion of replication.

3.3 Discussion

BRCA2 germline mutation predisposes to breast and ovarian cancer. Seemingly paradoxically, however, BRCA2 deficiency results in inviability both during mouse embryo development and in mouse cells themselves (Patel et al. 1998; Evers and Jonkers 2006; Kuznetsov et al. 2008; Badie et al. 2010). How the cell lethality is triggered in normal cells and bypassed during tumor formation remains unclear. Here, using a BRCA2 conditional system in a non-transformed human mammary epithelial cell line, we show that BRCA2 deficiency induces replication stress, resulting in single-stranded DNA lesions in G2, failure to complete DNA replication and concomitant 53BP1 NB formation in the subsequent G1 phase, to ultimately lead to p53-dependent G1 arrest

and cellular senescence **(Fig. 3-14)**. Independent results from other groups are in agreement with this model (Lai et al. 2017; Schoonen et al. 2017).

3.3.1 BRCA2 suppresses replication stress*

Our data provide mechanistic insight into how BRCA2 suppresses replication stress and under replication. First, BRCA2 serves to repair replication-associated DNA damage such as DSBs through HR, as it does in other contexts. Supporting this, we observe that BRCA2 deficiency leads to spontaneous DNA damage originating in S/G2 phases that persists into mitosis. In particular, at least a fraction of the G2 damage is characterized as hyper-resected DNA arising from activities of resection enzymes that are known to generate intermediates for strand invasion during HR, although other resection-independent mechanisms could also be involved, for example, ssDNA gap formed behind the fork that has been seen upon RAD51 impairment (Hashimoto et al. 2010; Zellweger et al. 2015). These lesions, if left unrepaired or inefficiently repaired, can in turn impede completion of DNA replication. For example, BRCA2 or RAD51 deficiency biases stalled fork-induced recombination towards long-tract gene conversion (Willis et al. 2014); more repair synthesis than during canonical HR may delay the completion of replication. Second, BRCA2 may facilitate DNA replication completion in a DSB-independent manner. In particular, RAD51-mediated fork reversal (Zellweger et al. 2015), followed by BRCA2-promoted strand invasion by RAD51, may allow lesion bypass without DNA breakage. Lastly, through its HR function, BRCA2 may additionally be involved in the following S phase to promote the resolution of lesions marked by 53BP1 NBs.

---

* Section 3.3.1 is adapted from Feng W, Jasin M. 2018. Homologous Recombination and Replication Fork Protection: BRCA2 and More! *Cold Spring Harb Symp Quant Biol*. (Under a Creative Commons license http://creativecommons.org/licenses/by/4.0/).

What is the cause of DNA under replication? BRCA2-deficient cells accumulate single-stranded DNA lesions in G2. Fork reversal, hyper-resection at DNA breaks (current study), and single-stranded DNA formed at or behind the forks (Kolinjivadi et al. 2017) can all contribute to these lesions. We propose that these persistent, unrepaired DNA lesions prevent timely completion of DNA replication. Thus, the sequelae of BRCA2 deficiency can be traced from S/G2 DNA lesions as the source of the G1 arrest to cell inviability as the consequence **(Fig. 3-14)**.

3.3.2 BRCA2 deficiency and mitotic abnormalities

The description of aberrant mitotic structures in BRCA2-deficient cells is not entirely unprecedented but has often been explained by mitotic-specific functions of BRCA2 (Tutt et al. 1999; Daniels et al. 2004; Choi et al. 2012; Mondal et al. 2012). While we do not rule out the possibility of a mitotic-specific function of BRCA2, the restoration of mitotic integrity in BRCA2-deficient cells by a pre-mitotic treatment – delayed mitotic entry – strongly suggests that the underlying lesions occur in the preceding cell cycle phases (i.e., DNA under replication in S phase). Moreover, the aberrant mitotic structures are associated with sites of DNA under replication. Delaying mitotic entry, as well as prolonging prometaphase, the stage when compensatory mitotic DNA synthesis occurs, also rescues G1 abnormalities (i.e., 53BP1 NB formation), further supporting the notion that lack of replication completion causes mitotic and G1 abnormalities upon BRCA2 deficiency.

3.3.3 Involvement of p53 after BRCA2 loss*

---

* Section 3.3.3 is adapted from Feng W, Jasin M. 2018. Homologous Recombination and Replication Fork Protection: BRCA2 and More! Cold Spring Harb Symp Quant Biol. (Under a Creative Commons license http://creativecommons.org/licenses/by/4.0/).

Our model predicts that the lethal phenotypes of BRCA2 disruption may be mitigated by inactivation of cell cycle arrest processes. The p53 pathway is induced upon BRCA2 loss and is responsible for the subsequent G1 arrest. Indeed, p53 loss partially restores cell proliferation to BRCA2-deficient cells. These observations provide insight into the frequent association of *TP53* mutations with BRCA2-mutated cancers (Ramus et al. 1999; Greenblatt et al. 2001; Roy et al. 2011), which parallels results from mouse systems (Connor et al. 1997; Lee et al. 1999; Jonkers et al. 2001; Bouwman et al. 2010). However, p53 inactivation only partially rescues MCF10A cells. While senescence and G1 arrest are substantially abrogated by p53 loss, apoptosis is not, indicating that a p53-independent apoptotic pathway prevents full rescue of viability in the absence of BRCA2. One possibility is the involvement of other p53 family members, i.e., p63 and p73, which play similar roles to p53 in multiple processes, including apoptosis, and have been shown to act redundantly in some contexts (Dotsch et al. 2010; Wang et al. 2017). Therefore, multiple pathways, both p53-dependent and –independent, work together to ultimately result in inviability of BRCA2-deficient cells **(Fig. 3-14)**.

p53 pathway activation in G1 could occur through several non-mutually exclusive ways. First, 53BP1 directly interacts with p53 and regulates p53-dependent G1 checkpoint arrest (Iwabuchi et al. 1994; Cuella-Martin et al. 2016). Therefore, p53 can be activated as a direct response to 53BP1 NBs. However, this interaction may not be the sole explanation for p53 activation, given that 53BP1 inactivation neither restores viability nor diminishes p53 induction in BRCA2-deficient mouse cells (Bouwman et al. 2010). Second, 53BP1 NBs mark DNA breaks due to improper resolution of under-replicated DNA during mitosis (Lukas et al. 2011; Naim et al. 2013; Ying et al. 2013); p53 activation can thus be triggered as a downstream event of DNA damage signaling. Consistent with this notion, a number of DNA damage response proteins reside in 53BP1 NBs (Lukas et al. 2011). In addition to 53BP1-related mechanisms, p53-

dependent G1 arrest may also be activated by mitotic errors independently of DNA damage (Kuffer et al. 2013; Ganem et al. 2014a; Pedersen et al. 2016). In summary, we propose that the replication stress in BRCA2-deficient cells leads to abnormalities in the subsequent M and G1 phases, which in turn trigger apoptosis together with p53-dependent G1 arrest and cellular senescence **(Fig. 3-14)**.

3.3.4 Implications for cancer biology

Our observation that BRCA2 deficiency induces replication stress adds a new dimension to a growing literature that replication stress is a key feature of precancerous lesions induced by oncogenes (Macheret and Halazonetis 2015). Unanticipated consequences of the replication stress induced by BRCA2 loss are mitotic abnormalities leading to G1 arrest and 53BP1 NB formation, which may be exploitable as a diagnostic biomarker for BRCA2 status in carriers. Whether the sequelae of replication stress that we observe with loss of BRCA2, in particular 53BP1 body formation, will be found more generally such as in oncogene-induced precancerous lesions will be important to determine.

Our studies also have implications for cancer therapy. Agents found to enhance 53BP1 NB formation may further sensitize BRCA2-deficient cancer cells to therapy. DNA under replication could also potentially be exploited as an Achilles heel to treat BRCA2-deficient cancers by targeting components in the mitotic DNA synthesis pathway. While a previous study demonstrated the activation of mitotic DNA synthesis in the presence of aphidicolin (Bhowmick et al. 2016), our finding here that mitotic DNA synthesis is activated upon BRCA2 loss even in the absence of exogenous replication stress suggests that it is more relied upon and therefore a promising target for intervention in BRCA2-deficient tumors.

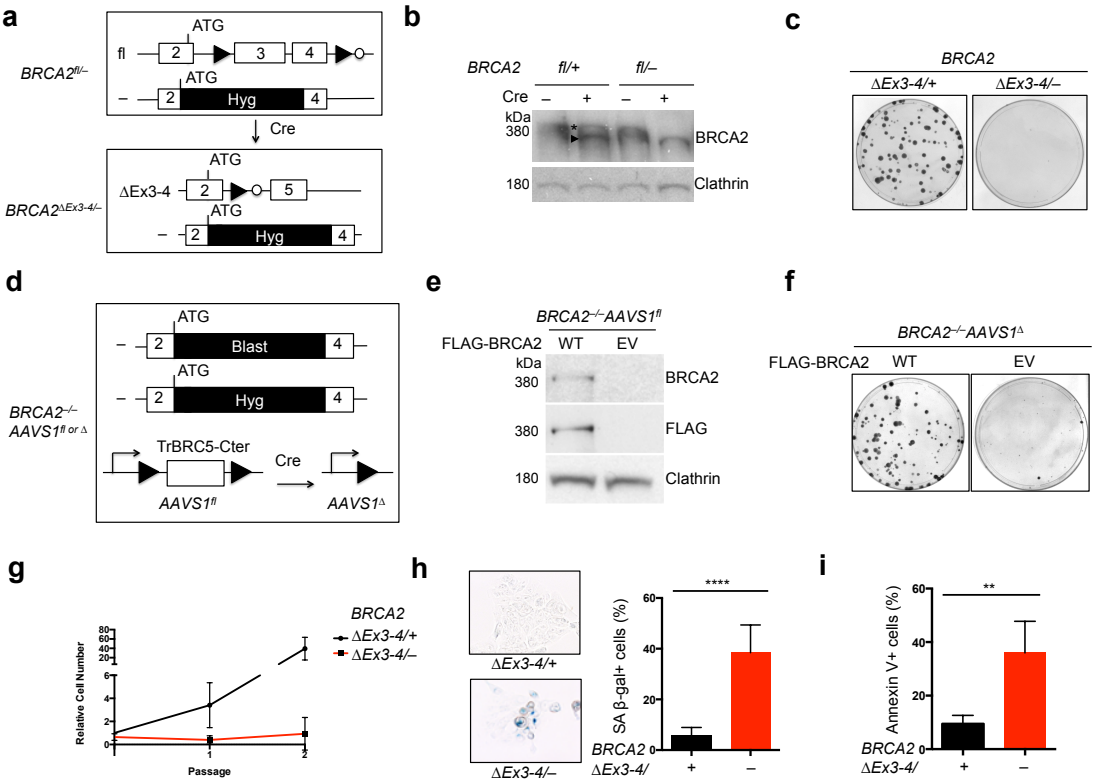

Figure 3-1. BRCA2 is essential for non-transformed human mammary MCF10A cell viability

a. Schematic of the *BRCA2* exon3-4-floxed conditional system in MCF10A cells (filled triangle, loxP site; open circle, FRT site; Hyg, hygromycin-resistance gene).

b. Western blot of *BRCA2* exon3-4-floxed cell extracts with or without Cre expression (asterisk, full-length BRCA2; arrowhead, ΔEx3-4 peptide). The BRCA2 antibody Ab-1 detects BRCA2 amino acids 1651-1821.

c. $BRCA2^{\Delta Ex3\text{-}4/-}$ cells were plated for clonogenic survival. Representative plates are shown.

d. Schematic of the $BRCA2^{-/-}AAVS1^{fl}$ conditional system in MCF10A cells. Blast, Blasticidin-resistance gene.

e. Western blot showing BRCA2 expression in stably-complemented $BRCA2^{-/-}AAVS1^{fl}$ cells (WT, wild-type BRCA2; EV, empty vector).

f. $BRCA2^{-/-}AAVS1^{\Delta}$ cells were plated for clonogenic survival.

g. $BRCA2^{\Delta Ex3\text{-}4/-}$ cells were serially passaged every 3 days. Cell number was determined at the end of each passage and normalized to the number of $BRCA2^{\Delta Ex3\text{-}4/+}$ cells at passage 0.

h. Cells were stained for senescence-associated β-galactosidase (SA β-gal). Left: representative images; Right: comparison of the percent SA β-gal+ cells.

i. Cells were quantified for apoptosis using Annexin V staining.

Error bars in this figure represent one standard deviation from the mean (s.d.). n>3. **, p<0.01; ****, p<0.0001 (unpaired two-tailed t test).

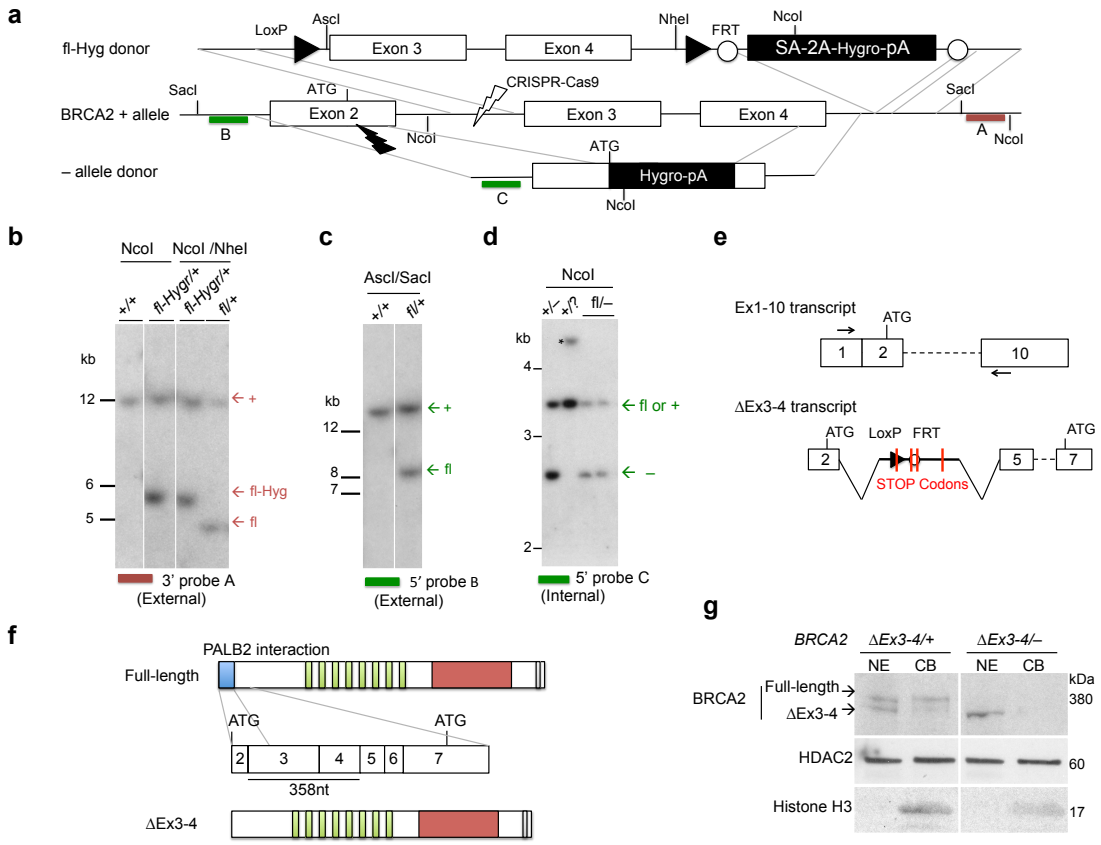

Figure 3-2. Generation of *BRCA2*$^{fl/–}$ and *BRCA2*$^{\Delta Ex3\text{-}4/–}$ cells

a. Schematic for generation of *BRCA2*$^{fl/–}$ cells by CRISPR-Cas9-mediated gene targeting. Donor fragments for generating the BRCA2 exon 3-4 floxed allele prior to Flp recombination (fl-Hyg) and the null (-) allele are shown. Restriction digestion sites for Southern blotting are indicated. SA-2A, splice acceptor followed by 2A self-cleaving peptide sequence; lightning symbols, CRISPR-Cas9 recognition sites; colored bold lines, probes used for Southern blotting.

b-d. Southern blots to confirm targeting of MCF10A cells. The correct bands for the various alleles are indicated by the arrows. Asterisk indicates an unexpected band with the corresponding allele designated with a question mark; this clone was not further interrogated.

e. RT-PCR strategy to detect splicing from the Δ*Ex3-4* transcript. Using primers that hybridize to BRCA2 exons 1 and 10, a product is detected that contains a portion of intron 2 spliced to intron 4 with several stop codons that are in frame with the normal BRCA2 start codon. The next in-frame ATG codon in exon 7 is indicated.

f. Schematic showing domains of BRCA2 protein expressed from + (full-length) and that predicted from the Δ*Ex3-4* allele (ΔEx3-4) if translation begins in exon 7. Additional ATGs downstream can also be used to give rise to a similar peptide.

g. Western blot of BRCA2 after subcellular protein fractionation, showing that the ΔEx3-4 peptide is defective in binding to chromatin (NE, soluble nuclear extract; CB, chromatin-bound fraction). The BRCA2 antibody Ab-1 detects BRCA2 amino acids 1651-1821.

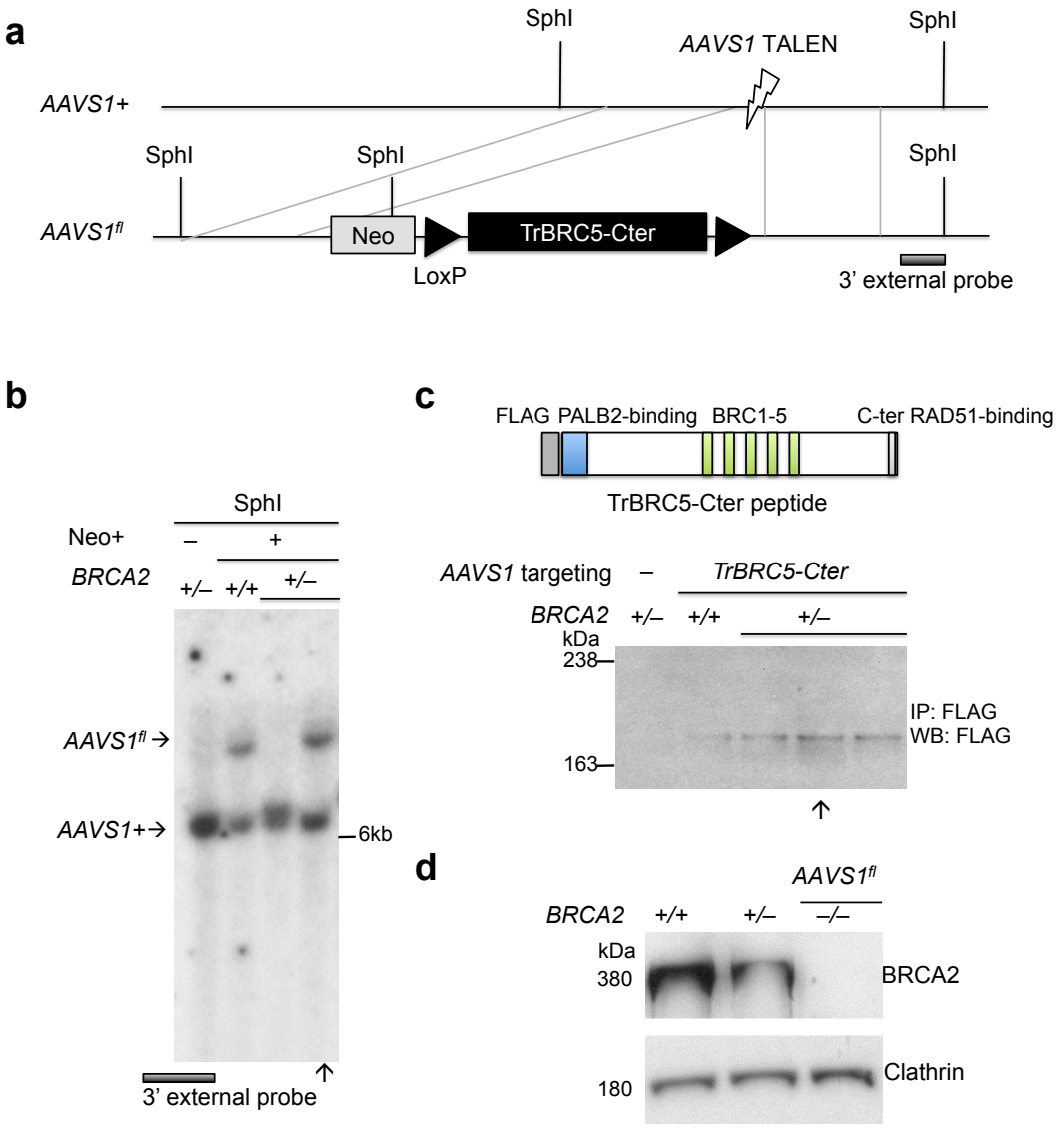

Figure 3-3. Generation and characterization of *BRCA2*$^{-/-}$*AAVS1*^{fl} cells
The *BRCA2* null (-) alleles were generated using the Hygro donor fragment shown in **Fig. 3-2a** and a cognate donor with a blasticidin-resistance gene replacing the hygromycin-resistance gene. The *AAVS1* targeting vector was introduced prior to generating the second *BRCA2* null allele.
a. Schematic of *AAVS1* targeting strategy. Restriction digestion sites and probes for Southern blotting are shown. Lightning symbol, *AAVS1* TALEN recognition sites; Neo, Neomycin-resistance gene cassette.
b. Southern blot to confirm correct gene targeting at the *AAVS1* locus in Neo+ clones. Vertical arrow indicates the clone chosen for subsequent experiments which has one targeted and one untargeted allele.
c. Western blot showing FLAG-tagged TrBRC5-Cter peptide expression by immuno-precipitation. Domain structure of the TrBRC-Cter peptide is shown at top. TrBRC5-Cter peptide expression is not detectible by direct FLAG Western blotting (i.e., without

enrichment by FLAG IP), suggesting low expression. Vertical arrow indicates the clone chosen for subsequent experiments.
d. Western blot showing loss of BRCA2 protein in *BRCA2–/–AAVS1*^{fl} cells.

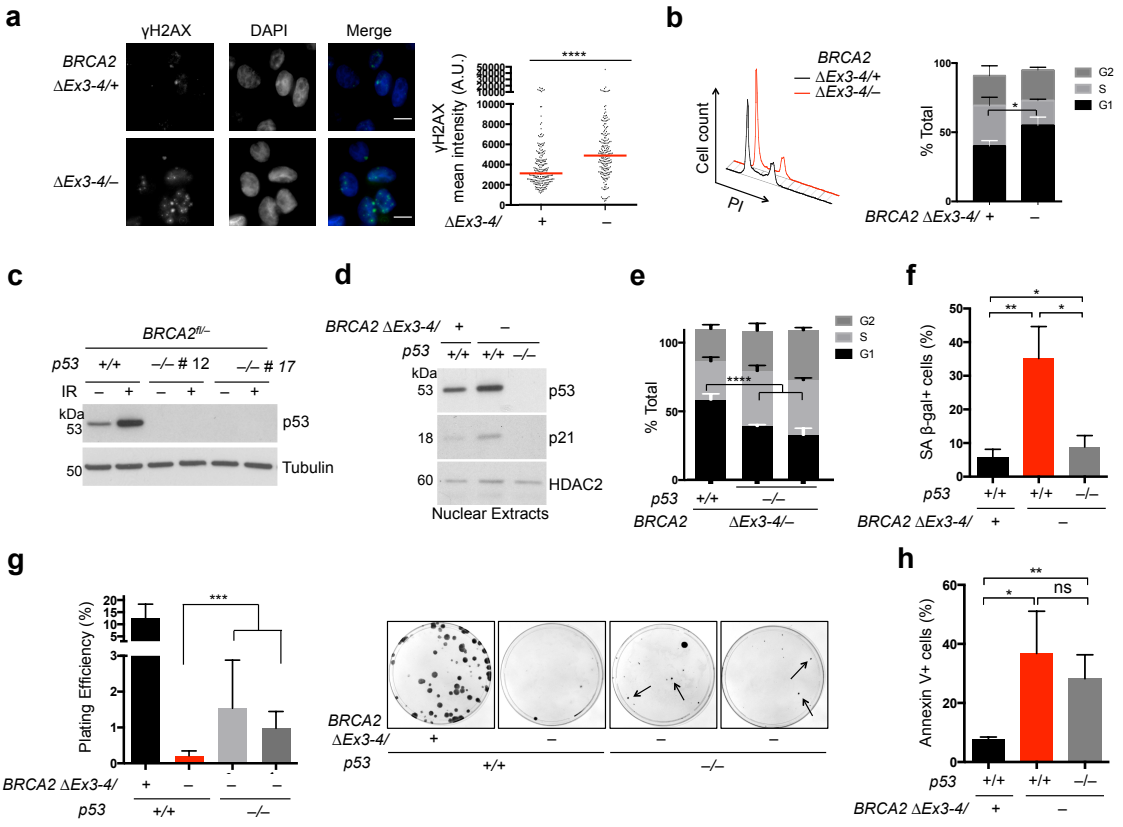

Figure 3-4. BRCA2 deficiency triggers spontaneous DNA damage and G1 arrest

a. *BRCA2*$^{\Delta Ex3\text{-}4/-}$ cells were immunostained for γ H2AX. DNA was counterstained with DAPI. Representative images (left) and quantification of γ H2AX mean nuclear intensity (right) are shown with analysis by a two-tailed Mann-Whitney test. Median γH2AX intensity, red bars. Scale bars, 10 µm.

b. Cell cycle analysis demonstrates an increase in the G1 fraction upon BRCA2 deficiency. Representative plots displaying results from the same amount of cells for both samples are shown on the left. An unpaired two-tailed t test was used for the analysis. n≥3.

c. Western blot showing p53 loss. Cells were harvested 2 h after 10 Gy irradiation (IR). Two independent *BRCA2*$^{fl/-}$*p53*$^{-/-}$ clones were analyzed.

d. Western blots of nuclear extracts prepared from the indicated cells.

e. Cell cycle analysis. An unpaired two-tailed t test was used for the analysis. n≥3.

f. Cellular senescence, as indicated by SA β-gal staining. An unpaired two-tailed t test was used for the analysis. n≥3.

g. p53 loss leads to a partial increase in clonogenic survival of BRCA2-deficient cells. Left: plating efficiency, as analyzed by an unpaired two-tailed t test. n≥3. Right: images of representative plates. Arrows highlight typical PCR-validated *BRCA2*$^{\Delta Ex3\text{-}4/-}$*p53*$^{-/-}$ colonies.

h. Apoptosis analysis using Annexin V staining. Analysis is by an unpaired two-tailed t test. n≥3.

Error bars, s.d. ns, not significant; *, p<0.05; **, p<0.01; ***, p<0.001; ****, p<0.0001.

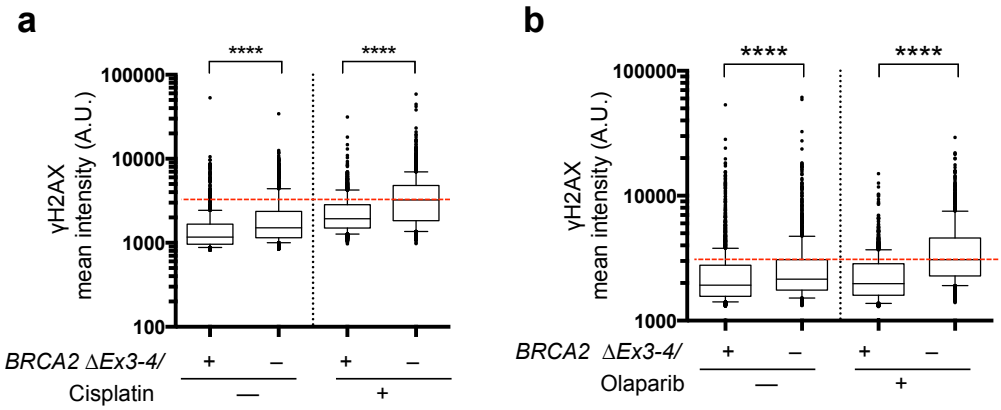

Figure 3-5. BRCA2 inactivation causes increased DNA damage
a. Cisplatin-induced γH2AX. Cells were treated with 5 μM cisplatin for 5 h and released for another 24 h before analysis. γH2AX mean nuclear intensities of >1000 individual cells are shown from one experiment, which is representative of three independent experiments, analyzed by a two-tailed Mann-Whitney test. Box and whiskers show the 10th and 90th percentiles. The dotted red line indicates the median of the *BRCA2* mutant cells exposed to cisplatin.
b. Olaparib-induced γH2AX. Cells were treated with 5 μM olaparib for 24 h before analysis as in **a** (representative of two independent experiments). The dotted red line indicates the median of the *BRCA2* mutant cells exposed to olaparib.
****, p<0.0001.

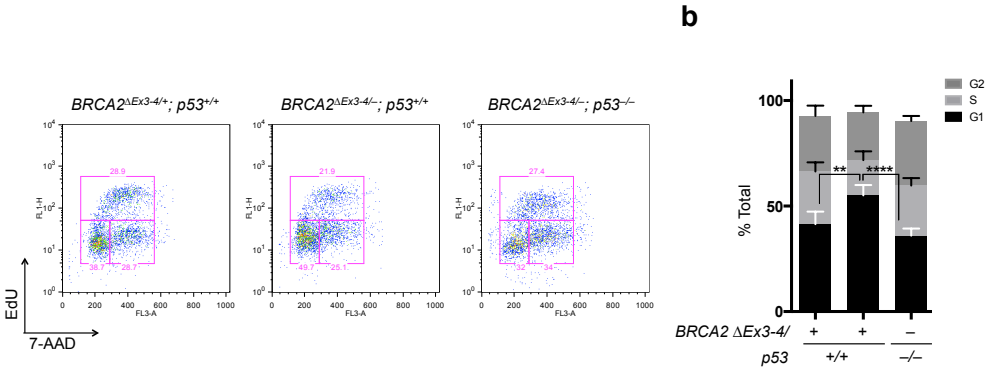

Figure 3-6. BRCA2-deficient cells show p53-dependent G1 arrest
a, b. Cells were incubated with EdU for 30 min before cell cycle analysis based on EdU intensity and DNA content (7-AAD staining). Representative flow cytometry profiles (**a**) and quantification (**b**) are shown, analyzed by an unpaired two-tailed t test. n≥3. Error bars, s.d. **, p<0.01; ****, p<0.0001.

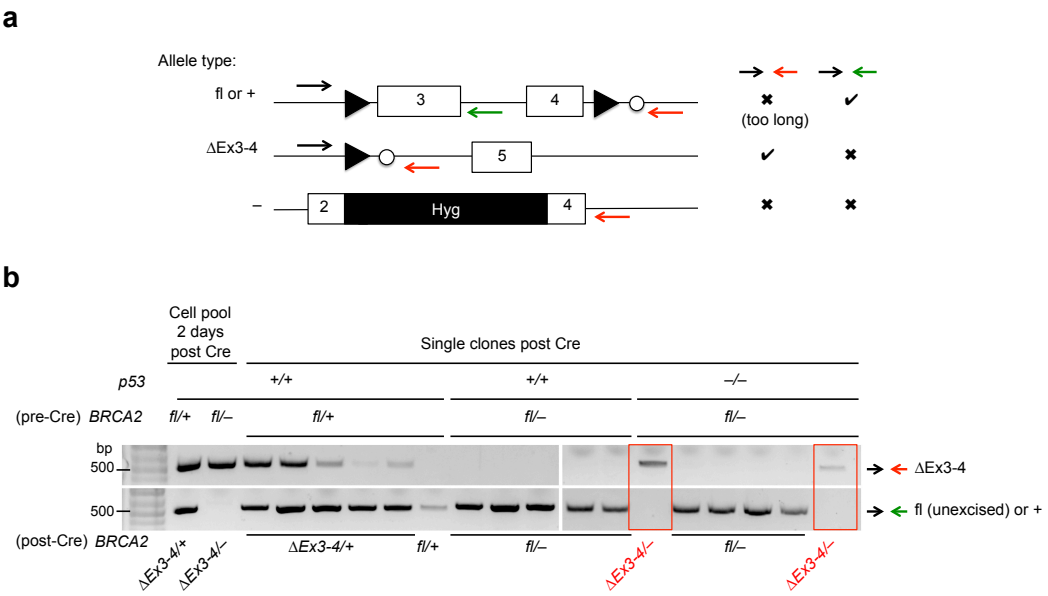

Figure 3-7. Validated *BRCA2*$^{\Delta Ex3\text{-}4/-}$ clones form in the absence of p53
a. Schematic of primer design to distinguish the different *BRCA2* alleles.
b. Representative DNA gel image showing the results of genotyping PCR for the indicated cells. PCR was performed using either cell pools two days after Cre expression (first two lanes) or single colonies that grew after Cre expression. Primer sets used are shown on the right. The genotypes determined from PCR results are shown below the gel. The clones confirmed to be *BRCA2*$^{\Delta Ex3\text{-}4/-}$ are highlighted. Note that the only *BRCA2*$^{\Delta Ex3\text{-}4/-}$ clones are *p53*$^{-/-}$.

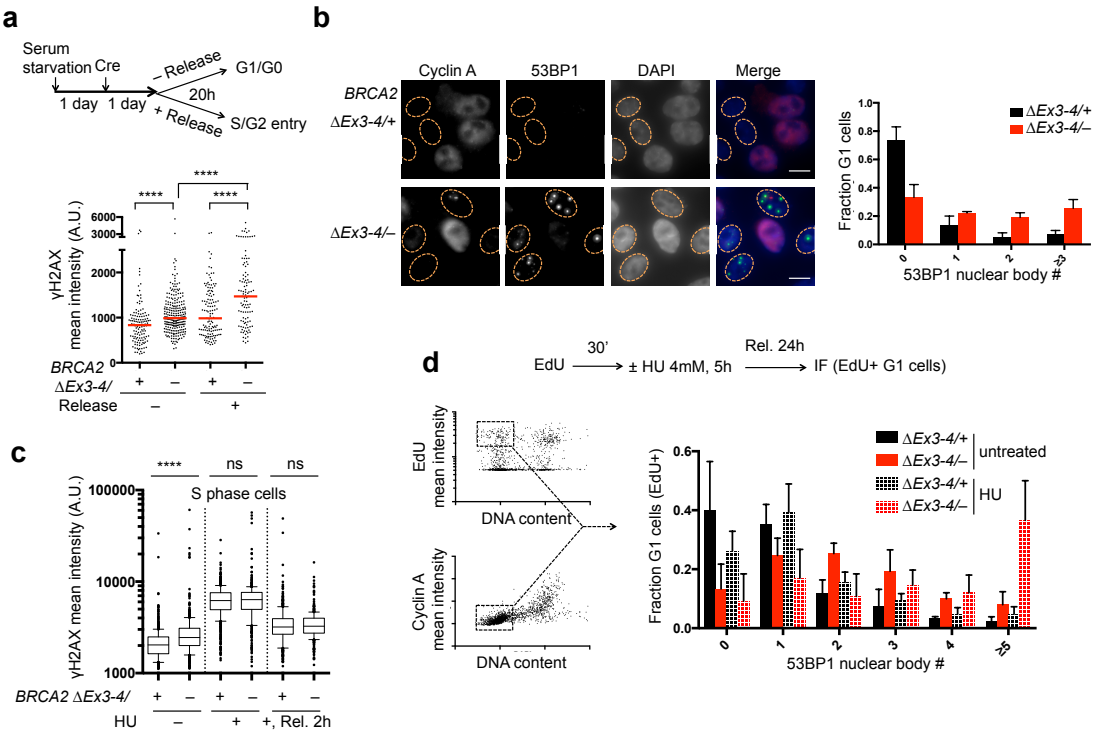

Figure 3-8. BRCA2 suppresses replication stress associated with G1 53BP1 nuclear bodies

a. *BRCA2*$^{\Delta Ex3\text{-}4/-}$ cells were serum starved with or without release, as in the schematic (top), and γ H2AX mean nuclear intensities were quantified (bottom). γ H2AX mean nuclear intensities are shown from one experiment, which is representative of two independent experiments. Median γH2AX intensity, red bars.

b. 53BP1 NB analysis in G1 phase. Cyclin A– nuclei (indicating G1 phase) are outlined (left). Quantification of 53BP1 NB distribution is shown (right). n=4. Scale bars, 10 μm.

c. S phase DNA damage analysis. Where indicated, cells were treated with EdU for 30min followed by HU treatment (4 mM, 5 h) with or without release (Rel.) before harvest. Quantification of γH2AX mean nuclear intensities is shown from one experiment, which is representative of two independent experiments. Box and whiskers show the 10th and 90th percentiles.

d. HU-induced 53BP1 NB formation analysis, as in the schematic (top). Sample plots for high content image cytometry analysis are shown on the left. The EdU+ G1 cell fraction (i.e., EdU+, cyclin A–, 1N DNA content) for 53BP1 NB quantification is highlighted. Quantification of 53BP1 NB distribution in EdU+ cells in G1 at the time of harvest is shown in the graph. n≥3.

Error bars, s.d. ns, not significant; ****, p<0.0001 (two-tailed Mann-Whitney test).

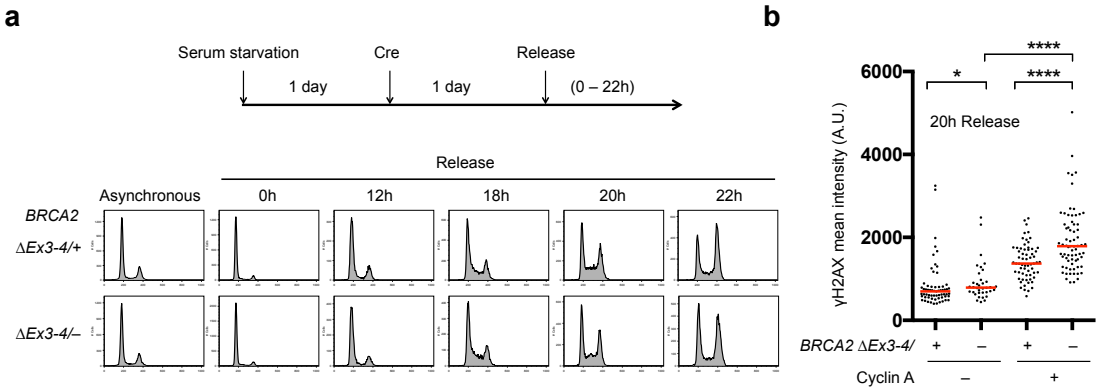

Figure 3-9. S/G2-associated DNA damage induction upon BRCA2 deficiency
a. Cell cycle analysis of *BRCA2*$^{\Delta Ex3\text{-}4/-}$ cells released from serum starvation at time points indicated in the schematic at top.
b. Cells released for 20 h in Fig. 4a were also analyzed for γH2AX mean nuclear intensity in cyclin A– and cyclin A+ cells. Median γH2AX intensity, red bars. γH2AX mean nuclear intensities are shown from one experiment, which is representative of two independent experiments, analyzed by a two-tailed Mann-Whitney test. *, $p<0.05$; ****, $p<0.0001$.

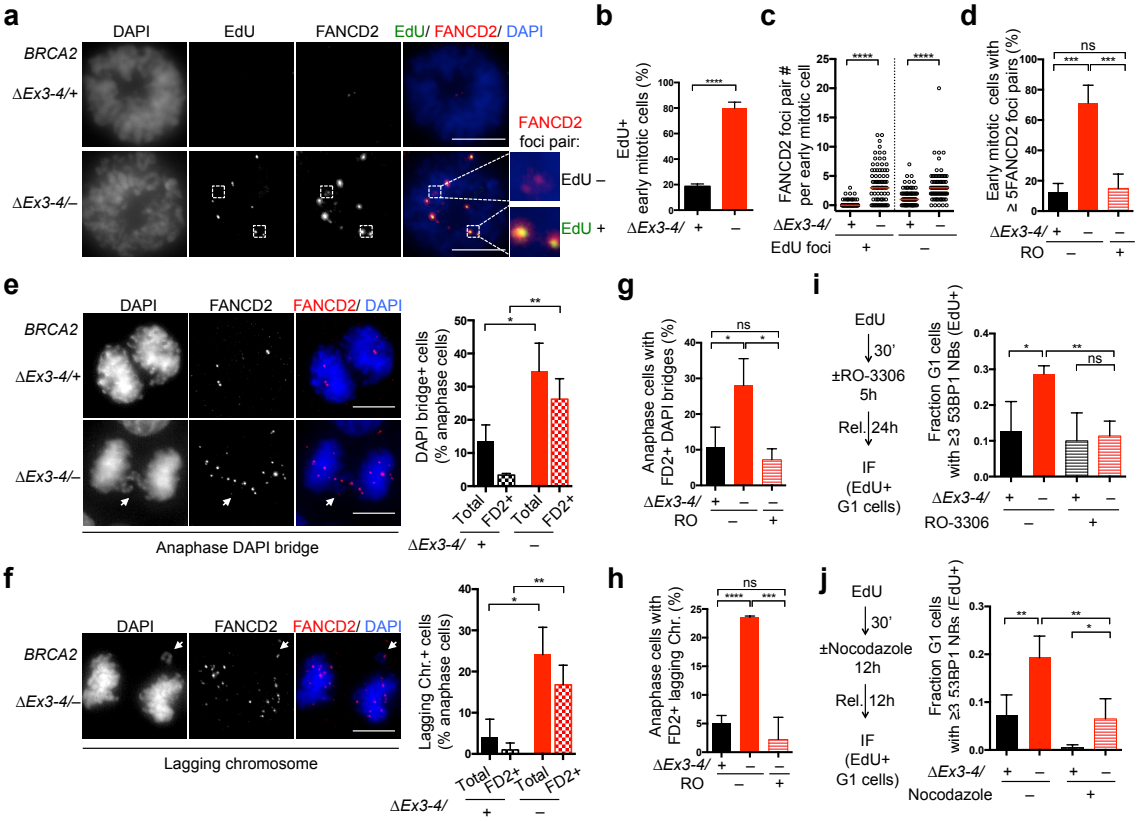

Figure 3-10. BRCA2 deficiency causes DNA under replication that results in abnormal mitoses

a-c. *BRCA2*$^{\Delta Ex3\text{-}4/-}$ cells were released for 22 h from serum starvation to increase mitotic cells, incubated with EdU for 1 h, and then analyzed for mitotic DNA synthesis. Early mitotic cells defined as being in prophase, prometaphase, or metaphase were analyzed for EdU foci that colocalize with FANCD2 foci pairs.

a. Representative images of mitotic DNA synthesis. Scale bars, 10 μm.

b. Percent early mitotic cells containing EdU foci, analyzed by an unpaired two-tailed t test. n=3.

c. FANCD2 foci pairs with or without EdU foci co-localization. Graphs represent the pooled results of three independent experiments, each analyzed by a two-tailed Mann-Whitney test. Median FANCD2 foci pair number, red bars.

d. FANCD2 foci pair analysis in early mitotic cells. Cells were untreated, or treated with the CDK1 inhibitor RO-3306 (10 μM, 24 h) to delay mitotic entry, and released for 1 h before analysis of FANCD2 foci pairs in early mitotic cells. Analysis is by an unpaired two-tailed t test. n=4.

e-h. Anaphase cells were analyzed for DAPI bridges (**e, g**) and lagging chromosomes (**f, h**). RO-3306 treatment (10 μM, 24 h with release for 1 h) was applied where indicated. Representative deconvolved images are shown on the left of **e** and **f**. n=3. Statistical analysis was by an unpaired two-tailed t test. FD2, FANCD2. Scale bars, 10 μm.

i, j. 53BP1 NB analysis with RO-3306 (10 μM, **i**) or nocodazole (100 ng ml^{-1}, **j**) treatment and released as in the schematic on the left. The fraction of EdU+ cells in G1 at the time of harvest that contains ≥3 53BP1 NBs is shown in the graph on the right. Analysis is by an unpaired two-tailed t test. n≥3.

Error bars, s.d. ns, not significant; *, p<0.05; **, p<0.01; ***, p<0.001; ****, p<0.0001.

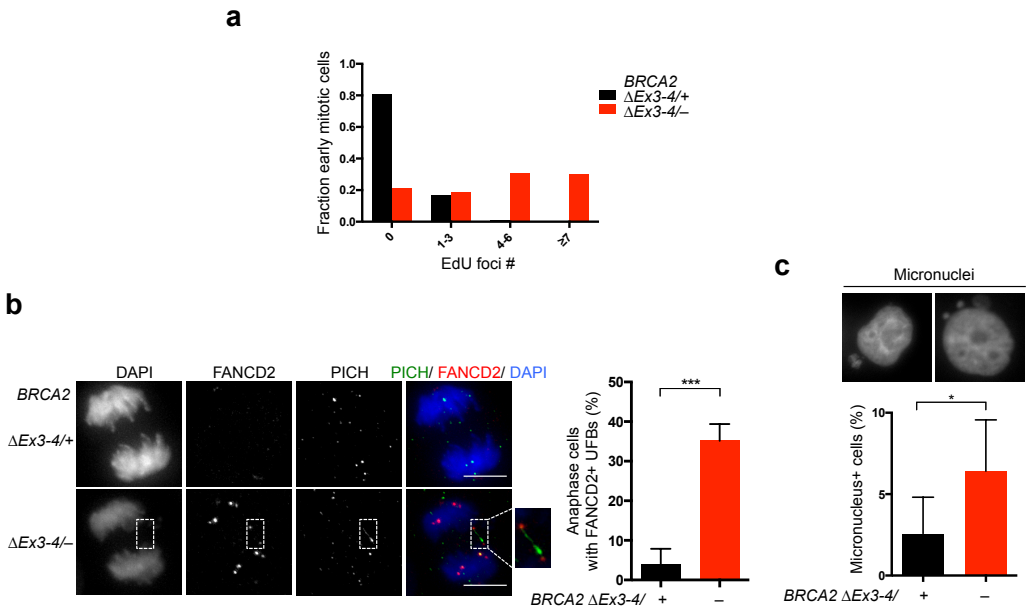

Figure 3-11. BRCA2 deficiency causes under replication and mitotic abnormalities
a. EdU foci distribution quantification of samples from **Fig. 3-10a** (pooled results of three independent experiments).
b. Anaphase cells were analyzed for UFBs with PICH staining. Representative deconvolved images with an inset magnifying the UFB flanked by FANCD2 foci (left) and quantification (right) are shown. n=3. Scale bars, 10 μm.
c. Percent micronucleus-containing cells. Representative images are shown (top). n>3. Scale bars, 10 μm.
Error bars, s.d. *, p<0.05; ***, p<0.001 (unpaired two-tailed t test).

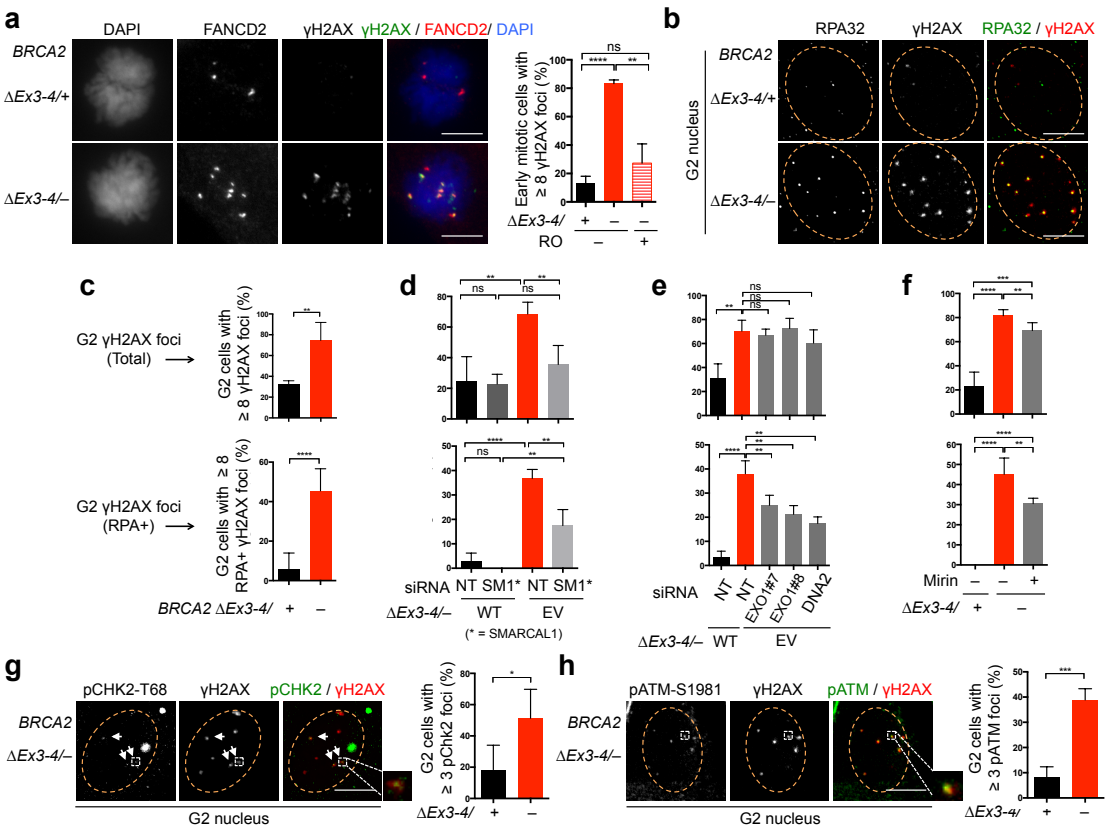

Figure 3-12. BRCA2-deficient cells accumulate single-stranded DNA lesions in G2
a. γH2AX foci analysis in early mitotic cells. Cells were untreated, or treated with RO-3306 (10 μM, 24 h) to delay mitotic entry, and released for 1 h before analysis of γH2AX and FANCD2 foci pairs in early mitotic cells. Representative images are shown (left). Analysis is by an unpaired two-tailed t test. n=3. Scale bars, 10 μm.
b-f. Cells treated with the indicated siRNAs or mirin (50 μM, 5h) were incubated with EdU for 30 min and then analyzed for γH2AX and RPA foci in G2 cells (EdU–, 2N DNA content). Representative deconvolved images are shown (**b**). Quantification of γH2AX foci (top, **c-f**) and RPA+ γH2AX foci (bottom, **c-f**) for BRCA2-deficient cells (**c**), cells transfected with siRNAs (**d**, SMARCAL1; **e**, EXO1 and DNA2), and cells treated with mirin (**f**) are shown. n≥3. Scale bars, 10 μm.
g, h. Cells were incubated with EdU as in **b** before analysis of γH2AX and pCHK2-T68 (**h**) or pATM-S1981 (**i**) foci in G2 cells. Representative deconvolved images with magnified inset highlighting foci colocalization are shown (left in each panel). n≥3. Scale bars, 10 μm.
Error bars, s.d. ns, not significant; *, p<0.05; **, p<0.01; ***, p<0.001; ****, p<0.0001 (unpaired two-tailed t test).

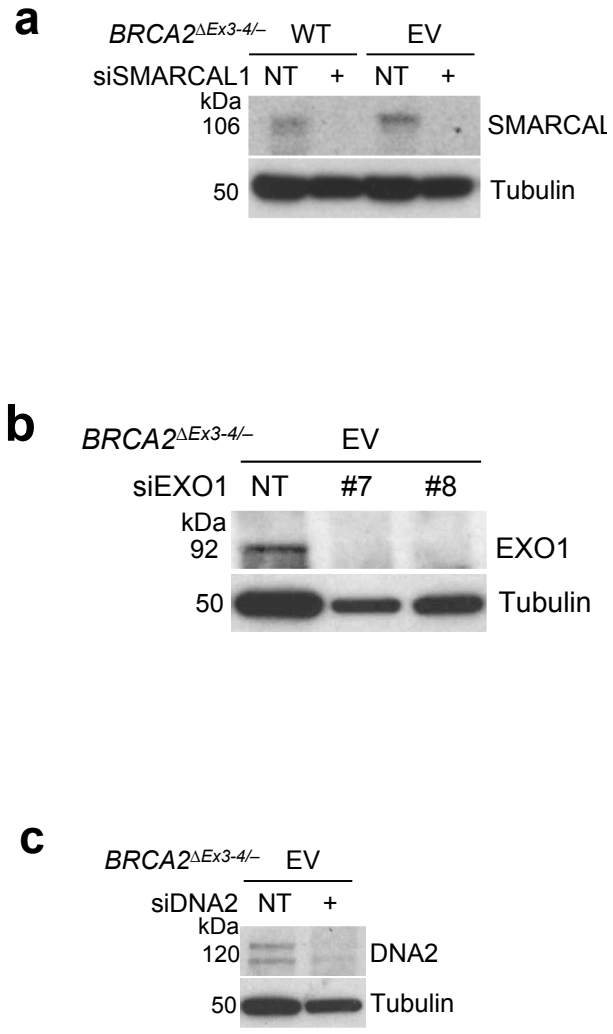

Figure 3-13. Validation of protein depletion by Western blot
a-c. Western blot showing SMARCAL1 (**a**), EXO1 (**b**) and DNA2 (**c**) knockdown.

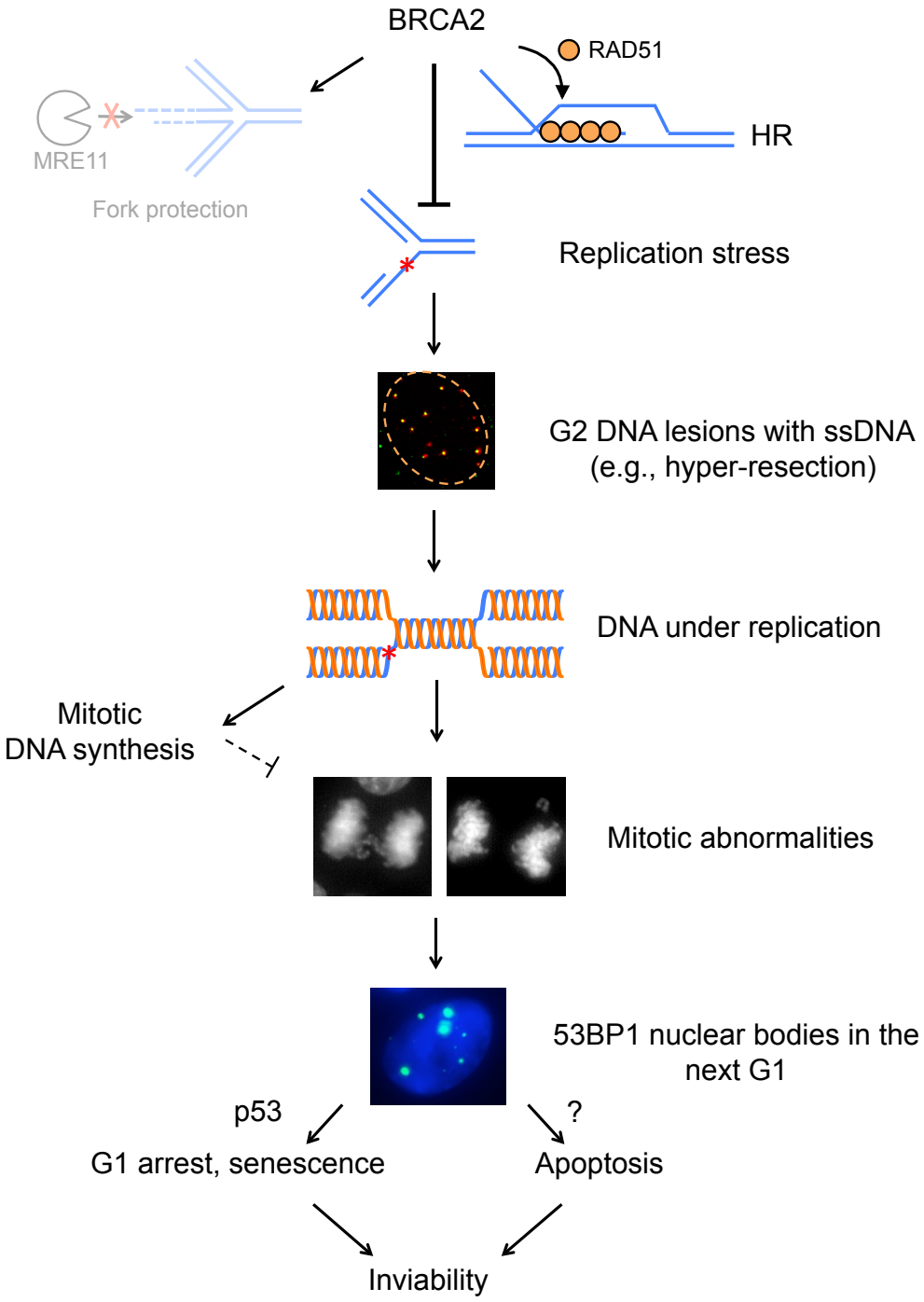

Figure 3-14. Model for replication stress and its aftermath in the absence of BRCA2

BRCA2 suppresses replication stress and DNA under replication in non-transformed cells primarily through RAD51-mediated HR repair of DNA damage. Protection of stalled replication forks from MRE11-mediated degradation plays a minor role (illustrated in chapter 4). Upon BRCA2 deficiency, single-stranded DNA lesions accumulate in G2, generated, in part, by fork reversal (not shown) and hyper-resection. Unrepaired DNA

damage perturbs the timely completion of DNA replication, leading to under replication. During early mitosis, the compensatory mitotic DNA synthesis pathway is insufficient, such that these unresolved DNA structures lead to anaphase abnormalities and formation of 53BP1 NBs in the next G1 phase. G1 arrest and cellular senescence mediated by p53 and p53-independent apoptosis are in turn triggered to ultimately result in cell inviability.

Chapter 4 Dissecting the contribution of homologous recombination and replication fork protection pathways*

4.1 Introduction

Tumor suppressor BRCA2 functions to protect genome integrity by playing critical roles in two processes: a well-established one in homologous recombination and a more recently described HR-independent one in the protection of stalled replication forks (Schlacher et al. 2011). HR is the best-characterized function of BRCA2, where it loads the RAD51 recombinase onto single-stranded DNA, which form a nucleoprotein filament to mediate homologous strand exchange (Prakash et al. 2015). This process is responsible for repairing DNA double-strand breaks (DSBs), which may include those generated by replication fork breakdown (Lomonosov et al. 2003). Due to impaired HR, BRCA2-deficient cells are hypersensitive to agents that cause DSBs, such as cross-linking agents and poly (ADP-ribose) polymerase (PARP) inhibitors. These sensitivities are being exploited in therapeutic approaches.

FP prevents degradation of nascent DNA strands at stalled replication forks by the MRE11 nuclease and requires BRCA1 and other Fanconi anemia proteins, as well as BRCA2 (Schlacher et al. 2011; Schlacher et al. 2012; Ying et al. 2012). Recently, MRE11 recruitment to stalled replication forks has been shown to be mediated by a number of proteins, including PARP1 (Ding et al. 2016; Ray Chaudhuri et al. 2016). HR and FP are functionally separable processes, despite sharing a requirement of key

---

* Chapter 4 is mainly adapted from Feng W, Jasin M. 2017. BRCA2 suppresses replication stress-induced mitotic and G1 abnormalities through homologous recombination. *Nat Commun* **8**: 525. (Under a Creative Commons license http://creativecommons.org/licenses/by/4.0/).

proteins (Schlacher et al. 2011; Schlacher et al. 2012; Ding et al. 2016; Ray Chaudhuri et al. 2016).

A series of HR factors including BRCA2 are essential for embryonic cell survival, establishing HR as an essential process in mammalian cells (Moynahan and Jasin 2010). Recently, however, the role of BRCA2 in the protection of stalled replication forks was reported to be sufficient to sustain viability of mouse embryonic stem (ES) cells and to confer resistance of tumor cells to crosslinking agents and PARP inhibitors even in the absence of functional HR (Ding et al. 2016; Ray Chaudhuri et al. 2016). These studies argue that HR may not be essential at least in the contexts tested. Nevertheless, although viable, these ES cells grow poorly, and FP alone is not capable of supporting embryo development (Ding et al. 2016). How the two pathways functionally interact to ensure genome integrity and cell viability in adult tissues, such as normal mammary cells to prevent breast cancer initiation, remains elusive.

To dissect the functional relationship between HR and FP, we took advantage of the BRCA2 MCF10A models (described in Chapter 3) and generated multiple separation-of-function systems. All results converge to a conclusion that HR, but not protection of stalled replication forks, is primarily responsible for suppressing replication stress and supporting cell viability. We propose HR as the major pathway to guard against replication stress, a hallmark of precancerous lesions.

4.2 Results

4.2.1 FP is a minor survival and repair pathway

To examine HR levels in the BRCA2-deficient human mammary cells, we used the stably integrated DR-GFP reporter that produces functional GFP only when a DSB introduced into the reporter is repaired through HR (Pierce et al. 1999). As expected, the

BRCA2-deficient cells showed a dramatic reduction in HR repair of the DSB (~10-fold, **Fig. 4-1a**). One hallmark of HR deficiency is hypersensitivity to cross-linking agents (e.g., cisplatin) and PARP inhibitors (e.g., olaparib) and mild sensitivity to irradiation (IR). In line with this view, treatment with either cisplatin or olaparib led to substantially higher levels of unrepaired DNA damage in *BRCA2*$^{\Delta Ex3\text{-}4/-}$ cells compared with *BRCA2*$^{\Delta Ex3\text{-}4/+}$ cells, as measured by the nuclear intensity of γH2AX **(Fig. 3-5)**. In addition, while both *BRCA2* genotypes displayed similar initial levels of IR-induced γH2AX, *BRCA2*$^{\Delta Ex3\text{-}4/-}$ cells showed slower repair kinetics **(Fig. 4-1b)**. The delayed repair was more pronounced in the S/G2 phases compared with G1, which is consistent with the cell-cycle phase preference for HR repair. Together, these results confirm that these human mammary cells have a severe HR deficiency upon BRCA2 deficiency.

We next performed DNA fiber assays to confirm that the BRCA2-deficient cells show degradation of nascent DNA strands at stalled replication forks that is dependent on MRE11 nuclease (Schlacher et al. 2011). We sequentially labeled the cells with a pulse of IdU (red), followed by CldU (green), which is preferentially lost in the absence of FP upon replication stress, in this case from the fork stalling agent hydroxyurea (HU) **(Fig. 4-2a)**. HU treatment triggered a substantially lower relative CldU tract length in BRCA2-deficient cells compared to control cells expressing wild-type BRCA2, indicating nascent strand degradation **(Fig. 4-2a)**. As expected, replication fork degradation was dependent upon MRE11 nuclease **(Fig. 4-2b, Fig. 4-3a)**. As a complementary approach, cells were treated with a single IdU pulse (red) before HU treatment. Again, BRCA2-deficient cells showed considerably shortened nascent strands (IdU-labeled) after HU treatment **(Fig. 4-3b)**, confirming that BRCA2 protects stalled forks. In addition to depletion of MRE11 itself, PARP1 deficiency was recently shown to rescue FP, as PARP1 mediates MRE11 chromatin recruitment during replication stress, but not HR

(Ding et al. 2016; Ray Chaudhuri et al. 2016), which we also observed **(Fig. 4-2b,c, Fig. 4-3c,d)**.

Restoration of nascent DNA strand stability at stalled forks was shown recently to be sufficient to confer viability to *Brca2* null mouse ES cells and cisplatin resistance to BRCA2-deficient mouse B cells and a human tumor cell line (Guillemette et al. 2015; Ding et al. 2016; Ray Chaudhuri et al. 2016). Surprisingly, PARP1 depletion failed to restore viability to the BRCA2-deficient MCF10A cells **(Fig. 4-2d)**. Moreover, PARP1 depletion failed to suppress cisplatin-induced γH2AX formation **(Fig. 4-2e)**.

As these results are contrary to those seen in other systems, we also generated *PARP1* knockouts in MCF10A cells using CRISPR-Cas9. Although both PARP1 heterozygosity and complete knockout restored FP, but not HR, to the BRCA2-deficient cells, neither restored cell viability **(Fig. 4-4a-d)**. We also examined the effects of PARP inhibition and MRE11 depletion which were also previously shown (Schlacher et al. 2011; Ding et al. 2016), and confirmed in our system, to prevent nascent strand degradation **(Fig. 4-2b, Fig. 4-4e)**. Again, neither treatment conferred a growth advantage to BRCA2-deficient cells **(Fig. 4-4f,g)**. Thus, in contrast to previous observations in mouse and tumor cells, our results suggest that FP is not sufficient to support cell viability or repair crosslink-induced DNA damage in these non-transformed human mammary epithelial cells.

We next asked whether protection of nascent DNA strand at stalled forks is necessary for cell survival and DNA repair. In hamster cells, mutating BRCA2 S3291 (S3291A) specifically abrogates FP without affecting HR (Schlacher et al. 2011), thus providing a separation of function mutation to distinguish the two functions. In this study, we investigated the S3291E mutation, which, like S3291A, also disrupts RAD51 binding to the BRCA2 C terminus (Esashi et al. 2005). To this end, we expressed the BRCA2

S3291E (BRCA2 SE) mutant at physiological levels in both BRCA2 conditional systems (*BRCA2*$^{-/-}$*AAVS1*$^{\Delta}$, **Fig. 4-2f**; *BRCA2*$^{\Delta Ex3\text{-}4/-}$, **Fig. 4-5a)**.

As expected, BRCA2 SE-complemented cells in both systems showed nascent strand degradation during HU treatment but only a mild or moderate HR defect **(Fig. 4-2g,h, Fig. 4-5b-d)**. Notably, BRCA2 SE-expressing cells were capable of forming colonies **(Fig. 4-2i, Fig. 4-5e,f),** demonstrating the ability of cells to proliferate in the absence of FP. In the *BRCA2*$^{-/-}$*AAVS1*$^{\Delta}$ system, colony number was fully restored by BRCA2 SE expression. In *BRCA2*$^{\Delta Ex3\text{-}4/-}$ cells, colony number was also significantly restored with BRCA2 SE expression and colonies were as large as those with BRCA2 WT. Nonetheless, plating efficiency of these cells was still reduced relative to WT-complemented cells, which may be related to the lack of full restoration of HR (see below), possibly due to slightly lower expression of BRCA2 SE, when compared either to BRCA2 WT in *BRCA2*$^{\Delta Ex3\text{-}4/-}$ cells or to BRCA2 SE in *BRCA2*$^{-/-}$*AAVS1*$^{\Delta}$ cells (**Fig. 4-5a,g**), although interference from the BRCA2$^{\Delta Ex3\text{-}4}$ peptide cannot be ruled out. Furthermore, BRCA2 SE substantially suppressed cisplatin-induced DNA damage formation in both systems, with only a marginal defect compared to BRCA2 WT **(Fig. 4-2j, Fig. 4-5h)**. Thus, protection of stalled replication forks is dispensable for cell survival and only plays a minor role in repairing cisplatin-induced DNA damage.

4.2.2 Replication stress suppression primarily associates with HR

Our earlier observations have demonstrated a critical role of BRCA2 in preventing replication stress, mitotic and G1 abnormalities and supporting cell survival (described in Chapter 3). To gain more mechanistic insight, we asked through which pathway, FP or HR, or both, does BRCA2 suppress replication stress using the above separation-of-function approaches. *BRCA2*$^{-/-}$*AAVS1*$^{\Delta}$ cells expressing the BRCA2 SE protein, which is specifically impaired in FP, had similarly low levels of mitotic DNA synthesis as cells

expressing BRCA2 WT **(Fig. 4-6a)**. BRCA2 SE complemented cell lines also showed few spontaneous and HU-induced G1 53BP1 NBs, similar to BRCA2 WT cells **(Fig. 4-6b-e)**. By contrast, *BRCA2*$^{\Delta Ex3\text{-}4/-}$ cells in which FP, but not HR, is restored through MRE11- or PARP1-deficiency showed high levels of HU-induced G1 53BP1 NBs **(Fig. 4-6f,g)**. Together, these results imply that protection of stalled replication forks does not play a major role in suppressing DNA under replication and replication stress, as marked by G1 53BP1 NBs.

Thus far, our results show a correlation between HR proficiency, suppression of DNA under replication/53BP1 NB formation, and cell viability: BRCA2 SE-expressing cells are at least partially competent in all aspects, whereas cells with combined BRCA2 and PARP1 deficiency are impaired in all aspects. Furthermore, a cross comparison of the effects of BRCA2 SE expression in the two conditional systems also reveals a correlation between HR activity and cell viability, as BRCA2 SE expression in *BRCA2*$^{-/-}$ *AAVS1*$^{\Delta}$ cells more completely restored both compared to in *BRCA2*$^{\Delta Ex3\text{-}4/-}$ cells (compare **Fig. 4-5d** with **Fig. 4-2h** and **Fig. 4-5e,f** with **Fig. 4-2i**).

To further investigate the importance of HR, we transiently depleted RAD51 **(Fig. 4-7a, Fig. 4-8a)**, the key strand exchange protein which acts immediately downstream of BRCA2 in HR (Prakash et al. 2015). Cells showed a dramatic reduction in HR when RAD51 was depleted **(Fig. 4-7b, Fig. 4-8b)**, as expected. RAD51 depletion also causes a substantial defect in repairing cisplatin-induced DNA damage, another hallmark of HR deficiency, to a similar extent as BRCA2-deficient cells (**Fig. 4-9a)**. However, protection of stalled replication forks was not adversely affected by RAD51 depletion **(Fig. 4-7c, Fig. 4-8c)**, consistent with recent observations (Thangavel et al. 2015) (further examined below). Based on these results, RAD51 depletion allowed us to investigate the consequences of disrupted HR independently of FP defects.

Notably, RAD51 depletion in WT-complemented *BRCA2*$^{\Delta Ex3\text{-}4/-}$ cells substantially induced mitotic DNA synthesis **(Fig. 4-7d, Fig. 4-9b)**. After HU treatment, these cells also displayed markedly elevated levels of G1 53BP1 NBs **(Fig. 4-7e)**. As shown in Chapter 3, BRCA2-deficient cells demonstrated an increase in G2 single-stranded DNA lesions that are correlated with under-replicated DNA **(Fig. 3-12)**. We considered the possibility that replication fork degradation is the cause of the observed ssDNA damage. However, BRCA2 SE expression in BRCA2-deficent cells effectively suppressed these G2 DNA lesions, despite impaired FP **(Fig. 4-7f, Fig. 4-8d)**. Conversely, RAD51 depletion, with HR but not FP deficiency, phenocopied BRCA2 deficiency in inducing ssDNA damage in G2, which was not further exacerbated by combined RAD51 and BRCA2 inactivation **(Fig. 4-7f)**. Together with our earlier results that fork reversal, DNA breakage and hyper resection contribute to formation of these lesions **(Fig. 3-12)**, our results suggest that BRCA2 functions through RAD51-mediated HR to prevent DNA damage accumulation in G2, likely through repair of the resected DNA breaks.

Concomitantly, cell survival was severely compromised in RAD51-depleted cells **(Fig. 4-7g, Fig. 4-8e)**. Thus, RAD51 depletion, with the consequent HR deficiency but adequate FP, is sufficient to cause replication stress associated with cell lethality. BRCA2 SE-complemented cells showed a small further decrease in colony formation upon RAD51 depletion compared to BRCA2 WT-complemented cells, although no further reduction in HR **(Fig. 4-7b,g, Fig. 4-8b,e)**, suggesting a compensatory role for FP in the absence of HR, although this warrants further investigation.

While consistent with recent observations (Thangavel et al. 2015), the above result that RAD51 depletion does not cause nascent strand degradation is surprising given previous findings from the lab using other approaches that have implicated RAD51 in FP (Schlacher et al. 2011; Schlacher et al. 2012). Interestingly, RAD51 depletion in *BRCA2*$^{\Delta Ex3\text{-}4/-}$ cells led to a partial restoration of FP **(Fig. 4-9c,d)**. Thus, while being

critical for FP, RAD51 is also involved in a BRCA2-independent process that is upstream of nascent strand degradation, such that the overall outcome of RAD51 depletion does not affect replication fork stability. Importantly, RAD51 and BRCA2 co-deficiency did not further elevate 53BP1 NBs **(Fig. 4-7h)**, indicating that RAD51 and BRCA2 function in the same pathway, which rules out that this putative RAD51-specific process plays a role in suppressing replication stress.

We also tested the possible involvement of fork restart. No detectible defects in resuming replication at stalled forks were observed in cells lacking RAD51, BRCA2, or both **(Fig. 4-9e)**, unlike a previous report using a tumor cell line with different treatment protocols (Petermann et al. 2010). Overall, our results suggest that HR is the primary pathway associated with the ability to suppress replication stress and support cell viability, while FP plays a minor, possibly compensatory role when HR activity is compromised.

4.3 Discussion

Tumor suppressor BRCA2 is a key player in preventing genome instability, a hallmark of cancer. In the last chapter, we have further shown that BRCA2 suppresses replication stress, which in its absence leads to abnormalities in subsequent cell cycle stages, ultimately resulting in cell lethality. Two genome integrity maintenance processes require BRCA2 activity: HR and FP, both of which are in turn relevant for cancer therapy and chemoresistance. The key mechanistic question that remains unresolved is about the relative contributions of these two pathways to genome integrity maintenance and cell viability. In this study, we provide evidence from a relatively normal human mammary cell line that the integrity of these processes mainly rely on the HR function of BRCA2.

4.3.1 Separation-of-function systems to dissect roles of HR and FP [*]

One key mechanistic question related to BRCA2 function is how it supports cell proliferation. In mouse models, disruption of HR proteins including BRCA2 generally leads to embryonic lethality, implicating HR as an essential process for mammalian cell survival (Moynahan and Jasin 2010). More recently, however, FP in the absence of HR has been reported to sustain viability of BRCA2-deficient cells, both mouse embryonic stem (ES) cells and tumor cells subjected to chemotherapy, arguing that HR may not be essential in these contexts (Ding et al. 2016; Ray Chaudhuri et al. 2016). Subsequent studies have also observed improved cell fitness (viability, chemoresistance) when nascent strand degradation is prevented, by suppressing either fork reversal (Taglialatela et al. 2017) or the RAD51 antagonist RADX (Dungrawala et al. 2017).

However, the correlation between FP and cell fitness does not always hold true. For example, cells with a mutation at the BRCA2 S3291 residue are severely disrupted in FP, but remain proficient in both unperturbed survival and preventing genome instability under PARP inhibitor/platinum treatment, presumably because HR is intact (Schlacher et al. 2011). In fact, fully restoring FP to BRCA2-deficient cells by perturbing different proteins (ZRANB3, MUS81, RADX) varies dramatically in the extent to which it leads to acquired chemoresistance, ranging from no resistance (Lemacon et al. 2017; Mijic et al. 2017) to partial or substantial resistance (Dungrawala et al. 2017; Rondinelli et al. 2017). Different cellular contexts could contribute to the varying experimental outcomes. Therefore, it is critical to determine the functional relationship between HR and FP for viability of normal human cells, particularly in BRCA2-relevant mammary cells.

---

[*] Section 4.3.1 is adapted from -. 2018. Homologous Recombination and Replication Fork Protection: BRCA2 and More! *Cold Spring Harb Symp Quant Biol*. (Under a Creative Commons license http://creativecommons.org/licenses/by/4.0/).

To approach this question, we generated multiple, complementary separation-of-function systems in MCF10A cells to distinguish the roles of HR and FP **(Fig. 4-10)**: HR was specifically disrupted by RAD51 depletion in wild-type cells, while FP was specifically impaired by BRCA2 SE expression or restored by MRE11 or PARP1 deficiency in BRCA2-deficient cells. Taken together, these systems demonstrate that protection of stalled forks plays a minor role in suppressing replication stress and promoting cell proliferation; rather, they support the conclusion that BRCA2 primarily functions through HR in these processes **(Fig. 3-14)**. We cannot formally exclude possible contributions of some as yet unknown BRCA2-RAD51-mediated process that is separable from strand invasion. However, thus far, the various genetic systems tested, with the potentially confounding pathways excluded (i.e., FP and restart), are consistent with a role of HR in preventing DNA under replication and its aftermath. This model can explain the viability of mice and humans whose cells show reasonable levels of HR but are nonetheless deficient in FP, for example, those with Fanconi anemia or *Brca2* hypomorphic mutation (McAllister et al. 2002; Nakanishi et al. 2005; Schlacher et al. 2011; Schlacher et al. 2012; Kass et al. 2016a).

4.3.2 Context-dependent pathway requirement for cell survival

At first glance, the finding of a minor role for FP, specifically, protection of nascent strands, is surprising considering its recently reported critical role in supporting viability of mouse ES cells and conferring chemoresistance to tumor cells (Ding et al. 2016; Ray Chaudhuri et al. 2016). We envision diverse pathway choices to maintain genomic integrity and/or support viability in different biological contexts **(Fig. 4-11)**. Given our results that the p53 pathway impedes cell survival, the threshold to survive BRCA2 loss, and HR loss more generally, may be lower in mouse ES cells due to their compromised p53-mediated G1/S checkpoint (Aladjem et al. 1998); thus, even with HR deficiency,

reducing DNA damage by protecting stalled forks may be sufficient for cell survival (Ding et al. 2016) **(Fig. 4-11b)**. However, FP is not sufficient to fully support embryonic development of *Brca2*-deficent mice (Ding et al. 2016) during which differentiation and the accompanying restoration of G1/S checkpoint function occur. Similarly, having survived the crisis of BRCA2 loss by p53 mutation and/or other means, tumor cells may be able to bypass the requirement for HR, such that restoration of FP is then sufficient to deal with replication stress from agents like olaparib and cisplatin, as recently observed (Ray Chaudhuri et al. 2016) **(Fig. 4-11c)**. However, it is important to note that HR is restored through reversion mutations in a substantial fraction of therapy-resistant human tumors (Kondrashova et al. 2017b; Lord and Ashworth 2017), such that HR reactivation cannot be underestimated as a major mechanism of therapy resistance. In agreement with a context-dependent pathway requirement, SMARCAL1 inactivation, preventing fork degradation, alleviates sensitivity to PARP inhibitors and cisplatin of BRCA1-depleted breast cancer MDA-MB-231 cells, but not MCF10A cells (Taglialatela et al. 2017). Future studies are needed to understand the relationship between these pathways and various cellular milieus.

In an effort to model normal mammary tissue, we used a non-transformed human mammary epithelial cell line, providing evidence that HR is more critical than FP for genome integrity and cell viability. We cannot rule out that the specific genetic background of MCF10A cells (Cowell et al. 2005) could influence our findings, such that experiments in other normal mammary contexts will be required to formally test the generalizability of our findings. Nevertheless, a high reliance on HR in mammary cells is supported by recent in vivo studies, showing particularly robust HR in mammary tissue compared to other tissues (Kass et al. 2016a). Collectively, these previous and our current studies using various systems lead us to propose the complexity of the

contribution that these genome integrity maintenance pathways (i.e., HR and FP) make in different biological systems.

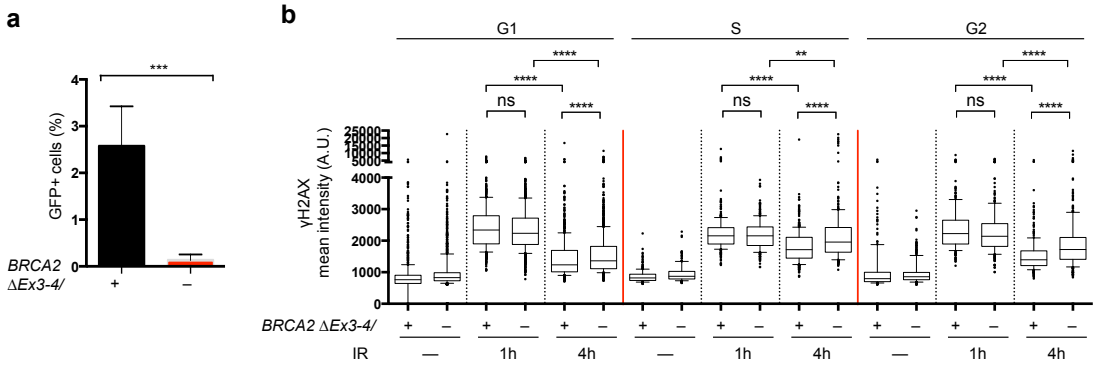

Figure 4-1. BRCA2 inactivation causes HR deficiency
a. HR analysis. *BRCA2*$^{\Delta Ex3\text{-}4/-}$ cells were infected with I-SceI-expressing lentivirus and the percent GFP+ cells was analyzed by an unpaired two-tailed t test. n>3. Error bars, s.d.
b. IR-induced γH2AX. Cells were irradiated with 5 Gy and harvested 1 or 4 h later. EdU was added to all samples 1h before harvest for analysis. Cell cycle stages were determined based on EdU and DAPI intensity. γH2AX mean nuclear intensities of cells from each cell cycle stage are shown from one experiment, which is representative of two independent experiments, analyzed by a two-tailed Mann-Whitney test.
ns, not significant; **, p<0.01; ***, p<0.001; ****, p<0.0001.

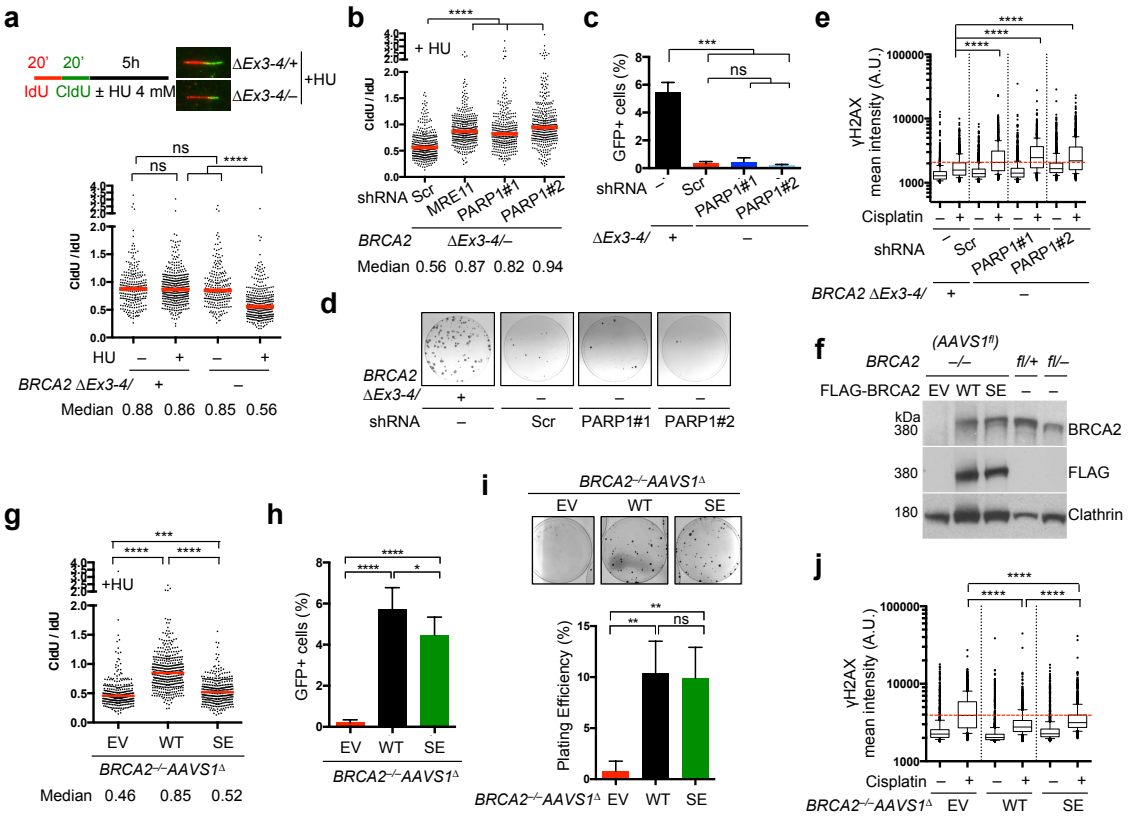

Figure 4-2. FP plays a minor role in cell viability and DNA repair

a. DNA fiber analysis to quantify FP. Schematic of the experimental design and representative images are shown in the inset. Median CldU/IdU tract length ratios are indicated in the graph (red bars). Graphs here and below represent the pooled results of >200 fibers per genotype from at least two independent experiments, analyzed by a two-tailed Mann-Whitney test.

b. Cells stably expressing the indicated shRNAs were analyzed for FP in the presence of HU by a two-tailed Mann-Whitney test. Scr, scrambled shRNA.

c. HR analysis. PARP1 knockdown cells were infected with I-SceI-expressing lentivirus and the percent GFP+ cells was analyzed by an unpaired two-tailed t test. n=3.

d. PARP1 knockdown cells were plated for clonogenic survival. Residual colonies from *BRCA2*$^{\Delta Ex3\text{-}4/-}$ plates were all were confirmed by PCR to have maintained the *BRCA2*$^{fl/-}$ genotype (i.e., escaped Cre recombination).

e. Cisplatin-induced γ H2AX. PARP1 knockdown cells were treated with 5 μM cisplatin for 5 h and released for another 24 h before analysis. γ H2AX mean nuclear intensities of >1000 individual cells are shown from one experiment, which is representative of three independent experiments, analyzed by a two-tailed Mann-Whitney test. The dotted red line indicates the median of *BRCA2* mutant cells treated with the scrambled shRNA exposed to cisplatin. A.U., arbitrary units. Box and whiskers show the 10th and 90th percentiles.

f. Western blotting of *BRCA2*$^{-/-}$*AAVS1*^{fl} cells stably expressing BRCA2 WT or BRCA2 SE.

g. DNA fiber analysis to quantify FP in the presence of HU. Median CldU/IdU tract length ratios are indicated (red bars), analyzed by a two-tailed Mann-Whitney test.

h. HR analysis, as in **c**. n>3.

i. Clonogenic survival analysis using an unpaired two-tailed t test. n=3.
j. Cisplatin-induced γ H2AX analysis, as in **e**. The dotted red line indicates the median of the *BRCA2*$^{-/-}$*AAVS1*$^{\Delta}$ cells exposed to cisplatin.
Error bars, s.d. ns, not significant; *, p<0.05; **, p<0.01; ***, p<0.001; ****, p<0.0001.

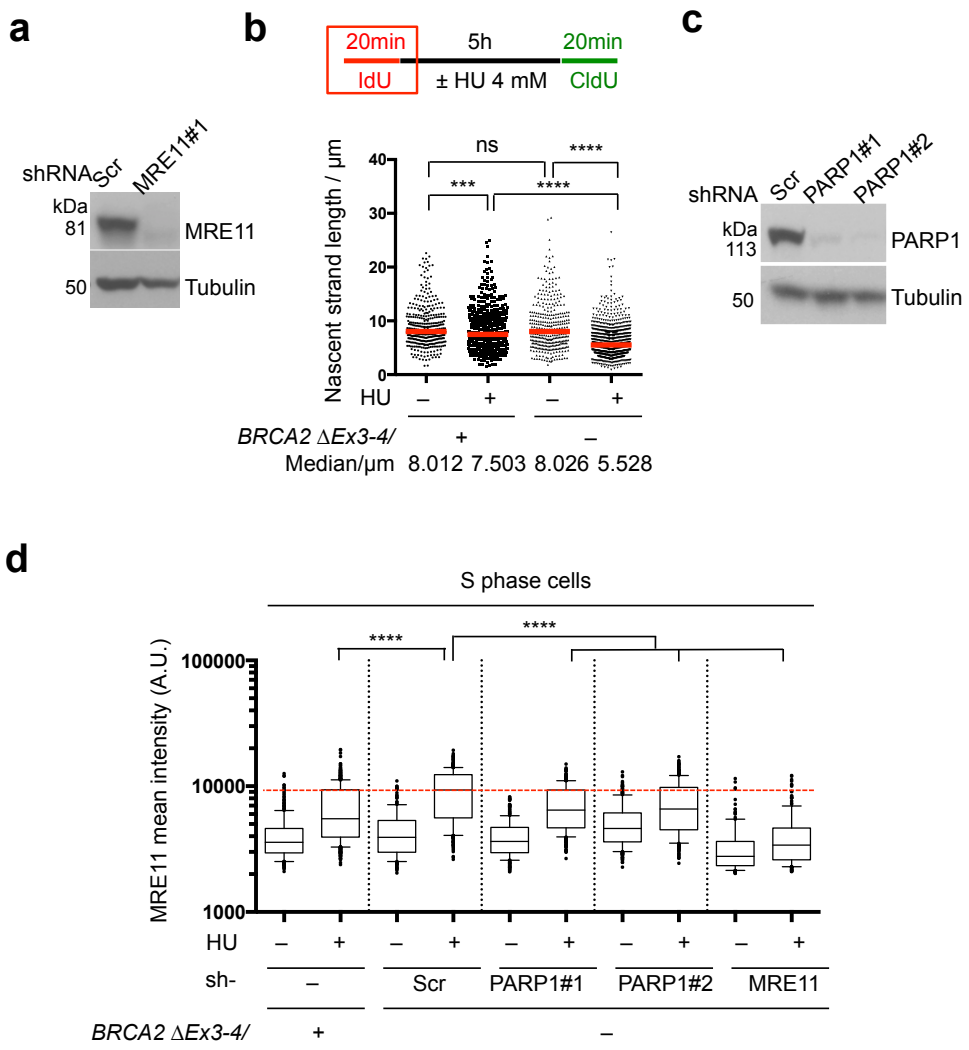

Figure 4-3. PARP1 mediates MRE11 chromatin recruitment upon replication stress
a. Western blot showing MRE11 knockdown (related to **Fig. 4-2b**).
b. DNA fiber analysis to quantify FP with or without HU treatment. A schematic of the experimental design is shown (top). IdU tract length was quantified to indicate nascent strand length. The median IdU tract lengths are indicated (red bars). Graphs represent the pooled results of >200 fibers per genotype from two independent experiments.
c. Western blot showing PARP1 knockdown (related to **Fig. 4-2b**).
d. MRE11 chromatin recruitment assay. PARP1 knockdown cells were either treated with EdU together with HU (4 mM) for 5 h or EdU alone for 1h before pre-extraction and analyzed for chromatin-bound MRE11. MRE11 mean nuclear intensities of EdU+ cells are shown from one experiment, which is representative of two independent experiments. The dotted red line indicates the median of the *BRCA2* mutant cells treated with the scrambled shRNA exposed to HU. Box and whiskers show the 10th and 90th percentiles. ns, not significant; ***, p<0.001; ****, p<0.0001 (two-tailed Mann-Whitney test).

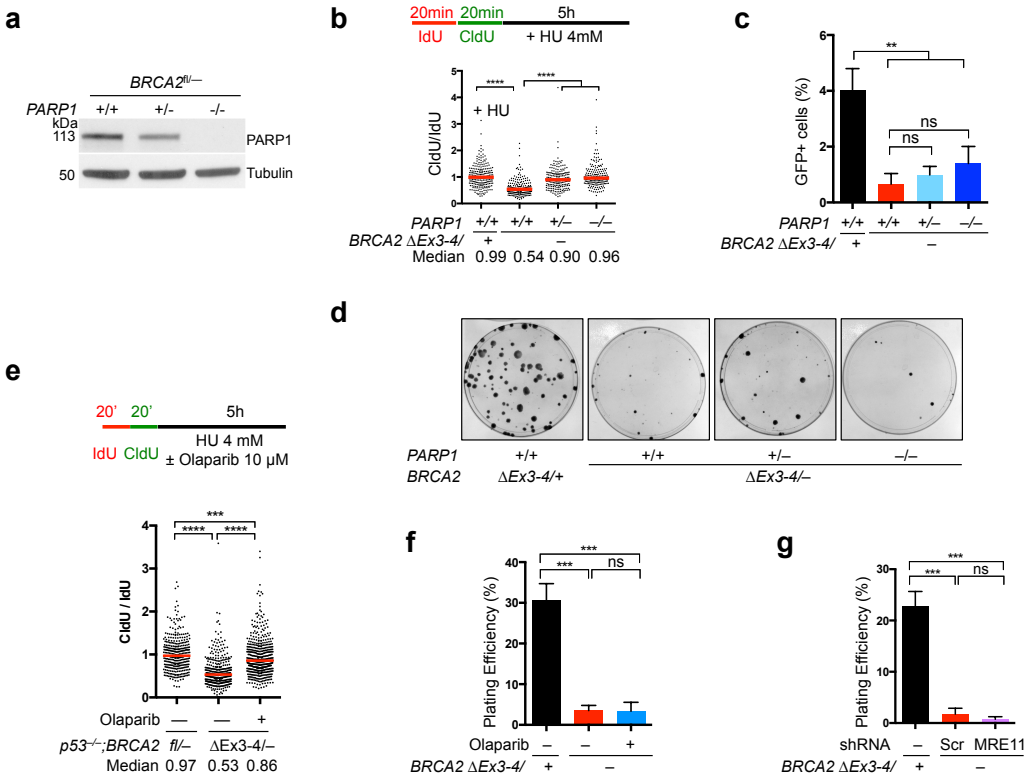

Figure 4-4. FP is not sufficient to support cell viability
a. Western blot showing PARP1 protein levels in indicated cells.
b. DNA fiber analysis to quantify FP in the presence of HU. Median CldU/IdU tract length ratios are indicated in the graph (red bars). Graphs represent the pooled results of >200 fibers per genotype from two independent experiments, analyzed by a two-tailed Mann-Whitney test.
c. HR analysis. Cells were infected with I-SceI-expressing lentivirus and the percent GFP+ cells was analyzed by an unpaired two-tailed t test. n=3.
d. Clonogenic survival. More than 40 of the residual colonies from each of the *BRCA2*$^{\Delta Ex3\text{-}4/-}$ plates were picked, and all were confirmed by PCR to have maintained the *BRCA2*$^{fl/-}$ genotype (i.e., escaped Cre recombination; primer design in **Fig. 3-7a**).
e. DNA fiber analysis. *BRCA2*$^{fl/-}$ *p53*$^{-/-}$ and *BRCA2*$^{\Delta Ex3\text{-}4/-}$ *p53*$^{-/-}$ cells (derived from pre- and post-Cre colonies from **Fig. 3-4g**, respectively) were analyzed for FP in the presence of HU, and in the latter case olaparib, as shown in the schematic above. Median CldU/IdU tract length ratios are indicated in the graph (red bars). Graphs represent the pooled results of >300 fibers per sample from three independent experiments, analyzed by a two-tailed Mann-Whitney test.
f. Cells were treated without or with olaparib (10 μM, 3 h) prior to Cre expression and then were plated for clonogenic survival, analyzed by an unpaired two-tailed t test. n=3.
g. Clonogenic survival analysis using an unpaired two-tailed t test. n=3.
Error bars, s.d. ns, not significant; **, p<0.01; ***, p<0.001; ****, p<0.0001.

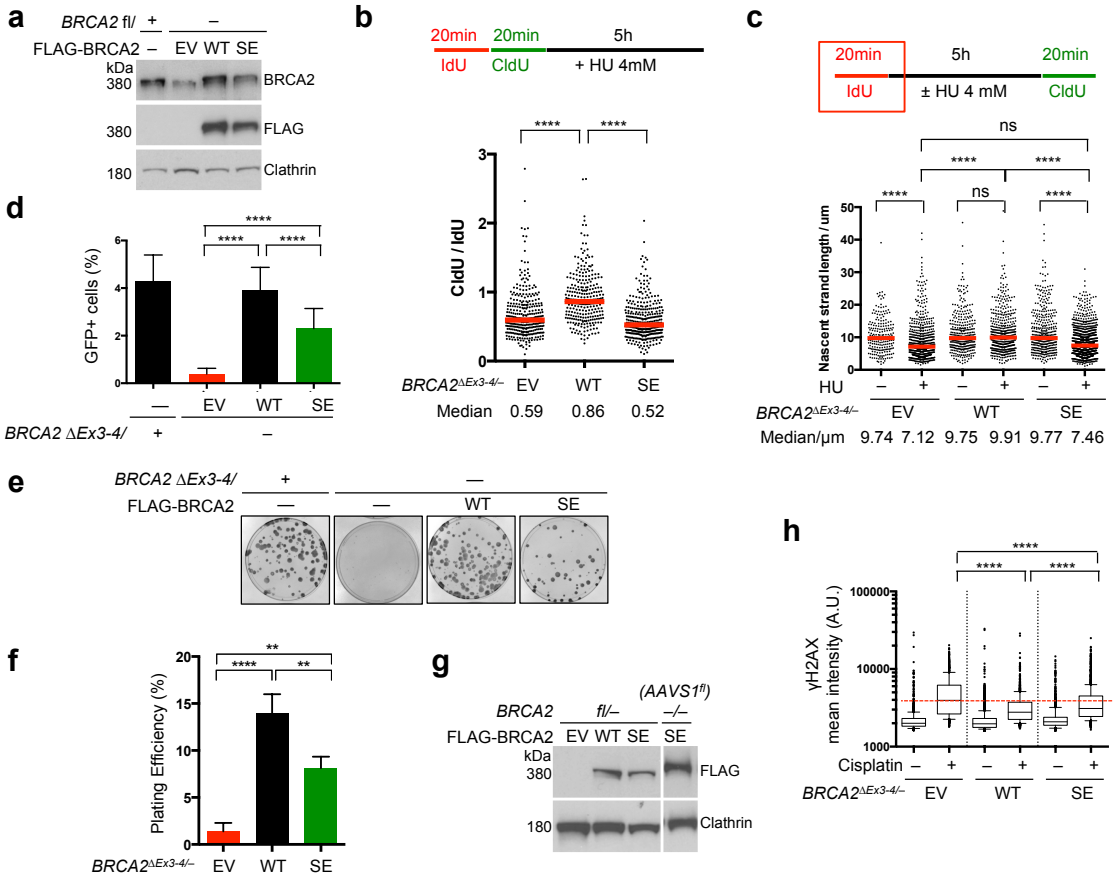

Figure 4-5. FP is not essential for cell viability or DNA repair

a. BRCA2 Western blot for *BRCA2*$^{fl/–}$ cells stably expressing FLAG-tagged BRCA2 WT or BRCA2 SE, and *BRCA2*$^{fl/+}$ cells as a control for endogenous BRCA2 protein level.

b,c. DNA fiber analysis of cells treated as shown at top to quantify FP. Median CldU/IdU tract length ratios (**b**) or IdU tract lengths (**c**) are indicated in the graph (red bars). Graphs represent the pooled results of >200 fibers per sample from at least two independent experiments, analyzed by a two-tailed Mann-Whitney test.

d. HR analysis. Cells were infected with I-SceI-expressing lentivirus and the percent GFP+ cells was analyzed by an unpaired two-tailed t test. n>3.

e, f. Clonogenic survival. Representative plates (**e**) and quantification of plating efficiency (**f**) are shown, analyzed by an unpaired two-tailed t test. n=4.

g. Western blot to compare stably transfected FLAG-tagged BRCA2 transgene expression in *BRCA2*$^{fl/–}$ and *BRCA2*$^{–/–}$*AAVS1*^{fl} cells. Note the BRCA2 SE expression is higher in the *AAVS1*^{fl} system than in the *BRCA2*$^{fl/–}$ system.

h. Cisplatin-induced γH2AX. Cells were treated with 5 μM cisplatin for 5 h and released for another 24 h before analysis. γH2AX mean nuclear intensities of >1000 individual cells are shown from one experiment, which is representative of two independent experiments, analyzed by a two-tailed Mann-Whitney test. Box and whiskers show the 10th and 90th percentiles. The dotted red line indicates the median of the *BRCA2*$^{ΔEx3-4/–}$ cells exposed to cisplatin.

Error bars, s.d. ns, not significant; **, p<0.01; ****, p<0.0001.

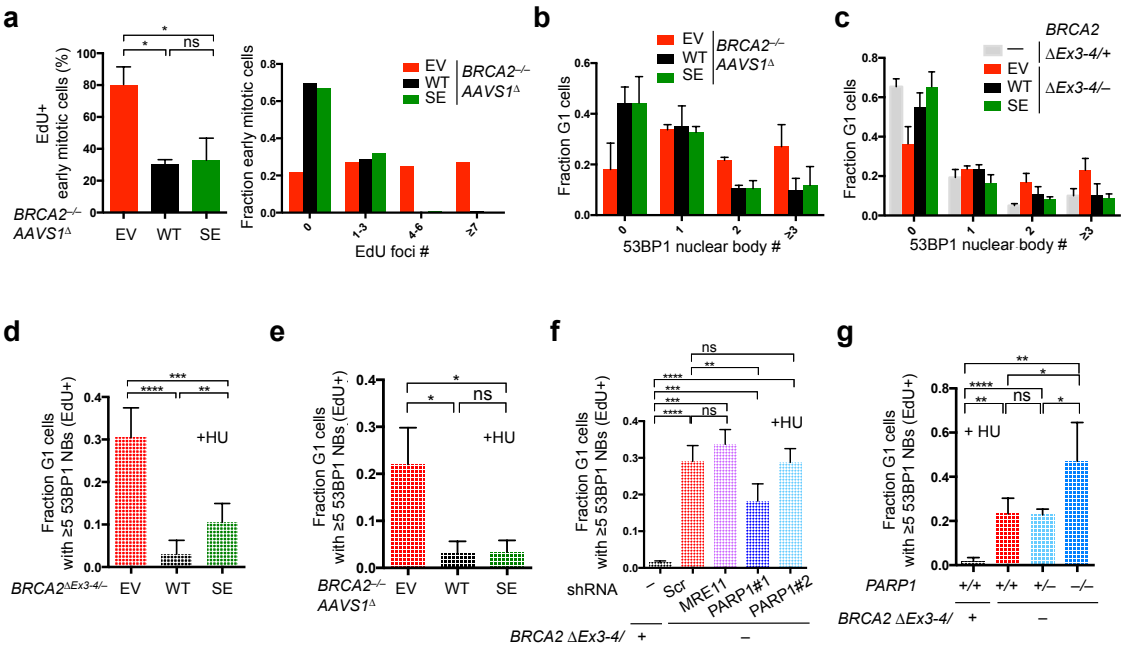

Figure 4-6. FP is a minor replication stress suppression pathway

a. Analysis of mitotic DNA synthesis in *BRCA2*$^{-/-}$*AAVS1*$^{\Delta}$ cells complemented by BRCA2 WT or BRCA2 SE. Cells were released for 22 h from serum starvation to increase mitotic cells, incubated with EdU 1 h, and then analyzed for mitotic DNA synthesis. Early mitotic cells, defined as being in prophase, prometaphase, or metaphase, were analyzed for EdU foci that colocalize with FANCD2 foci pairs. The percent early mitotic cells containing EdU foci (left, n=3) or EdU foci distribution in these cells (right, pooled results of three independent experiments) was quantified.

b, c. Spontaneous 53BP1 NB analysis in G1 in both *BRCA2*$^{\Delta Ex3\text{-}4/-}$ cells **(b)** and *BRCA2*$^{-/-}$*AAVS1*$^{\Delta}$ cells **(c)** complemented by BRCA2 WT or BRCA2 SE. n≥3.

d-g. HU-induced 53BP1 NB formation analysis, as in **Figure 3-8d,** using complemented *BRCA2*$^{\Delta Ex3\text{-}4/-}$ cells (**d**) or *BRCA2*$^{-/-}$ *AAVS1*$^{\Delta}$ cells (**e**), stable MRE11 or PARP1 knockdown *BRCA2*$^{\Delta Ex3\text{-}4/-}$ cells (**f**), and *BRCA2*$^{\Delta Ex3\text{-}4/-}$ cells with the indicated *PARP1* genotype (**g**). n≥3.

Error bars, s.d. ns, not significant; *, p<0.05; **, p<0.01; ***, p<0.001; ****, p<0.0001 (unpaired two-tailed t test).

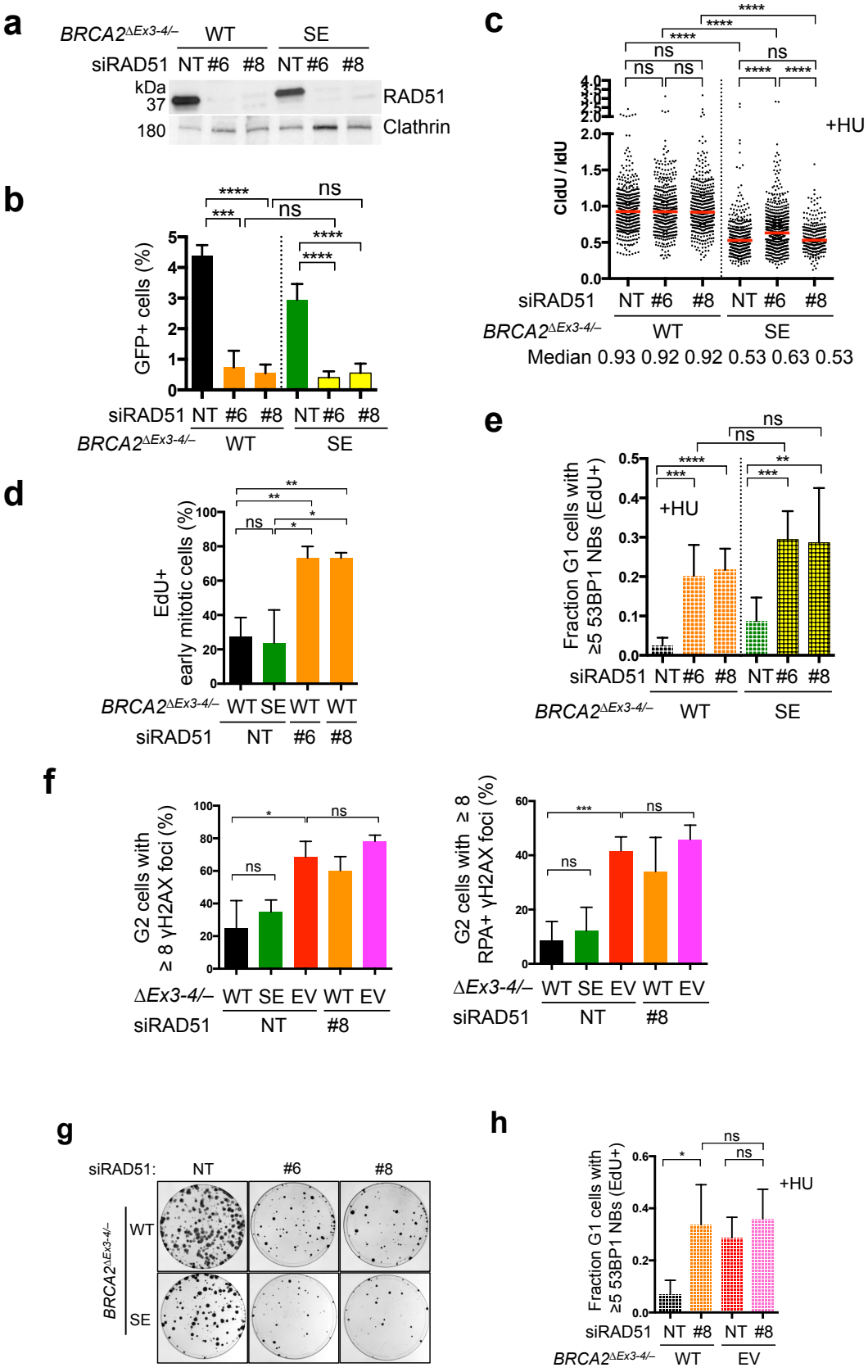
a
BRCA2ΔEx3-4/–
WT
SE
siRAD51 NT #6 #8 NT #6 #8
kDa
37
180
RAD51
Clathrin
b
GFP+ cells (%)
siRAD51 NT #6 #8 NT #6 #8
BRCA2ΔEx3-4/– WT SE
c
CldU / IdU
+HU
siRAD51 NT #6 #8 NT #6 #8
BRCA2ΔEx3-4/– WT SE
Median 0.93 0.92 0.92 0.53 0.63 0.53
d
EdU+ early mitotic cells (%)
BRCA2ΔEx3-4/– WT SE WT WT
siRAD51 NT #6 #8
e
Fraction G1 cells with ≥5 53BP1 NBs (EdU+)
+HU
siRAD51 NT #6 #8 NT #6 #8
BRCA2ΔEx3-4/– WT SE
f
G2 cells with ≥ 8 γH2AX foci (%)
ΔEx3-4/– WT SE EV WT EV
siRAD51 NT #8
G2 cells with ≥ 8 RPA+ γH2AX foci (%)
ΔEx3-4/– WT SE EV WT EV
siRAD51 NT #8
g
siRAD51: NT #6 #8
BRCA2ΔEx3-4/–
WT
SE
h
Fraction G1 cells with ≥5 53BP1 NBs (EdU+)
+HU
siRAD51 NT #8 NT #8
BRCA2ΔEx3-4/– WT EV

Figure 4-7. HR proficiency is associated with replication stress suppression and cell viability

a. Western blot showing RAD51 knockdown in *BRCA2*$^{\Delta Ex3\text{-}4/-}$ cells stably expressing BRCA2 WT or BRCA2 SE. NT, non targeting siRNA.

b. HR analysis. Cells expressing RAD51 siRNAs were infected with I-SceI-expressing lentivirus and the percent GFP+ cells was analyzed by an unpaired two-tailed t test. n≥3.

c. Cells expressing RAD51 siRNAs were analyzed for FP in the presence of HU. Median CldU/IdU tract length ratios are indicated in the graph (red bars). Graphs represent the pooled results of >300 fibers per genotype from at least three independent experiments, analyzed by a two-tailed Mann-Whitney test.

d. Cells expressing RAD51 siRNAs were released for 22 h from serum starvation to increase mitotic cells, incubated with EdU 1 h, and then analyzed for mitotic DNA synthesis. Early mitotic cells, defined as being in prophase, prometaphase, or metaphase, were analyzed for EdU foci that colocalize with FANCD2 foci pairs. The percent early mitotic cells containing EdU foci were analyzed by an unpaired two-tailed t test. n=3.

e. HU-induced 53BP1 NB formation analysis, as in **Figure 3-8d**, using cells expressing RAD51 siRNAs. Statistical analysis was by an unpaired two-tailed t test. n≥4.

f. Cells treated with the indicated RAD51 siRNA were incubated with EdU for 30 min and then analyzed for γH2AX and RPA foci in G2 cells (EdU–, 2N DNA content). Quantification of γH2AX foci (left) and RPA+ γ H2AX foci (right) are shown. n≥3.

g. RAD51 depletion in *BRCA2*$^{\Delta Ex3\text{-}4/-}$ cells stably expressing BRCA2 WT or BRCA2 SE leads to a reduction in clonogenic survival.

h. HU-induced 53BP1 NB formation analysis, as in **Figure 3-8d**, using cells transfected with RAD51 siRNAs. Statistical analysis was by an unpaired two-tailed t test. n=4.

Error bars, s.d. ns, not significant; *, p<0.05; **, p<0.01; ***, p<0.001; ****, p<0.0001.

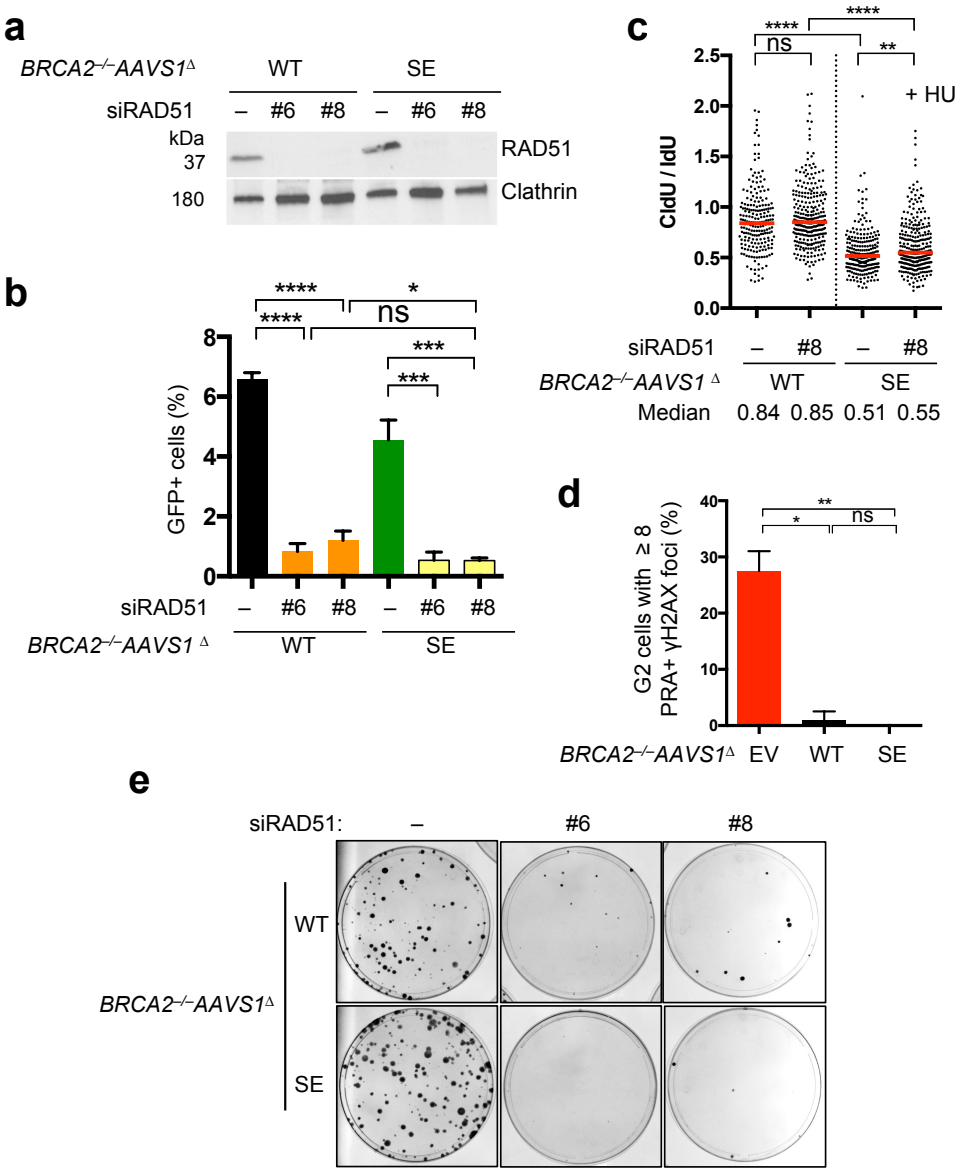

Figure 4-8. HR is critical for cell viability and limiting G2 DNA damage
a. Western blot showing RAD51 knockdown in *BRCA2*$^{-/-}$*AAVS1*$^{\Delta}$ cells stably expressing BRCA2 WT or BRCA2 SE.
b. HR analysis. Cells expressing RAD51 siRNAs were infected with I-SceI-expressing lentivirus and the percent GFP+ cells was analyzed by an unpaired two-tailed t test. n=3. Error bars, s.d.
c. Cells expressing RAD51 siRNAs were analyzed for FP in the presence of HU. Median CldU/IdU tract length ratios are indicated in the graph (red bars). Graphs represent the pooled results of > 200 fibers per genotype from two independent experiments, analyzed by a two-tailed Mann-Whitney test.
d. BRCA2–/–AAVS1$^{\Delta}$ cells complemented with BRCA2 expression vectors were incubated with EdU for 30 min before quantification of RPA+ γH2AX foci in G2 cells (EdU–, 2N DNA content) cells, analyzed by an unpaired two-tailed t test. n=2. Error bars, s.d.

e. RAD51 depletion in *BRCA2*$^{-/-}$*AAVS1*$^{\Delta}$ cells stably expressing BRCA2 WT or BRCA2 SE leads to a severe reduction in clonogenic survival.
ns, not significant; *, p<0.05; **, p<0.01; ***, p<0.001; ****, p<0.0001.

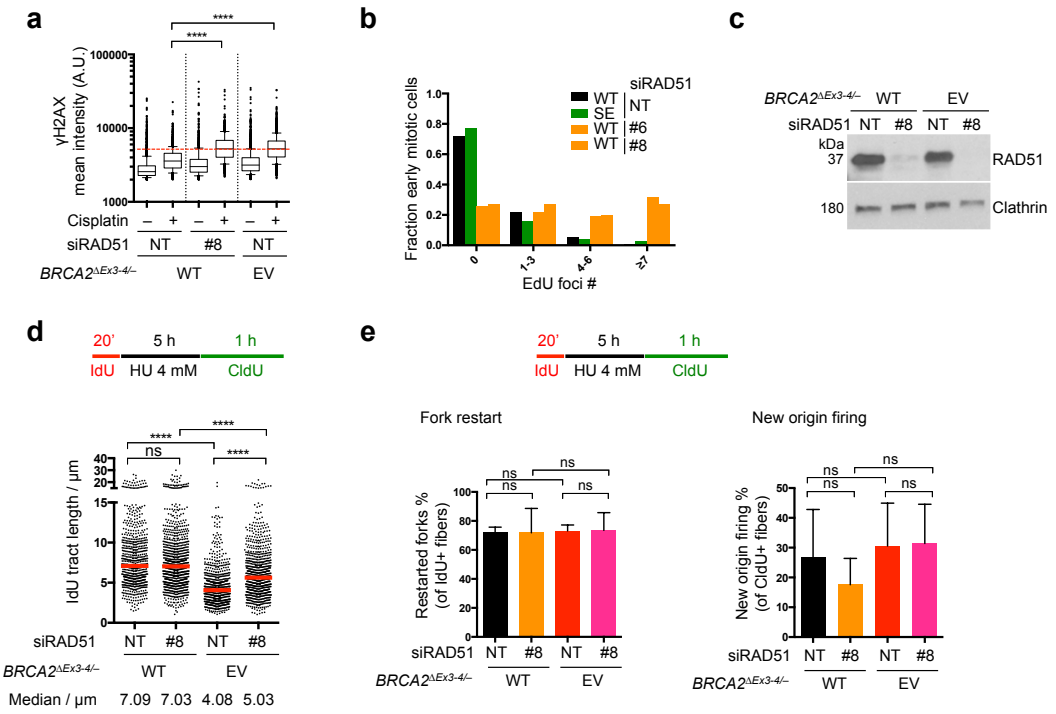

Figure 4-9. Effects of RAD51 depletion on BRCA2-deficient cells

a. Cisplatin-induced γH2AX. Cells were treated with 5 µM cisplatin for 5 h and released for another 24 h before analysis. γH2AX mean nuclear intensities of >1000 individual cells are shown from one experiment, which is representative of three independent experiments, analyzed by a two-tailed Mann-Whitney test. Box and whiskers show the 10th and 90th percentiles. The dotted red line indicates the median of the NT (non targeting) siRNA-treated, EV-transfected *BRCA2*$^{\Delta Ex3\text{-}4/-}$ cells exposed to cisplatin.

b. EdU foci distribution of samples from **Fig. 4-7d** (pooled results of three independent experiments).

c. Western blots showing RAD51 knockdown in indicated cells.

d. DNA fiber analysis to quantify FP with HU treatment. A schematic of the experimental design is shown (top). Median IdU tract lengths are indicated in the graph (red bars). Graphs represent the pooled results of > 600 fibers per genotype from four independent experiments, analyzed by a two-tailed Mann-Whitney test.

e. DNA fiber analysis to quantify fork restart with HU treatment. A schematic of the experimental design is shown (top). Frequency quantifications of restarted forks (lower left) and newly fired origins (lower right) are shown, analyzed by an unpaired two-tailed t test. n=4. Error bars, s.d.

ns, not significant; ****, p<0.0001.

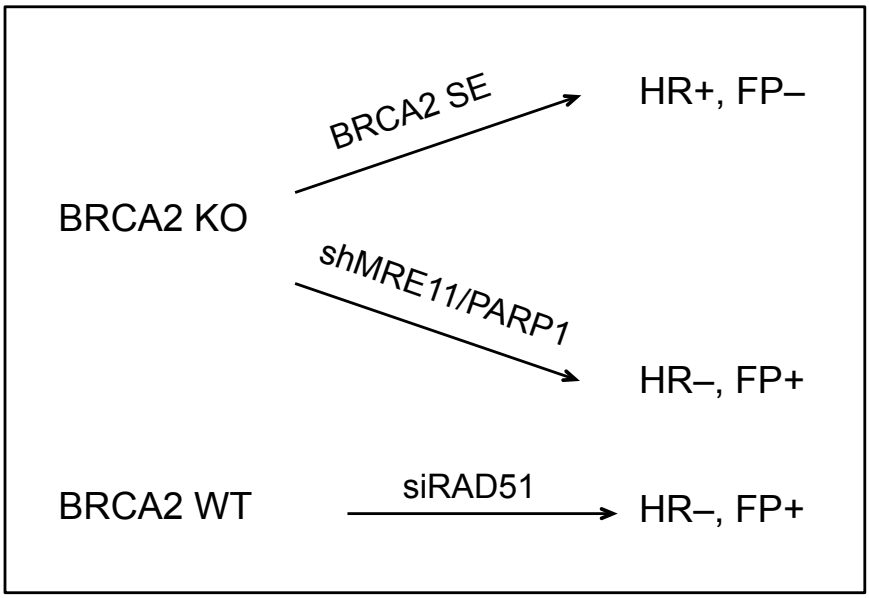

Figure 4-10. Separation-of-function systems to study HR and FP functions. Summarization of the three separation-of-function systems to dissect the individual contributions of HR and FP pathways generated in this chapter.

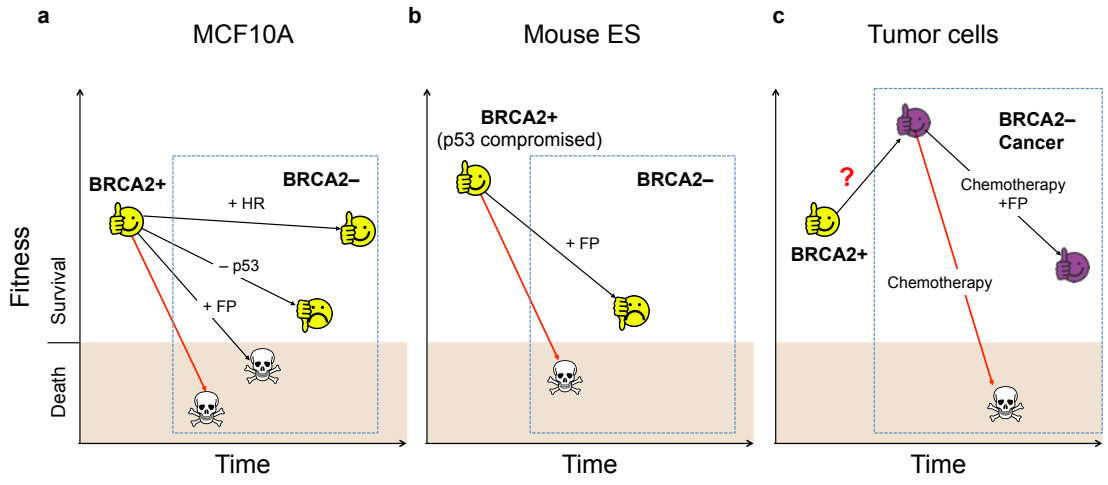

Figure 4-11. Context-dependent requirement for HR versus FP for cell survival. Differential requirements for HR and FP are observed to reach the threshold of cell viability in different contexts of BRCA2 deficiency, as highlighted in the dashed blue boxes. BRCA2 loss alone (untreated or with chemotherapy) (red arrows) is shown as a baseline for comparison to BRCA2 loss with the indicated additional genetic alterations (black arrows).
a. Nontransformed mammary epithelial cells MCF10A do not survive BRCA2 loss. Restoration of HR, but not FP, re-establishes cell viability. p53 loss fails to suppress apoptosis and only partially rescues cell proliferation.
b. In mouse ES cells, FP restoration is sufficient to rescue cell survival after BRCA2 loss. These cells may have a higher tolerance to DNA damage than MCF10A cells due to a compromised p53 response.
c. In BRCA2-deficient tumor cells, FP is also sufficient to overcome the viability threshold to confer chemoresistance. Presumably, these cells have evolved to survive BRCA2 loss and aberrantly proliferate (purple face) and thus may have a higher tolerance to DNA damage.

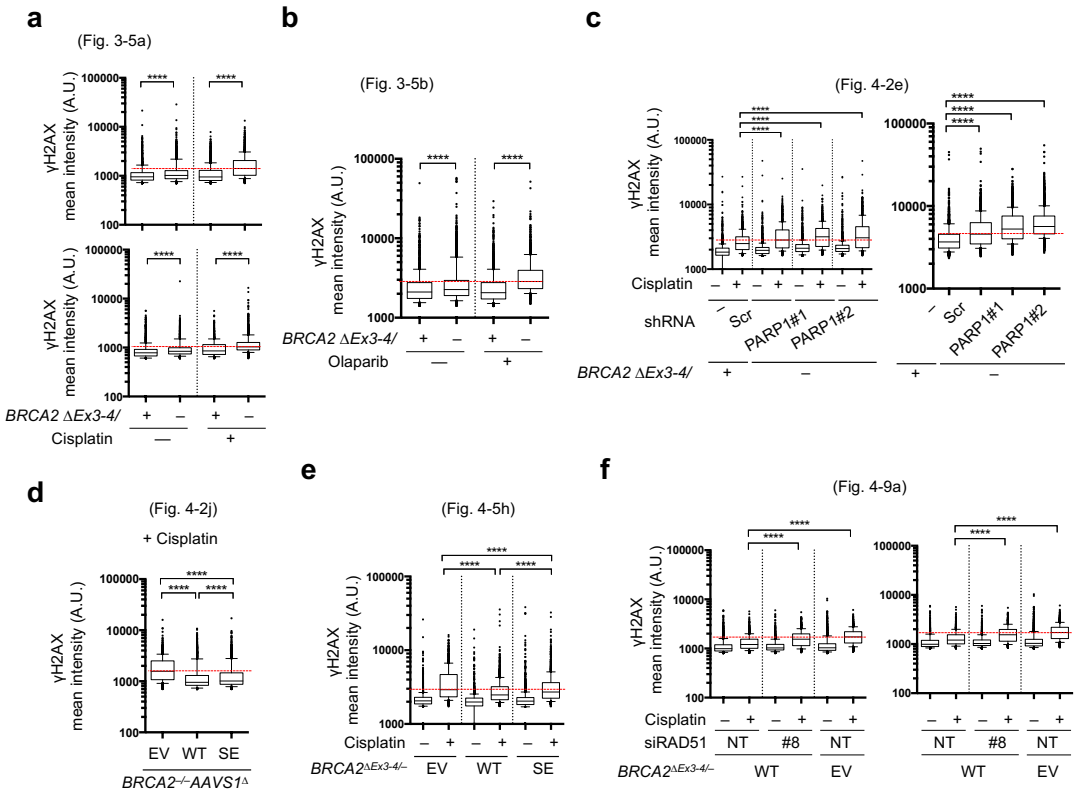

Figure 4-12. γH2AX intensity replicates for the indicated figures

Chapter 5 53BP1 nuclear body-marked replication stress in a human mammary cell model of BRCA2 deficiency

5.1 Introduction

While sharing many key players, including BRCA2, HR and FP are both genetically and functionally separable processes (Feng and Jasin 2018). Our mechanistic understanding of FP has recently advanced by the discovery of the role of replication fork reversal, where a fork regresses to form a four-way “chicken foot”-like structure (Neelsen and Lopes 2015) (reviewed in chapter 1). In a FP-deficient background, reversed forks serve as the substrate for subsequent nascent strand degradation by nucleases (Kolinjivadi et al. 2017; Lemacon et al. 2017; Mijic et al. 2017; Taglialatela et al. 2017). An HR defect in *BRCA1/2*-mutated cancers was initially leveraged to develop synthetic-lethality-based therapeutic strategies, while subsequent restoration of HR and/or possibly FP in tumors confers resistance (Chen et al. 2018). The relative contribution of HR, FP, and now fork reversal to genome integrity is complex and may be contingent upon the cellular context (Feng and Jasin 2018).

Modeling BRCA2 deficiency in a non-transformed background may provide insight into the early events that initiate *BRCA2*-mutated breast cancer formation. To this end, we recently leveraged the CRISPR (Clustered Regularly Interspaced Short Palindromic Repeats)-Cas9 tools to generate two *BRCA2* conditional models in MCF10A cells (Feng and Jasin 2017), a non-transformed human mammary epithelial cell line (Soule et al. 1990). In the process, we also developed a CRISPR-Cas9-based approach for allele-specific gene targeting at the *BRCA2* locus.

With these *BRCA2* conditional models, we demonstrated that BRCA2 deficiency leads to replication stress and DNA under replication that in turn causes abnormalities during mitosis and 53BP1 NB formation in the subsequent G1 phase, accompanied by a p53-mediated G1 arrest and ultimately cell lethality (Feng and Jasin 2017). In dissecting the relative contribution of the HR and FP pathways, we provided evidence that cell viability and replication stress suppression are mainly mediated by the HR function of BRCA2, but not FP, in these non-transformed human mammary epithelial cells (Feng and Jasin 2017). Here, we further explore the consequences of BRCA2 deficiency, with a focus on 53BP1 NBs, in particular their possible upstream triggers and downstream link with p53 activation. The role of the fork reversal protein SMARCAL1 and its functional interaction with BRCA2 is also examined.

5.2 Results and discussion

5.2.1 Allele-specific editing of the *BRCA2* locus

While generating the two BRCA2 conditional models in MCF10A cells (Feng and Jasin 2017), CRISPR-Cas9-facilitated gene targeting was employed to achieve the desired editing outcome. One of the *BRCA2* conditional systems we described involved first targeting two loxP sites to flank exons 3 and 4 of one allele (*fl)*; the remaining *WT* allele was targeted using a promoterless selectable marker inserted at the *BRCA2* start codon (Hyg-targeted) **(Fig. 5-1**) (Feng and Jasin 2017). However, the start codon resides in exon 2, which is present in both the *fl* and *WT* alleles. Therefore, one technical challenge we anticipated was to specifically target the *WT* allele with the Hyg-targeting vector, while leaving exon 2 of the *fl* allele intact (**Fig. 5-2a**).

To this end, we developed a method to achieve allele-specific targeting, which we benchmarked in *BRCA2*$^{+/+}$ cells to demonstrate its generality. We first sequenced the

BRCA2 exon 2 region and identified a single nucleotide polymorphism (SNP). The sgRNA was then designed specifically for the allele containing the G nucleotide SNP ("G allele") residing towards the 3' end of the sgRNA sequence (**Fig. 5-2a**), i.e., the seed region of the sgRNA that is sensitive to mismatches (Fu et al. 2013; Hsu et al. 2013; Pattanayak et al. 2013). The post-transfection clones showing Hyg resistance were screened by a PCR specific for the Hyg cassette correctly integrated at the *BRCA2* locus (**Fig. 5-2b**). To characterize the other allele in the positive clones, PCR was performed with a reverse primer specific to an untargeted *BRCA2* allele. All clones tested exhibited a positive PCR product, indicating monoallelic gene targeting with the Hyg cassette (**Fig. 5-2b**). Sequencing of these PCR products revealed a strong bias (95.2%, 19/20) towards the allele with the A nucleotide SNP ("A allele"), such that Hyg targeting predominantly occurred at the G allele (**Fig. 5-2c,d**). Therefore, polymorphism of even a single nucleotide at the sgRNA site can strongly bias targeting towards one specific allele. We then applied this strategy to our *BRCA2*$^{fl/+}$ cells, in this case targeting the A allele with the Hyg cassette using an A allele-specific sgRNA, as the prior *fl* targeting turned out to occur to the G allele (**Fig. 5-1**).

Achieving allele discrimination provides advantages for a variety of applications. For example, selectively disrupting or correcting dominant disease-causing alleles has potential clinical value. Accomplishing allele discrimination can also benefit basic research, such as achieving allele-specific imaging or studying one particular allele of interest, e.g. the maternal vs. the paternal allele. While alleles can be effectively distinguished via CRISPR approaches in cases where a unique PAM is present in one allele (Shin et al. 2016; Maass et al. 2018), discrimination between alleles with single nucleotide mismatches within the sgRNA site is conceptually challenging given the promiscuity of sgRNA recognition (Fu et al. 2013; Hsu et al. 2013; Pattanayak et al. 2013). In this regard, previous studies have shown promise in utilizing SNPs in the

sgRNA target regions to achieve allele-specific mutagenesis (Yoshimi et al. 2014; Smith et al. 2015; Burnight et al. 2017; Gao et al. 2018; Pingjuan et al. 2018). Our results now extend allele-specific applications to HR-mediated gene targeting. Notably, allele selectivity can be further improved with a truncated sgRNA design (Pingjuan et al. 2018), since it displays an even lower tolerance to mismatches (Fu et al. 2014). These efforts have substantially broadened the scope of allele-specific applications to achieve various desired outcomes.

5.2.2 Replication stress-vulnerable sites in BRCA2-deficient cells

One previously unappreciated consequence of BRCA2 deficiency recently uncovered by others and us is the manifestation of S/G2 repair defects in later cell cycle stages, resulting in 53BP1 NB formation in the subsequent G1 phase (Feng and Jasin 2017; Lai et al. 2017). What remains mysterious is the source of the replication stress. Understanding how 53BP1 NBs are formed is key to addressing this question.

53BP1 NBs were initially reported to mark common fragile sites (CFSs). Treatment with low-dose aphidicolin (APH) is a commonly used method to specifically induce CFS instability (Durkin and Glover 2007). It acts by perturbing DNA replication (polymerase α) without substantially affecting cell cycle progression, leading to breakage at the fragile sites in mitosis, termed CFS expression. The same treatment was found to massively stimulate formation of 53BP1 NBs at CFSs (Harrigan et al. 2011; Lukas et al. 2011). By contrast, high doses of another replication inhibitor, hydroxyurea (HU), which does not display CFS selectivity, presumably due to a different a mode of action (in part, nucleotide pool depletion) (Durkin and Glover 2007), fails to induce 53BP1 NBs (Harrigan et al. 2011). Thus, in genetically unmodified cells, 53BP1 NB formation appears to be associated with CFS expression.

To explore the sources of 53BP1 NBs arising from BRCA2 deficiency, we first benchmarked how control MCF10A cells respond to different replication stresses induced by APH and HU. BRCA2-proficient cells displayed ≥5-fold increase in these NBs with low doses of APH (**Fig. 5-3a**), consistent with a recent report (Arora et al. 2017). 53BP1 NBs were somewhat increased with HU treatment (Feng and Jasin 2017), but the level did not reach that seen with APH and this trend was not statistically significant (**Fig. 5-3b**). These results are consistent with previous findings (Harrigan et al. 2011), showing that conditions that induce CFS expression (low-dose APH) lead to 53BP1 NB formation, while HU exerts a minimal response at the dosage used.

Notably, upon BRCA2 disruption, the level of 53BP1 NBs was further elevated not only by HU (Feng and Jasin 2017), but also by APH (**Fig. 5-3**). Interestingly, BRCA2-deficient cells displayed a level of spontaneous 53BP1 NBs that was comparable to that of BRCA2-proficient cells treated with low-dose APH (**Fig. 5-3a**), which provides an estimation of the level of spontaneous replication stress in these BRCA2-disrupted cells. Thus, BRCA2 suppresses replication stress that perturbs CFSs as well as other genomic sequences. This stress in turn leads to 53BP1 NB formation when BRCA2 function is compromised.

We have previously shown that HU-induced replication stress is relieved by the HR function of BRCA2 (Feng and Jasin 2017). Thus, HR disruption leads to fragility of genomic regions with distinct properties from those of CFSs upon HU. These properties are reminiscent of the recently discovered early replication fragile sites (ERFSs), which are characterized as regions bound by a set of DNA repair proteins, including the HR protein BRCA1, and prone to breakage in response to HU but not low-dose APH (Barlow et al. 2013). Since BRCA2-deficient cells display a high level of replication stress under both HU and low-dose APH treatment, multiple processes likely contribute to the replication stress seen in these cells. For example, BRCA2 prevents R-loop

accumulation (Bhatia et al. 2014; Tan et al. 2017) and maintains the integrity of telomeres (Badie et al. 2010) and G-quadruplex-forming sites (Zimmer et al. 2016). Presumably these regions are more susceptible to replication stress and become fragile upon BRCA2 loss. It would be interesting for future studies to determine the full set of genomic regions that are particularly unstable upon BRCA2 deficiency and uncover the mechanism(s) of DNA fragility.

5.2.3 Link between 53BP1 NBs and p53 activation

53BP1 NBs form in G1, the cell cycle stage at which BRCA2-deficient cells arrest due to p53 activation (Feng and Jasin 2017). To further characterize the link between 53BP1 NBs and p53 activation in BRCA2-deficient cells, we performed image analysis to determine whether the two proteins colocalize. Indeed, a substantial fraction (~60%) of 53BP1 NBs contained p53 and its active, phosphorylated form, p53-pS15 (**Fig. 5-4a,b,d,e**). This colocalization occurred irrespective of BRCA2 status, although we observed a slight, but reproducible increase in the frequency of NBs with p53 signals in BRCA2-deficient cells (**Fig. 5-4b,e**), possibly reflecting a positive feedback regulation of p53 levels in stressed conditions (Harris and Levine 2005). However, as a consequence of increased NB abundance, BRCA2 deficiency led to a marked elevation of both p53- and p53-pS15-positive 53BP1 NBs in G1 phase (**Fig. 5-4c,f**). Indeed, BRCA2 disruption is accompanied with an increase in spontaneous p53 levels in various systems (Patel et al. 1998; Carlos et al. 2013; Feng and Jasin 2017). Importantly, p53 disruption did not affect 53BP1 NB formation (**Fig. 5-4g**), suggesting that p53 functions downstream of the DNA lesions marked by 53BP1. Together, these results establish that 53BP1 NBs are spatially linked to p53 activation.

53BP1 NBs could activate p53 at multiple levels (Feng and Jasin 2018), either directly through 53BP1-p53 interaction (Iwabuchi et al. 1994) or indirectly through the

downstream DNA damage response. The underlying DNA lesions within the NBs may serve to activate signaling networks, including the p53 pathway. Indeed, 53BP1 NBs contain various components involved in the DNA damage response, including the master regulator ATM in its activated, phosphorylated form (pATM S1981) (Lukas et al. 2011), which directly stabilizes and activates p53 (Shiloh and Ziv 2013). Together, our results are consistent with a model that these nuclear compartments marked by 53BP1 serve as a signaling hub to recruit and activate p53. However, so far their relationship remains correlative and additional studies are needed to determine whether the relationship is causal and, if so, what are the mechanisms.

In addition to p53 activation, 53BP1 NBs may play other roles in BRCA2-deficient cells. For example, 53BP1 NBs sequester and shield the underlying sites of DNA damage (Lukas et al. 2011). In the setting of CFS expression, removing 53BP1 enhances DNA break manifestation (Lukas et al. 2011). Thus, perturbing 53BP1 in BRCA2-deficient cells may similarly aggravate DNA break deprotection and thereby synergistically exacerbate genome instability phenotypes. This hypothesis, if found to be true, could potentially be exploited to develop novel synthetic lethal therapies for BRCA2-deficient cancers.

5.2.4 Functional interplay between SMARCAL1 and BRCA2

Having uncovered some unusual aspects of BRCA2 deficiency, our BRCA2 conditional systems also afford the opportunity to dissect the contribution of two pathways, HR and FP. To this end, we developed multiple separation-of-function approaches to specifically perturb one pathway while keeping the other intact. These approaches converge on the conclusion that HR, rather than FP, plays the critical role in suppressing replication stress to support MCF10A cell survival (Feng and Jasin 2017).

Replication fork reversal has emerged as a new aspect in dictating the outcome of FP versus fork degradation, with multiple studies suggesting that forks that have not reversed will not be degraded (Quinet et al. 2017; Feng and Jasin 2018). We therefore examined the impact of fork reversal on replication stress by depleting SMARCAL1, a DNA translocase known to exhibit fork reversion activity (Betous et al. 2012; Betous et al. 2013; Couch et al. 2013). In BRCA2-deficient cells, SMARCAL1 inactivation suppressed fork degradation (**Fig. 5-5a**), consistent with recent observations (Kolinjivadi et al. 2017; Taglialatela et al. 2017) and the model that fork reversal acts as a prerequisite for nascent strand degradation (**Fig. 5-5b**). While FP was rescued, 53BP1 NBs were not significantly reduced in HU-treated BRCA2-deficient cells by SMARCAL1 depletion (**Fig. 5-5c**). Supporting these observations, inactivating ZRANB3, another DNA translocase that catalyzes fork reversal, also fails to abolish HU-induced chromosomal aberrations in BRCA2-deficient cells (Mijic et al. 2017). These results further corroborate our previous conclusions that FP is not critical for replication stress suppression.

These data recapitulate previous results that SMARCAL1-mediated fork reversal plays a critical role in promoting nascent strand degradation upon replication stress (Kolinjivadi et al. 2017; Taglialatela et al. 2017), adding to the expanding recent literature that implicates this process in the pathways involved in FP suppression (Feng and Jasin 2018). FP restoration achieved by SMARCAL1 inactivation also represents an additional separation-of-function approach to study the contributions of the FP pathway in BRCA2- (and more generally HR-) deficient cells. The failure of FP to abolish the high replication stress found in BRCA2-deficient cells is in agreement with our previous findings obtained with orthogonal approaches (Feng and Jasin 2017). Thus, although FP alone suffices to restore genome integrity in HR-deficient cancer cells under various genotoxic stresses (Ray Chaudhuri et al. 2016), our results argue that FP plays a minor role in the relatively normal MCF10A cells. These apparent discrepancies could be due to distinct rate-

limiting stresses that occur under different cellular contexts, e.g., under cancerous versus non-transformed states (Feng and Jasin 2018). Future studies using additional non-transformed cell lines are needed to further validate this model.

Since fork reversal, either in excess or when limited, could cause DNA damage (Betous et al. 2012; Ciccia et al. 2012; Couch et al. 2013; Neelsen et al. 2013), we examined whether SMARCAL1 impacts replication stress in BRCA2 WT cells. Interestingly, SMARCAL1 depletion by itself led to a modest enhancement of HU-triggered 53BP1 NB formation (**Fig. 5-5c**). Given our previous findings that HR is critical to suppress replication stress (Feng and Jasin 2017), the observed induction in 53BP1 NBs is reminiscent of a role of SMARCAL1 in HR, as has been reported in the fly system (Holsclaw and Sekelsky 2017). To determine the HR function of SMARCAL1 in MCF10A cells, we employed the DR-GFP reporter that is stably integrated as a single copy to assay HR activity (Pierce et al. 1999; Kondrashova et al. 2017b) (**Fig. 5-5d**). Indeed, SMARCAL1 depletion led to a reduction in HR, although only to a moderate extent compared with that observed in cells depleted of the core HR component RAD51 (Moynahan and Jasin 2010) (**Fig. 5-5d**). Thus, SMARCAL1 depletion by itself exerts a small increase in 53BP1 NB formation that may be associated with its minor role in HR. We conclude that SMARCAL1 plays a minor role in suppressing replication stress when BRCA2 is present. In sum, our previous (Feng and Jasin 2017) and current results are all consistent with a model that HR plays a critical role in suppressing replication stress leading to 53BP1 NBs, whereas neither protection nor regression of replication forks substantially contributes to this process.

5.3 Concluding remarks

We have previously shown that BRCA2 suppresses DNA replication stress through HR (Feng and Jasin 2017). We have now expanded on these findings, investigating three

aspects of the replication stress triggered as a consequence of BRCA2 inactivation. First, we show that BRCA2-deficient cells are sensitized to two types of replication stress, those induced by HU and by low-dose APH. Second, 53BP1 NBs spatially link replication stress to downstream p53 activation in G1 phase. Finally, disrupting fork reversal by SMARCAL1 depletion ameliorates the FP defect in BRCA2-deficient cells, but does not restrain 53BP1 NB formation, further corroborating our previous model that FP plays a minor role in suppressing replication stress in MCF10A cells.

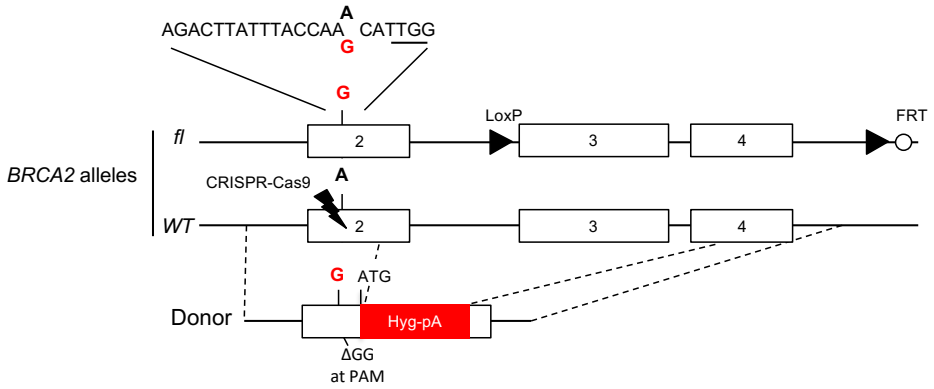

Figure 5-1. Gene targeting at the *WT* allele of *BRCA2*$^{fl/+}$ cells.
Schematic for generation of *BRCA2*$^{fl/-}$ cells described in (Feng and Jasin 2017). The Hyg cassette was designed to be specifically targeted to the *BRCA2 WT*, but not the *fl* allele. Unlike in **Fig. 5-2**, the target allele (*WT*) contains the A nucleotide SNP, so an A allele-specific sgRNA was designed to achieve the Hyg cassette targeting (with a paired nickase strategy, see methods). Filled triangles, loxP sites; open circle, FRT site. Other symbols are as described in the legends of **Fig. 5-2a**.

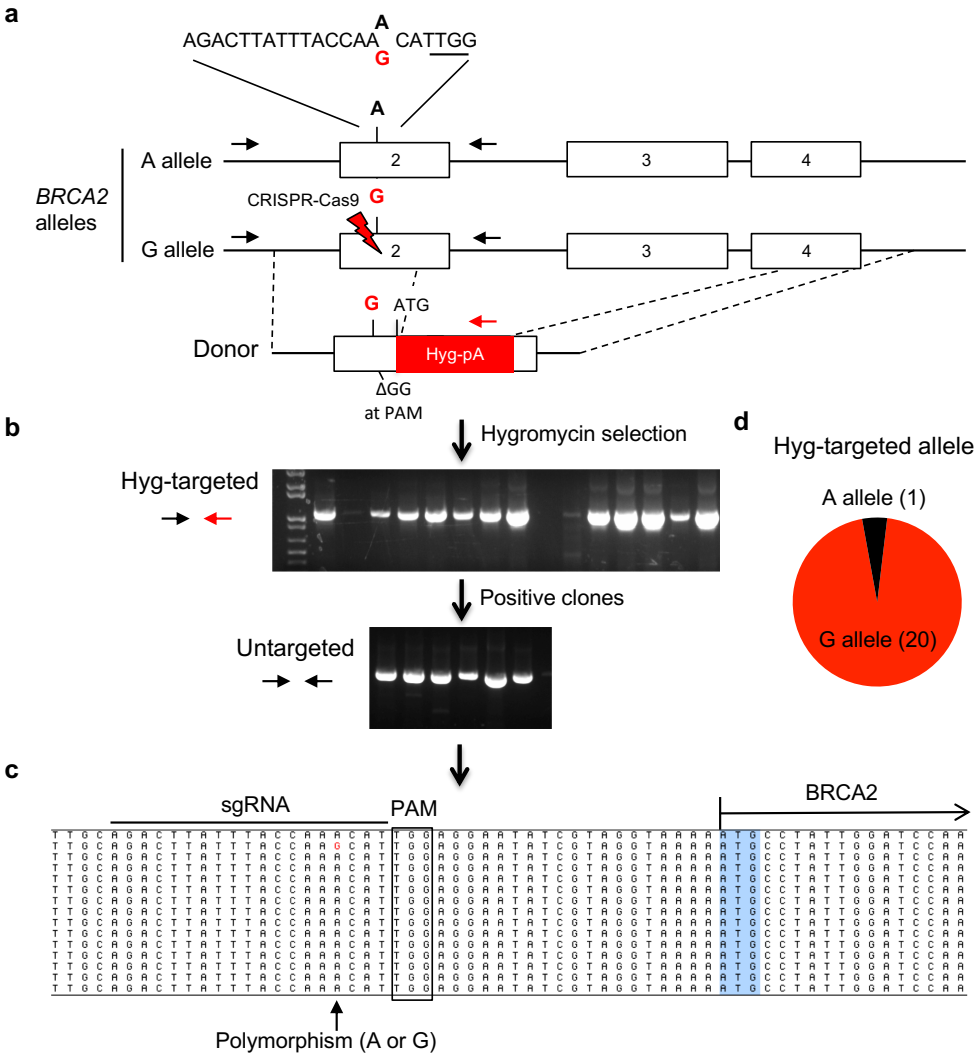

Figure 5-2. Presence of a SNP at the BRCA2 sgRNA site facilitates allele-specific gene editing.

a. Schematic for specifically targeting one *BRCA2* allele in MCF10A cells with a Hyg cassette. The BRCA2 sequence containing the A/G SNP is shown; the sgRNA sequence specifically targets the G allele (PAM sequence underlined). The donor fragment for generating the Hyg-targeted *BRCA2* null allele also contains the G SNP but it is close by to a disrupted PAM sequence (ΔGG). Primer sites for PCR are indicated. Hyg, promoterless hygromycin-resistance gene; lightning bolt, CRISPR-Cas9 cleavage site.

b. Genotyping PCR using primer sets as indicated in **a**. After transfection with plasmids expressing Cas9, the sgRNA, and the donor fragment, hygromycin resistant clones were subjected to a PCR to identify those that underwent successful Hyg gene targeting. PCR specific to the untargeted allele was then performed in the positive clones. A positive product is indicative of monoallelic targeting.

c. Sequences of the untargeted-allele-specific PCR products obtained in **b**. Positions of the sgRNA recognition region, PAM site, SNP site, and BRCA2 coding region are indicated.

d. Hyg targeting overwhelmingly occurred at the G allele. The number of clones for each genotype at the Hyg-targeted allele is shown in parentheses, as inferred from results in **c**.

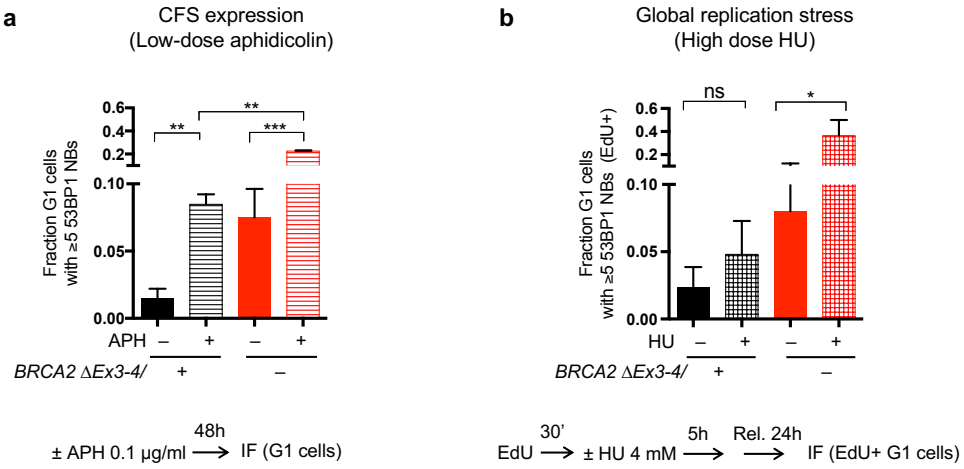

Figure 5-3. BRCA2 suppresses replication stress induced by both low-dose APH, which selectively triggers CFS expression, and HU, a more global inducer of replication stress.

a. BRCA2 deficiency further exacerbates 53BP1 NB formation in cells treated with low-dose APH. Population of *BRCA2*$^{fl/-}$ MCF10A cells after acute lentiviral transduction of self-deleting Cre recombinase (Pfeifer et al. 2001), hereafter named *BRCA2*$^{\Delta Ex3-4/-}$ (Feng and Jasin 2017), were analyzed for 53BP1 NB formation induced by continuous exposure to low-dose APH, as in the schematic at bottom. The fraction of G1 cells (cyclinA-negative with 2N DNA content) containing ≥ 5 53BP1 NBs as determined by immunofluorescence (IF) is shown.

b. BRCA2 deficiency leads to 53BP1 NB formation in cells treated with HU. Cells were analyzed for HU-induced 53BP1 NB formation, as in the schematic at bottom. EdU was used to label S phase cells at the time of HU treatment, which was followed by a release of the cells into the next G1 phase. EdU-positive, G1 cells (cyclinA-negative with 2N DNA content) were analyzed by IF. Note that unlike low-dose APH in **a**, HU treatment dramatically induced 53BP1 NB formation specifically in BRCA2-deficient, but not control cells. (Adapted from (Feng and Jasin 2017) under a Creative Commons license http://creativecommons.org/licenses/by/4.0/.)

Error bars in this figure represent one standard deviation from the mean (s.d.). n≥2. ns, not significant; *, p<0.05; **, p<0.01; ***, p<0.001 (unpaired two-tailed t test).

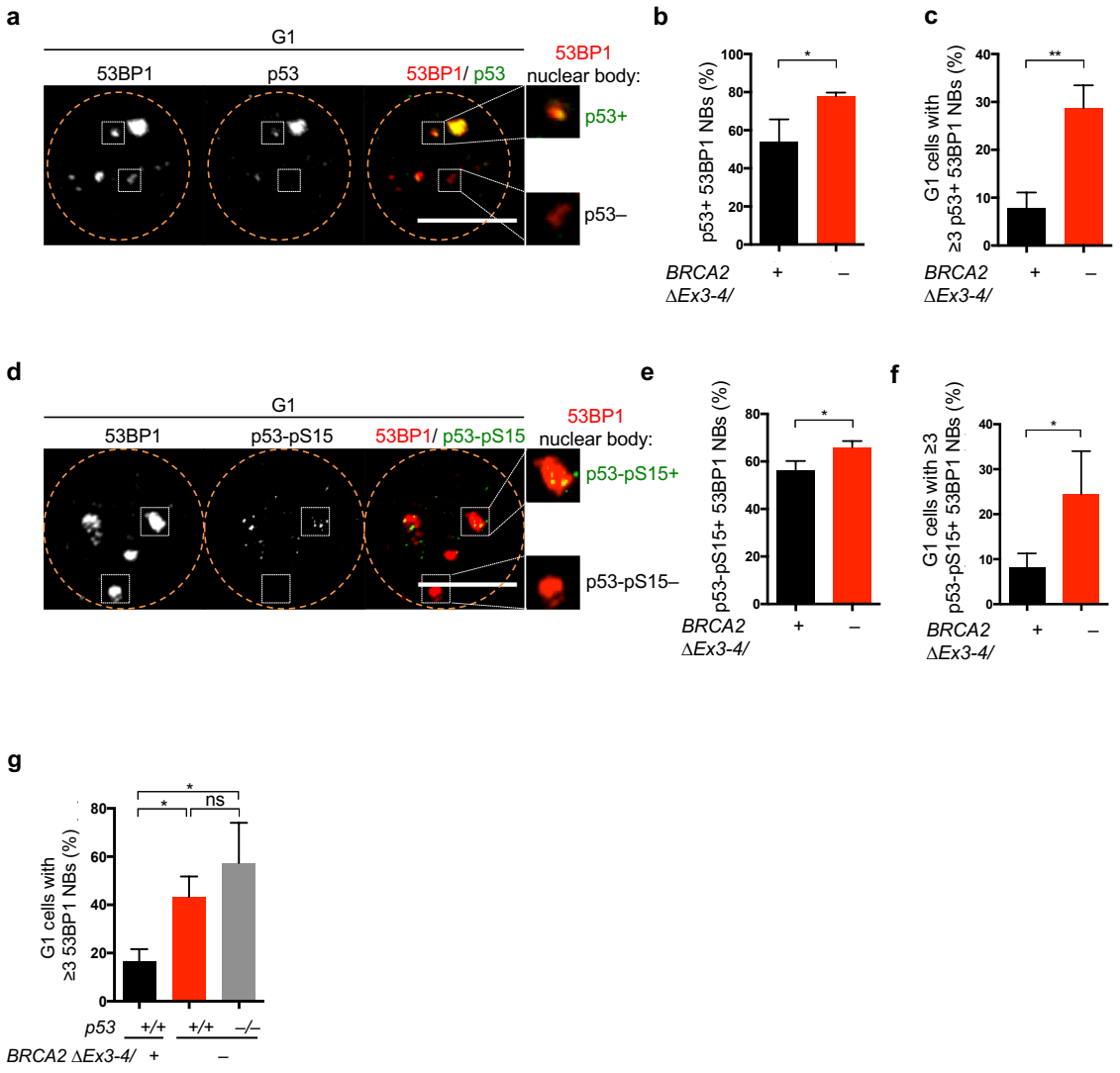

Figure 5-4. 53BP1 NB formation is associated with p53 activation.
a-f. Frequent 53BP1 NB formation with p53 colocalization in G1 phase in BRCA2-deficient cells. Representative deconvolved images are shown with G1 nuclei (EdU-negative with 2N DNA content) outlined (**a, d**). Cells were pulse labeled with EdU for 30 min before IF. 53BP1 NB formation and colocalization with p53 or p53-pS15 was quantified as in (**b, c**) and (**e, f**), respectively. Scale bars, 10 μm.
g. p53 loss does not significantly affect G1 53BP1 NB formation in BRCA2-deficient cells. Error bars in this figure represent one standard deviation from the mean (s.d.). n=3. ns, not significant; *, p<0.05; **, p<0.01 (unpaired two-tailed t test).

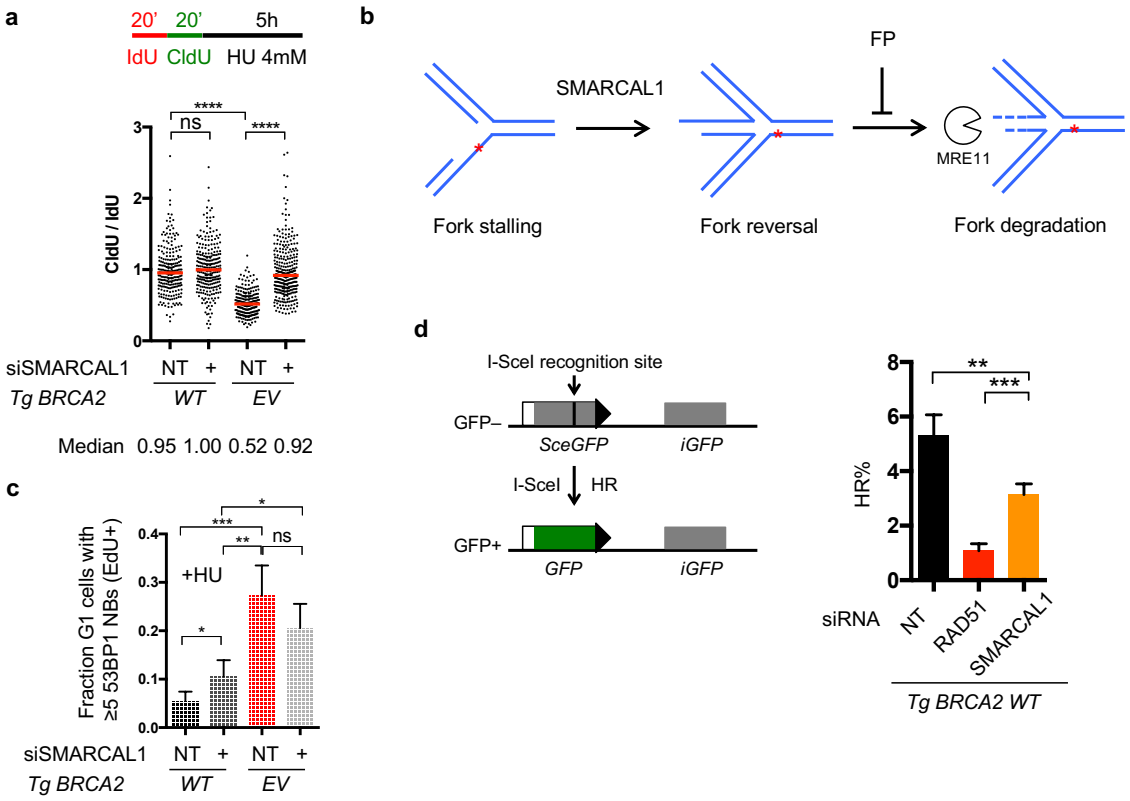

Figure 5-5. SMARCAL1 disruption in BRCA2-deficient cells restores FP but cells still maintain high 53BP1 NB levels.

a. SMARCAL1 depletion restores FP to BRCA2-deficient cells. *BRCA2*$^{\Delta Ex3\text{-}4/-}$ cells expressing a WT BRCA2 transgene (*Tg BRCA2 WT*) or containing an empty vector (*EV*) were depleted of SMARCAL1 with siRNA. DNA fiber analysis was performed to quantify FP. Schematic of the experimental design is shown at top. Median CldU/IdU tract length ratios are indicated in the graph (red bars). Graphs represent the pooled results of >250 fibers per genotype from two independent experiments, analyzed by a two-tailed Mann-Whitney test. NT, non targeting siRNA.

b. A model depicting fork reversal as a step prior to fork degradation, based on recent studies. Upon fork stalling, replication forks are subject to reversal, a process mediated by DNA translocases including SMARCAL1. The resulting reversed forks serve as the entry point for subsequent nascent strand degradation, a reaction catalyzed by MRE11 nuclease and antagonized by the BRCA2-mediated FP pathway.

c. 53BP1 NBs are not significantly diminished in BRCA2-deficient cells by restoration of FP through SMARCAL1 depletion. *BRCA2*$^{\Delta Ex3\text{-}4/-}$ cells with or without the *BRCA2* transgene were depleted of SMARCAL1 and analyzed for HU-induced 53BP1 NB formation, as in Fig. **5-3b**. Statistical analysis was by an unpaired two-tailed t test. n=4.

d. SMARCAL1 depletion leads to an intermediate HR defect. A schematic of the DR-GFP reporter as a readout of HR activity is shown (left). *BRCA2*$^{\Delta Ex3\text{-}4/-}$*;Tg BRCA2 WT* cells depleted of SMARCAL1 or RAD51 were infected with I-SceI-expressing lentivirus and the percent GFP+ cells was analyzed by an unpaired two-tailed t test (right). n≥3. Error bars s.d. ns, not significant; *p < 0.05; **p < 0.01; ***p < 0.001

Chapter 6 Conclusions and perspective*

Mutations in the tumor suppressor *BRCA2* predominantly predispose to breast cancer. Paradoxically, while loss of BRCA2 promotes tumor formation, it also causes cell lethality, although how lethality is triggered is unclear. In my thesis, we generate *BRCA2* conditional non-transformed human mammary epithelial cell lines using CRISPR-Cas9. Our work shows that cells are inviable upon BRCA2 loss, which leads to replication stress associated with under replication, causing mitotic abnormalities, 53BP1 NB formation in the ensuing G1 phase, and G1 arrest. Unexpected from other systems, the role of BRCA2 in homologous recombination, but not in stalled FP, is primarily associated with supporting human mammary epithelial cell viability, and, moreover, preventing replication stress, a hallmark of pre-cancerous lesions. Thus, our work uncovers a DNA under replication-53BP1 NB formation-G1 arrest axis as an unanticipated outcome of homologous recombination deficiency, which triggers cell lethality and, we propose, serves as a barrier that must be overcome for tumor formation.

6.1 Consequences of BRCA2 deficiency in MCF10A cells

One puzzle in the field is that, while predisposing to cancer, BRCA2 deficiency paradoxically leads to inviability in mice, both in embryos and in cells (Patel et al. 1998; Evers and Jonkers 2006; Kuznetsov et al. 2008; Badie et al. 2010). Therefore, a gap in our understanding needs to be bridged between the immediate consequence of cell

* Chapter 6 (except section 6.3, 6.4) is adapted from -. 2018. Homologous Recombination and Replication Fork Protection: BRCA2 and More! Cold Spring Harb Symp Quant Biol. (Under a Creative Commons license http://creativecommons.org/licenses/by/4.0/).

inviability and the long-term tumor susceptibility from BRCA2 deficiency. In addition, while BRCA2 loss is expected to impair HR in all tissues (Kass et al. 2016a), it predominantly predisposes to cancer in the breast and ovary. Resolution of these paradoxes requires a cellular model from a disease-relevant tissue, such as human mammary epithelial cells.

We set out to approach these questions by generating BRCA2 conditional models in a non-transformed human mammary epithelial cell line with a relatively stable genome (MCF10A; (Soule et al. 1990; Cowell et al. 2005)). This study reveals that BRCA2-deficiency-triggered cell lethality is conserved in these relatively normal human mammary cells (Feng and Jasin 2017). BRCA2 deficiency leads to cell cycle arrest in G1, a surprising result considering that BRCA2 functions in genome integrity maintenance pathways that are active in S and G2. To reconcile these seemingly counterintuitive results, we traced the source of DNA lesions that occur upon BRCA2 loss. We found that BRCA2 inactivation leads to DNA under replication, which in turn causes abnormalities during mitosis and 53BP1 NB formation in the subsequent G1 phase associated with a p53-dependent cell cycle arrest (Feng and Jasin 2017) (**Fig. 3-14**). Other independent studies have similar findings in different systems (Lai et al. 2017; Schoonen et al. 2017). Notably, while mitotic abnormalities have previously been associated with BRCA2 deficiency (Tutt et al. 1999; Daniels et al. 2004; Laulier et al. 2011; Choi et al. 2012; Mondal et al. 2012), we establish that it is the pre-mitotic stresses from the S and G2 phases that cause the subsequent aberrations (chromosome mis-segregation, 53BP1 NB formation), given that delaying mitotic entry abrogates these abnormalities (Feng and Jasin 2017).

6.2 Genetic background of MCF10A cells

In the thesis, MCF10A cells are considered as a model for relatively normal human mammary epithelial cells for the following reasons, as initially described (Soule et al. 1990): First, although immortalized, MCF10A cells are non-transformed, showing lack of anchorage-independent growth in vitro and lack of tumorigenicity in vivo. Second, they retain dependence on hormones and growth factors in culture, another feature shared with normal breast epithelium. Third, these cells maintain a stable karyotype and near diploidy. Notably, under 3D culture, MCF10A cells can form a spherical, acinar architecture that recapitulates some characteristics of glandular epithelium in vivo (Muthuswamy et al. 2001; Debnath et al. 2002).

Although MCF10A cells serve as an approximation of a physiological context, several potentially confounding limitations still exist and should be recognized. Despite displaying a stable karyotype, MCF10A cells are not cytogenetically normal (Soule et al. 1990), harboring structural variations that notably include biallelic loss of *CDKN2A* (encoding tumor suppressor p14/16) (Cowell et al. 2005). Moreover, MCF10A cells express telomerase which is critical for immortalization. Notably, telomerase has recently been shown to exert catastrophic impacts on genome integrity in some genetic backgrounds (Margalef et al. 2018). We cannot formally rule out the possibility that these genetic alterations may influence cell behavior either on their own or by interacting with BRCA2 loss. Nevertheless, the recue experiments argue that the observed phenotypes are indeed BRCA2-specific. The “DNA under replication-mitotic abnormality-53BP1 NB-G1 arrest” axis that we observed is corroborated by an independent study using different cell lines (Lai et al. 2017), which further minimizes the possible contributions from any cell-type-specific effects.

Molecular profiling analyses suggest MCF10A cells belong to a basal lineage subtype (Neve et al. 2006; Kao et al. 2009). By contrast, tumors with *BRCA2* mutations are predominantly luminal (Roy et al. 2011). However, it should be noted that, across all

breast cancer patients, the basal subtype is still well represented among those with *BRCA2*-mutated cancers, such that studies using the MCF10A models that we generated are clinically meaningful. The advent of organoid culture approaches of breast tumors (Duarte et al. 2018; Sachs et al. 2018) will make it feasible to study BRCA2 function in diverse genetic backgrounds.

6.3 Contributions of HR and FP to genome integrity and cell fitness

HR has been established as an essential process at the level of cells as well as organisms. The major underlying evidence is that severe functional disruption of the series of core HR factors such as BRCA2 almost invariably results in mouse embryonic lethality and defects in cell proliferation (Moynahan and Jasin 2010; Prakash et al. 2015). This view remains a widely accepted convention until the recent emergence of the FP pathway. Initially discovered in hamster cells, FP disruption by itself from an HR-proficient background only generates relatively subtle phenotypes, conferring a mild level of genome instability only under exogenous stresses, without discernible defects in spontaneous cell survival or sensitivity to PARP inhibitor (Schlacher et al. 2011). However, interesting findings were made from the converse experiments, namely, restoration of FP function in BRCA1/2-deficient settings. FP reactivation correlates with survival of mESCs and chemoresistance of cancer cells from an otherwise BRCA1/2-deficent backgrounds (Guillemette et al. 2015; Ray Chaudhuri et al. 2016). Importantly, HR remains deficient in these settings, arguing for the first time that HR can be a dispensable process as long as FP is intact.

Thus, FP is emerging as a pivotal process not only for understanding BRCA2 functions but also with potential clinical impacts. Interestingly, an ever-expanding list of canonical HR proteins turn out to contribute to the FP process as well (Feng and Jasin

2018). An immediate question emerges then, among the previously established severe phenotypes from disruption of HR genes, how many of them are actually attributable to HR loss per se, or rather to the accompanying ablation of the FP process, or a interaction of deficiency of both processes? Addressing questions like this not only helps delineate the repair pathway networks under homeostasis and disease, but also improves our understanding of therapy resistance mechanisms, potentially benefiting development of novel therapies. However, what makes the situation even more complicated is fact that FP is not fully correlated with genome integrity and cell survival either (discussed above). Different genetic manipulations and/or cellular contexts likely contribute to the diverse findings.

To approach this question in a disease-related cell type, we generated three independent separation-of-function systems in MCF10A cells (**Fig. 4-10**). FP, but not HR, is selectively disrupted through expression of a mutant BRCA2 peptide (BRCA2 S3291E) or restored by MRE11 or PARP1 ablation in BRCA2-deficent cells (Feng and Jasin 2017). In the third system, HR, but not FP, is selectively impaired by RAD51 depletion in BRCA2 wild-type cells (Feng and Jasin 2017).

We note that in the separation-of-function systems, while one pathway is perturbed, the other pathway is not completely normal (BRCA2 S3291E) and other cellular processes are affected (RAD51 depletion). Although caution should be used, these complications do not compromise the interpretations within the scope of the experiments in this thesis. For example, while BRCA2 S3291E complementation leads to an equivalent FP defect in both conditional systems, it results in varying extents of HR reduction, be it a minor defect (20%) in the AAVS1 system or a more pronounced defect (~40%) in the ΔEx3-4 system. This latter finding could be explained by lower BRCA2 S3291E protein levels and/or the presence of the residual BRCA2 ΔEx3-4 peptide in the ΔEx3-4 system. The more pronounced HR defect correlates with the lower plating

efficiency. Thus, our results are internally consistent: FP is not required for viability, while HR proficiency associates with cell viability (partial or nearly complete). Further, HR proficiency tracks with suppression of all aspects of replication stress. Given this internal consistency, while not perfect, the BRCA2 S3291E mutant is a valid separation-of-function mutant to evaluate FP-independent processes. Similarly, RAD51 depletion not only perturbed HR but also disrupted fork reversal. Nonetheless, the possible involvement of fork reversal was ruled out as discussed in chapter 4.

Collectively, all three systems unambiguously demonstrate that HR, but not FP is critical to suppress replication stress and support cell viability in this non-transformed human mammary cell line (Feng and Jasin 2017). Thus, HR and FP are differentially required for cell viability and genome integrity in different cell lines. How easy it is to meet the survival threshold, and thereby dictate the outcome of pathway restoration, may depend on the cellular context (**Fig. 4-11**) (discussed in Chapter 4).

6.4 Replication stress as a general barrier against tumor formation

Our study from MCF10A models provides insight into the notion that loss of a tumor suppressor gene and/or gain of genome instability, both of which are hallmarks of cancer, can actually lead to deleterious outcome. We propose that the increased replication stress in response to BRCA2 deficiency serve as a barrier that prospective tumor cells need to overcome to achieve malignancy. This notion adds to the well appreciated, tumor-suppressive roles of replication stress in the context of oncogene-induced hyper proliferation (Macheret and Halazonetis 2015). Nevertheless, the nature of the replication challenges under these different contexts may be inherently different. Oncogene-induced stress is largely due to the following non-exclusive reasons: deregulated origin firing, replication-transcription conflicts and nucleotide shortage.

These aberrations are largely linked to the nature of pre-mature S phase entry as a result of excessive cell growth stimulated by the oncogene, although some oncogenes are directly involved in deregulating some of the above aspects (discussed in chapter 1).

By contrast, BRCA2 deficiency, and likely caretaker-type of tumor suppressors in general, does not promote an unscheduled G1 entry. Since BRCA2 is prominently involved in either preventing (by FP) or repairing (by HR) DNA damage, it is possible that BRCA2 deficiency unveils some intrinsically damage-prone regions in the genome. CFSs and ERFSs are two of these examples (discussed in chapters 1 and 5). DNA lesions can form ahead of forks to serve as a trigger of replication stress. For example, the unscheduled R-loop formation (Bhatia et al. 2014; Shivji et al. 2018) can directly interfere with DNA replication in the absence of BRCA2. DNA damage can also occur as a result of the replication stress not being properly resolved. Therefore, BRCA2 deficiency may not lead to an active disruption of DNA replication in general, but instead passively reveal problems naturally encountered by replication forks, and amplify these problems due to a lack of repair. So far it remains an open question the exact nature of the "BRCA2-deficiency-susceptible" sites. Revealing these genomic regions will be critical to elucidating the mechanisms of replication stress underlying BRCA2 deficiency, and thereby provide insight into the additional tumor formation barrier. These studies may also shed light on the prominent mutational signatures associated with HR deficiency (Nik-Zainal et al. 2016; Davies et al. 2017).

6.5 Possible mechanisms to form tumors with *BRCA2* mutations

We anticipate a multitude of potential mechanisms cells can evolve to overcome the deleterious effects of acute BRCA2 loss. First, the cells can rewire repair pathways to suppress the occurrence of DNA damage, including replication stress as discussed

above, to a tolerable level. The aforementioned FP restoration represents a mechanism for cancer cells to survive chemotherapy. Although FP is not sufficient to support MCF10A cell survival in the absence of BRCA2, it is possible that alteration of other repair processes is involved. The rescue could occur by restoration of HR itself or activation of other HR-independent processes. Regarding the former possibility, it is well known that HR activity from BRCA1-deficient cells can be restored by disrupting 53BP1 or factors downstream (Bunting et al. 2010; Callen et al. 2013; Di Virgilio et al. 2013; Zimmermann et al. 2013; Xu et al. 2015), which bypasses the requirement for BRCA1 in DNA end resection. However, thus far HR suppressors in a *BRCA2* mutant background remain to be identified.

Second, if DNA damage still occurs at a substantial level, tumor cells may develop compensatory pathways to prevent further detrimental outcomes. We show that aberrations of *BRCA2* mutant cells extend beyond the S and G2 phases. The various forms of abnormalities during mitosis and 53BP1 NBs in the subsequent G1 phase are all downstream consequences of BRCA2 dysfunction. The deleterious effects of these aberrant products on cell fitness are highlighted by the arrest of cells in the G1, but not S or G2 phases, the cell cycle stages when DNA damage origins. Of relevance, we show that a prolonged G2 phase and, where tested, prometaphase are sufficient to abolish these later abnormalities. One immediate inference from these observations is that BRCA2-deficient cells may become viable by simply extending the duration of the G2 phase and/or prometaphase. Interestingly, checkpoints from both phases are compromised upon BRCA2 disruption (Menzel et al. 2011; Choi et al. 2012). It would be interesting for future studies to test if restoration of checkpoint defects in BRCA2-deficient cells suffices to support cell survival. Alternatively, tumor cells may also maintain a viable status by enhancing the compensatory repair pathways, such as the mitotic DNA synthesis in early mitosis.

Third, the cells may evolve ways to abrogate the growth-suppressive DNA damage responses. p53 inactivation represents one well-studied mechanism. However, at least in our MCF10A model, p53 disruption only rescues survival of BRCA2-deficient cells to a minimal extent. Therefore, additional, p53-independent growth-inhibitory processes may be activated in response to DNA damage and need to be overcome to achieve cell outgrowth (discussed in chapter 3).

Fourth, tissue microenvironment may also contribute to influencing tumor cell survival. This notion is particularly relevant for *BRCA2*-mutated cancers, given their preference for breast and ovarian tissue origins. Presumably, these tissues may provide a niche (e.g., a hormone-rich one) that is favorable for outgrowth of *BRCA2* mutant cells. In addition, immune systems may also be involved in modulating cell fate. A wave of recent discoveries converges to build a remarkable link between cGAS-STING immune pathways and abnormal cellular processes (reviewed in chapter 1). Among the immune-triggering anomalous products are stressed replication forks and micronuclei (Harding et al. 2017; Mackenzie et al. 2017; Bakhoum et al. 2018; Coquel et al. 2018), both of which are prominent in BRCA2-deficient cells, as we show. The resulting cGAS-STING pathway activation may elicit either a positive or negative impact on cancer cells, in a cell autonomous or non-autonomous manner. Therefore, it remains an interesting open question whether, and if so to what direction, these immune pathways affect BRCA2-deficient tumor formation.

Finally, while the thesis project and the above discussions are all concerned with consequences of a total loss of BRCA2 functions, it emerges that *BRCA2* heterozygosity also impacts genome integrity and may be clinically meaningful. Although a loss of heterozygosity was initially thought to invariably occur in tumor cells from *BRCA2* mutation carriers (Smith et al. 1992; Gudmundsson et al. 1995), it was later noticed from an analysis with a small patient cohort that loss of the remaining wild-type *BRCA2* allele

does not always occur in breast tumors (King et al. 2007). This trend is now expanded to a much larger sample size, showing compelling evidence that the wild-type *BRCA2* allele is still retained in a substantial portion of cancers with *BRCA2* germline mutations, particularly those from the breast (Maxwell et al. 2017; Huang et al. 2018). In a *Kras*-mutant-driven mouse pancreatic cancer model, it was shown that *Brca2* heterozygous germline mutation promotes tumor formation. Importantly, the resulting tumor cells still retain the wild-type *Brca2* allele (Skoulidis et al. 2010). A recent study adds insight into the heterozygous effects of BRCA2 deficiency, providing evidence that cells with monoallelic inactivation of BRCA2 are sensitized to aldehyde-induced genome instability due to a selective degradation of the remaining BRCA2 protein (Tan et al. 2017). Thus, an inherited *BRCA2* mutation may compromise genome integrity without overtly influencing cell viability, which can serve as a favorable platform to foster cancer evolution.

In summary, we envision that mammary cells with an inherited *BRCA2* mutant allele may have been under evolution in their genome before reaching the stage of malignancy. Although *BRCA2* heterozygous cells do not show spontaneous genome instability or overt defects in HR or FP, their genome is prone to damage by formaldehyde, which can be derived either endogenously as a cellular metabolite or exogenously from the environment (Tan et al. 2017). The insipid challenge to genome integrity, if proven in vivo, may contribute to an increasing chance of obtaining additional genomic alterations, including loss of the second *BRCA2* allele as well as evolution of mechanisms that allow for survival of complete BRCA2 loss. At the point of biallelic *BRCA2* inactivation, the cells display massive genome instability, which in turn enables acquisition of additional altercations that ultimately lead to malignancy. Alternatively, *BRCA2* heterozygous cells may accumulate by chance the mutations needed for tumor initiation. Under this circumstance, tumors may form with one *BRCA2* allele still intact.

6.6 Implications for cancer therapy

More than a decade ago, seminal work on PARP inhibition opened a new avenue of exploiting synthetic lethality to target cancers with BRCA1/2 deficiency (Bryant et al. 2005; Farmer et al. 2005). PARP inhibitors have clearly demonstrated promise with FDA approval for ovarian and, more recently, breast cancer treatment. Underlying mechanisms for the hypersensitivity of *BRCA1/2*-mutant tumor cells to PARP inhibition include accumulation of single-strand breaks and especially trapping of PARP protein on DNA to impede replication, both of which lead to lesions that require HR to be repaired (Lord and Ashworth 2017). Impaired mitotic progression may also promote PARP inhibition-associated cytotoxicity (Schoonen et al. 2017). Indeed, our observations that BRCA2-deficient cells display massive abnormalities during mitotic progression are in support of this model (Feng and Jasin 2017).

Despite the promise, PARP inhibitor therapies are challenged by tumor relapse with acquired resistance (Lord and Ashworth 2017). Thus, novel independent strategies to target *BRCA1/2* cancers may complement current therapies. Exploiting an increasing dependence of HR-deficient cells on minor DSB repair pathways has led to the discovery of novel targets for synthetic lethality: POLθ, which plays a role in microhomology-mediated end joining (Ceccaldi et al. 2015; Mateos-Gomez et al. 2015), and RAD52, a non-essential HR factor which becomes essential for the residual HR in BRCA1/2-deficient cells (Feng et al. 2011; Lok et al. 2013),

Recent studies including the current work described here have suggested another strategy to target that involves the phenomenon of mitotic DNA synthesis. Even under unperturbed conditions, BRCA2 prevents DNA under replication (Feng and Jasin 2017; Lai et al. 2017), such that in the absence of BRCA2 mitotic DNA synthesis is

activated (Feng and Jasin 2017; Lai et al. 2017), presumably as a last resort to complete DNA replication and prevent mitotic catastrophe (Minocherhomji et al. 2015; Bhowmick et al. 2016). A potential target in this pathway is RAD52, which is proposed to help prime mitotic DNA synthesis (Bhowmick et al. 2016). Other mitotic DNA synthesis components include MUS81 or SLX4, (Minocherhomji et al. 2015), loss of which impairs survival of BRCA2-deficient cancer cells (Lai et al. 2017). Interestingly, in contrast to the case of otherwise unperturbed cell proliferation, upon PARP inhibition MUS81 depletion paradoxically improves the viability of BRCA2-deficient cells, as discussed above (Rondinelli et al. 2017). Given that the critical pathways for cell survival may vary under different stresses, the importance of the accurate design of therapy strategies cannot be overstated.

BIBLIOGRAPHY

Aladjem MI, Spike BT, Rodewald LW, Hope TJ, Klemm M, Jaenisch R, Wahl GM. 1998. ES cells do not activate p53-dependent stress responses and undergo p53-independent apoptosis in response to DNA damage. *Curr Biol* **8**: 145-155.

Andreassen PR, Lohez OD, Lacroix FB, Margolis RL. 2001. Tetraploid state induces p53-dependent arrest of nontransformed mammalian cells in G1. *Mol Biol Cell* **12**: 1315-1328.

Anglana M, Apiou F, Bensimon A, Debatisse M. 2003. Dynamics of DNA replication in mammalian somatic cells: nucleotide pool modulates origin choice and interorigin spacing. *Cell* **114**: 385-394.

Antoniou A, Pharoah PDP, Narod S, Risch HA, Eyfjord JE, Hopper JL, Loman N, Olsson H, Johannsson O, Borg Å et al. 2003. Average Risks of Breast and Ovarian Cancer Associated with BRCA1 or BRCA2 Mutations Detected in Case Series Unselected for Family History: A Combined Analysis of 22 Studies. *The American Journal of Human Genetics* **72**: 1117-1130.

Arora M, Moser J, Phadke H, Basha AA, Spencer SL. 2017. Endogenous Replication Stress in Mother Cells Leads to Quiescence of Daughter Cells. *Cell Rep* **19**: 1351-1364.

Ayoub N, Rajendra E, Su X, Jeyasekharan AD, Mahen R, Venkitaraman AR. 2009. The carboxyl terminus of Brca2 links the disassembly of Rad51 complexes to mitotic entry. *Curr Biol* **19**: 1075-1085.

Badie S, Escandell JM, Bouwman P, Carlos AR, Thanasoula M, Gallardo MM, Suram A, Jaco I, Benitez J, Herbig U et al. 2010. BRCA2 acts as a RAD51 loader to facilitate telomere replication and capping. *Nat Struct Mol Biol* **17**: 1461-1469.

Bakhoum SF, Ngo B, Laughney AM, Cavallo JA, Murphy CJ, Ly P, Shah P, Sriram RK, Watkins TBK, Taunk NK et al. 2018. Chromosomal instability drives metastasis through a cytosolic DNA response. *Nature* **553**: 467-472.

Barlow JH, Faryabi RB, Callen E, Wong N, Malhowski A, Chen HT, Gutierrez-Cruz G, Sun HW, McKinnon P, Wright G et al. 2013. Identification of early replicating fragile sites that contribute to genome instability. *Cell* **152**: 620-632.

Barnes DE, Lindahl T. 2004. Repair and genetic consequences of endogenous DNA base damage in mammalian cells. *Annu Rev Genet* **38**: 445-476.

Bartkova J, Horejsi Z, Koed K, Kramer A, Tort F, Zieger K, Guldberg P, Sehested M, Nesland JM, Lukas C et al. 2005. DNA damage response as a candidate anti-cancer barrier in early human tumorigenesis. *Nature* **434**: 864-870.

Bartkova J, Rezaei N, Liontos M, Karakaidos P, Kletsas D, Issaeva N, Vassiliou LV, Kolettas E, Niforou K, Zoumpourlis VC et al. 2006. Oncogene-induced senescence is part of the tumorigenesis barrier imposed by DNA damage checkpoints. *Nature* **444**: 633-637.

Baumann C, Korner R, Hofmann K, Nigg EA. 2007. PICH, a centromere-associated SNF2 family ATPase, is regulated by Plk1 and required for the spindle checkpoint. *Cell* **128**: 101-114.

Beach RR, Ricci-Tam C, Brennan CM, Moomau CA, Hsu PH, Hua B, Silberman RE, Springer M, Amon A. 2017. Aneuploidy Causes Non-genetic Individuality. *Cell* **169**: 229-242 e221.

Berti M, Vindigni A. 2016. Replication stress: getting back on track. *Nat Struct Mol Biol* **23**: 103-109.

Bester AC, Roniger M, Oren YS, Im MM, Sarni D, Chaoat M, Bensimon A, Zamir G, Shewach DS, Kerem B. 2011. Nucleotide deficiency promotes genomic instability in early stages of cancer development. *Cell* **145**: 435-446.

Betous R, Couch FB, Mason AC, Eichman BF, Manosas M, Cortez D. 2013. Substrate-selective repair and restart of replication forks by DNA translocases. *Cell Rep* **3**: 1958-1969.

Betous R, Mason AC, Rambo RP, Bansbach CE, Badu-Nkansah A, Sirbu BM, Eichman BF, Cortez D. 2012. SMARCAL1 catalyzes fork regression and Holliday junction migration to maintain genome stability during DNA replication. *Genes Dev* **26**: 151-162.

Bhatia V, Barroso SI, Garcia-Rubio ML, Tumini E, Herrera-Moyano E, Aguilera A. 2014. BRCA2 prevents R-loop accumulation and associates with TREX-2 mRNA export factor PCID2. *Nature* **511**: 362-365.

Bhowmick R, Minocherhomji S, Hickson ID. 2016. RAD52 Facilitates Mitotic DNA Synthesis Following Replication Stress. *Mol Cell* **64**: 1117-1126.

Bignell G, Micklem G, Stratton MR, Ashworth A, Wooster R. 1997. The BRC repeats are conserved in mammalian BRCA2 proteins. *Hum Mol Genet* **6**: 53-58.

Biswas K, Das R, Alter BP, Kuznetsov SG, Stauffer S, North SL, Burkett S, Brody LC, Meyer S, Byrd RA et al. 2011. A comprehensive functional characterization of BRCA2 variants associated with Fanconi anemia using mouse ES cell-based assay. *Blood* **118**: 2430-2442.

Biswas K, Das R, Eggington JM, Qiao H, North SL, Stauffer S, Burkett SS, Martin BK, Southon E, Sizemore SC et al. 2012. Functional evaluation of BRCA2 variants mapping to the PALB2-binding and C-terminal DNA-binding domains using a mouse ES cell-based assay. *Hum Mol Genet* **21**: 3993-4006.

Bizard AH, Hickson ID. 2018. Anaphase: a fortune-teller of genomic instability. *Curr Opin Cell Biol* **52**: 112-119.

Bouwman P, Aly A, Escandell JM, Pieterse M, Bartkova J, van der Gulden H, Hiddingh S, Thanasoula M, Kulkarni A, Yang Q et al. 2010. 53BP1 loss rescues BRCA1 deficiency and is associated with triple-negative and BRCA-mutated breast cancers. *Nat Struct Mol Biol* **17**: 688-695.

Bouwman P, Drost R, Klijn C, Pieterse M, van der Gulden H, Song JY, Szuhai K, Jonkers J. 2011. Loss of p53 partially rescues embryonic development of Palb2 knockout mice but does not foster haploinsufficiency of Palb2 in tumour suppression. *The Journal of pathology* **224**: 10-21.

Bouwman P, van der Gulden H, van der Heijden I, Drost R, Klijn CN, Prasetyanti P, Pieterse M, Wientjens E, Seibler J, Hogervorst FB et al. 2013. A high-

throughput functional complementation assay for classification of BRCA1 missense variants. *Cancer Discov* **3**: 1142-1155.

Bowman-Colin C, Xia B, Bunting S, Klijn C, Drost R, Bouwman P, Fineman L, Chen X, Culhane AC, Cai H et al. 2013. Palb2 synergizes with Trp53 to suppress mammary tumor formation in a model of inherited breast cancer. *Proceedings of the National Academy of Sciences of the United States of America* **110**: 8632-8637.

Braig M, Lee S, Loddenkemper C, Rudolph C, Peters AH, Schlegelberger B, Stein H, Dorken B, Jenuwein T, Schmitt CA. 2005. Oncogene-induced senescence as an initial barrier in lymphoma development. *Nature* **436**: 660-665.

Branzei D, Foiani M. 2010. Maintaining genome stability at the replication fork. *Nat Rev Mol Cell Biol* **11**: 208-219.

Bryant HE, Schultz N, Thomas HD, Parker KM, Flower D, Lopez E, Kyle S, Meuth M, Curtin NJ, Helleday T. 2005. Specific killing of BRCA2-deficient tumours with inhibitors of poly(ADP-ribose) polymerase. *Nature* **434**: 913-917.

Bunting SF, Callen E, Wong N, Chen HT, Polato F, Gunn A, Bothmer A, Feldhahn N, Fernandez-Capetillo O, Cao L et al. 2010. 53BP1 inhibits homologous recombination in Brca1-deficient cells by blocking resection of DNA breaks. *Cell* **141**: 243-254.

Burnight ER, Gupta M, Wiley LA, Anfinson KR, Tran A, Triboulet R, Hoffmann JM, Klaahsen DL, Andorf JL, Jiao C et al. 2017. Using CRISPR-Cas9 to Generate Gene-Corrected Autologous iPSCs for the Treatment of Inherited Retinal Degeneration. *Mol Ther* **25**: 1999-2013.

Burrell RA, McClelland SE, Endesfelder D, Groth P, Weller MC, Shaikh N, Domingo E, Kanu N, Dewhurst SM, Gronroos E et al. 2013a. Replication stress links structural and numerical cancer chromosomal instability. *Nature* **494**: 492-496.

Burrell RA, McGranahan N, Bartek J, Swanton C. 2013b. The causes and consequences of genetic heterogeneity in cancer evolution. *Nature* **501**: 338-345.

Cadet J, Wagner JR. 2013. DNA base damage by reactive oxygen species, oxidizing agents, and UV radiation. *Cold Spring Harb Perspect Biol* **5**.

Cahill DP, Kinzler KW, Vogelstein B, Lengauer C. 1999. Genetic instability and darwinian selection in tumours. *Trends Cell Biol* **9**: M57-60.

Callen E, Di Virgilio M, Kruhlak MJ, Nieto-Soler M, Wong N, Chen HT, Faryabi RB, Polato F, Santos M, Starnes LM et al. 2013. 53BP1 mediates productive and mutagenic DNA repair through distinct phosphoprotein interactions. *Cell* **153**: 1266-1280.

Carlos AR, Escandell JM, Kotsantis P, Suwaki N, Bouwman P, Badie S, Folio C, Benitez J, Gomez-Lopez G, Pisano DG et al. 2013. ARF triggers senescence in Brca2-deficient cells by altering the spectrum of p53 transcriptional targets. *Nat Commun* **4**: 2697.

Carreira A, Hilario J, Amitani I, Baskin RJ, Shivji MK, Venkitaraman AR, Kowalczykowski SC. 2009. The BRC repeats of BRCA2 modulate the DNA-binding selectivity of RAD51. *Cell* **136**: 1032-1043.

Carreira A, Kowalczykowski SC. 2011. Two classes of BRC repeats in BRCA2 promote RAD51 nucleoprotein filament function by distinct mechanisms. *Proceedings of the National Academy of Sciences of the United States of America* **108**: 10448-10453.

Ceccaldi R, Liu JC, Amunugama R, Hajdu I, Primack B, Petalcorin MI, O'Connor KW, Konstantinopoulos PA, Elledge SJ, Boulton SJ et al. 2015. Homologous-recombination-deficient tumours are dependent on Poltheta-mediated repair. *Nature* **518**: 258-262.

Ceccaldi R, Sarangi P, D'Andrea AD. 2016. The Fanconi anaemia pathway: new players and new functions. *Nat Rev Mol Cell Biol* **17**: 337-349.

Chan KL, North PS, Hickson ID. 2007. BLM is required for faithful chromosome segregation and its localization defines a class of ultrafine anaphase bridges. *EMBO J* **26**: 3397-3409.

Chan KL, Palmai-Pallag T, Ying S, Hickson ID. 2009. Replication stress induces sister-chromatid bridging at fragile site loci in mitosis. *Nat Cell Biol* **11**: 753-760.

Chan YW, Fugger K, West SC. 2018. Unresolved recombination intermediates lead to ultra-fine anaphase bridges, chromosome breaks and aberrations. *Nat Cell Biol* **20**: 92-103.

Chang S, Biswas K, Martin BK, Stauffer S, Sharan SK. 2009. Expression of human BRCA1 variants in mouse ES cells allows functional analysis of BRCA1 mutations. *The Journal of clinical investigation* **119**: 3160-3171.

Cheeseman IM. 2014. The kinetochore. *Cold Spring Harb Perspect Biol* **6**: a015826.

Chen C-C, Feng W, Lim PX, Kass EM, Jasin M. 2018. Homology-Directed Repair and the Role of BRCA1, BRCA2, and Related Proteins in Genome Integrity and Cancer. *Annual Review of Cancer Biology* **2**: 313-336.

Chen CF, Chen PL, Zhong Q, Sharp ZD, Lee WH. 1999. Expression of BRC repeats in breast cancer cells disrupts the BRCA2-Rad51 complex and leads to radiation hypersensitivity and loss of G(2)/M checkpoint control. *J Biol Chem* **274**: 32931-32935.

Chen J, Silver DP, Walpita D, Cantor SB, Gazdar AF, Tomlinson G, Couch FJ, Weber BL, Ashley T, Livingston DM et al. 1998a. Stable interaction between the products of the BRCA1 and BRCA2 tumor suppressor genes in mitotic and meiotic cells. *Mol Cell* **2**: 317-328.

Chen PL, Chen CF, Chen Y, Xiao J, Sharp ZD, Lee WH. 1998b. The BRC repeats in BRCA2 are critical for RAD51 binding and resistance to methyl methanesulfonate treatment. *Proceedings of the National Academy of Sciences of the United States of America* **95**: 5287-5292.

Chen Q, Sun L, Chen ZJ. 2016. Regulation and function of the cGAS-STING pathway of cytosolic DNA sensing. *Nat Immunol* **17**: 1142-1149.

Chen YA, Shen YL, Hsia HY, Tiang YP, Sung TL, Chen LY. 2017. Extrachromosomal telomere repeat DNA is linked to ALT development via cGAS-STING DNA sensing pathway. *Nat Struct Mol Biol* **24**: 1124-1131.

Chen Z, Trotman LC, Shaffer D, Lin HK, Dotan ZA, Niki M, Koutcher JA, Scher HI, Ludwig T, Gerald W et al. 2005. Crucial role of p53-dependent cellular senescence in suppression of Pten-deficient tumorigenesis. *Nature* **436**: 725-730.

Choi E, Park PG, Lee HO, Lee YK, Kang GH, Lee JW, Han W, Lee HC, Noh DY, Lekomtsev S et al. 2012. BRCA2 fine-tunes the spindle assembly checkpoint through reinforcement of BubR1 acetylation. *Dev Cell* **22**: 295-308.

Ciccia A, Elledge SJ. 2010. The DNA damage response: making it safe to play with knives. *Mol Cell* **40**: 179-204.

Ciccia A, Nimonkar AV, Hu Y, Hajdu I, Achar YJ, Izhar L, Petit SA, Adamson B, Yoon JC, Kowalczykowski SC et al. 2012. Polyubiquitinated PCNA recruits the ZRANB3 translocase to maintain genomic integrity after replication stress. *Mol Cell* **47**: 396-409.

Cimini D, Howell B, Maddox P, Khodjakov A, Degrassi F, Salmon ED. 2001. Merotelic kinetochore orientation is a major mechanism of aneuploidy in mitotic mammalian tissue cells. *J Cell Biol* **153**: 517-527.

Collado M, Gil J, Efeyan A, Guerra C, Schuhmacher AJ, Barradas M, Benguria A, Zaballos A, Flores JM, Barbacid M et al. 2005. Tumour biology: senescence in premalignant tumours. *Nature* **436**: 642.

Connor F, Bertwistle D, Mee PJ, Ross GM, Swift S, Grigorieva E, Tybulewicz VL, Ashworth A. 1997. Tumorigenesis and a DNA repair defect in mice with a truncating Brca2 mutation. *Nat Genet* **17**: 423-430.

Coquel F, Silva MJ, Techer H, Zadorozhny K, Sharma S, Nieminuszczy J, Mettling C, Dardillac E, Barthe A, Schmitz AL et al. 2018. SAMHD1 acts at stalled replication forks to prevent interferon induction. *Nature* **557**: 57-61.

Cortez D. 2015. Preventing replication fork collapse to maintain genome integrity. *DNA Repair (Amst)* **32**: 149-157.

Couch FB, Bansbach CE, Driscoll R, Luzwick JW, Glick GG, Betous R, Carroll CM, Jung SY, Qin J, Cimprich KA et al. 2013. ATR phosphorylates SMARCAL1 to prevent replication fork collapse. *Genes Dev* **27**: 1610-1623.

Cowell JK, LaDuca J, Rossi MR, Burkhardt T, Nowak NJ, Matsui S. 2005. Molecular characterization of the t(3;9) associated with immortalization in the MCF10A cell line. *Cancer Genet Cytogenet* **163**: 23-29.

Crasta K, Ganem NJ, Dagher R, Lantermann AB, Ivanova EV, Pan Y, Nezi L, Protopopov A, Chowdhury D, Pellman D. 2012. DNA breaks and chromosome pulverization from errors in mitosis. *Nature* **482**: 53-58.

Cuella-Martin R, Oliveira C, Lockstone HE, Snellenberg S, Grolmusova N, Chapman JR. 2016. 53BP1 Integrates DNA Repair and p53-Dependent Cell Fate Decisions via Distinct Mechanisms. *Mol Cell* **64**: 51-64.

D'Andrea AD. 2010. Susceptibility pathways in Fanconi's anemia and breast cancer. *N Engl J Med* **362**: 1909-1919.

Dang CV, O'Donnell KA, Zeller KI, Nguyen T, Osthus RC, Li F. 2006. The c-Myc target gene network. *Semin Cancer Biol* **16**: 253-264.

Daniels MJ, Wang Y, Lee M, Venkitaraman AR. 2004. Abnormal cytokinesis in cells deficient in the breast cancer susceptibility protein BRCA2. *Science* **306**: 876-879.

Davies AA, Masson JY, McIlwraith MJ, Stasiak AZ, Stasiak A, Venkitaraman AR, West SC. 2001. Role of BRCA2 in control of the RAD51 recombination and DNA repair protein. *Mol Cell* **7**: 273-282.

Davies H, Glodzik D, Morganella S, Yates LR, Staaf J, Zou X, Ramakrishna M, Martin S, Boyault S, Sieuwerts AM et al. 2017. HRDetect is a predictor of BRCA1 and BRCA2 deficiency based on mutational signatures. *Nat Med* **23**: 517-525.

Davies OR, Pellegrini L. 2007. Interaction with the BRCA2 C terminus protects RAD51-DNA filaments from disassembly by BRC repeats. *Nat Struct Mol Biol* **14**: 475-483.

Davoli T, Uno H, Wooten EC, Elledge SJ. 2017. Tumor aneuploidy correlates with markers of immune evasion and with reduced response to immunotherapy. *Science* **355**.

Davoli T, Xu AW, Mengwasser KE, Sack LM, Yoon JC, Park PJ, Elledge SJ. 2013. Cumulative haploinsufficiency and triplosensitivity drive aneuploidy patterns and shape the cancer genome. *Cell* **155**: 948-962.

Debnath J, Mills KR, Collins NL, Reginato MJ, Muthuswamy SK, Brugge JS. 2002. The role of apoptosis in creating and maintaining luminal space within normal and oncogene-expressing mammary acini. *Cell* **111**: 29-40.

Dehe PM, Gaillard PH. 2017. Control of structure-specific endonucleases to maintain genome stability. *Nat Rev Mol Cell Biol* **18**: 315-330.

Di Micco R, Fumagalli M, Cicalese A, Piccinin S, Gasparini P, Luise C, Schurra C, Garre M, Nuciforo PG, Bensimon A et al. 2006. Oncogene-induced senescence is a DNA damage response triggered by DNA hyper-replication. *Nature* **444**: 638-642.

Di Virgilio M, Callen E, Yamane A, Zhang W, Jankovic M, Gitlin AD, Feldhahn N, Resch W, Oliveira TY, Chait BT et al. 2013. Rif1 prevents resection of DNA breaks and promotes immunoglobulin class switching. *Science* **339**: 711-715.

Ding L, Ley TJ, Larson DE, Miller CA, Koboldt DC, Welch JS, Ritchey JK, Young MA, Lamprecht T, McLellan MD et al. 2012. Clonal evolution in relapsed acute myeloid leukaemia revealed by whole-genome sequencing. *Nature* **481**: 506-510.

Ding X, Ray Chaudhuri A, Callen E, Pang Y, Biswas K, Klarmann KD, Martin BK, Burkett S, Cleveland L, Stauffer S et al. 2016. Synthetic viability by BRCA2 and PARP1/ARTD1 deficiencies. *Nat Commun* **7**: 12425.

Dominguez-Sola D, Ying CY, Grandori C, Ruggiero L, Chen B, Li M, Galloway DA, Gu W, Gautier J, Dalla-Favera R. 2007. Non-transcriptional control of DNA replication by c-Myc. *Nature* **448**: 445-451.

Dotsch V, Bernassola F, Coutandin D, Candi E, Melino G. 2010. p63 and p73, the ancestors of p53. *Cold Spring Harb Perspect Biol* **2**: a004887.

Dou Z, Ghosh K, Vizioli MG, Zhu J, Sen P, Wangensteen KJ, Simithy J, Lan Y, Lin Y, Zhou Z et al. 2017. Cytoplasmic chromatin triggers inflammation in senescence and cancer. *Nature* **550**: 402-406.

Duarte AA, Gogola E, Sachs N, Barazas M, Annunziato S, J RdR, Velds A, Blatter S, Houthuijzen JM, van de Ven M et al. 2018. BRCA-deficient mouse mammary tumor organoids to study cancer-drug resistance. *Nat Methods* **15**: 134-140.

Dungrawala H, Bhat KP, Le Meur R, Chazin WJ, Ding X, Sharan SK, Wessel SR, Sathe AA, Zhao R, Cortez D. 2017. RADX Promotes Genome Stability and Modulates Chemosensitivity by Regulating RAD51 at Replication Forks. *Mol Cell* **67**: 374-386 e375.

Durkin SG, Glover TW. 2007. Chromosome fragile sites. *Annu Rev Genet* **41**: 169-192.
Edwards SL, Brough R, Lord CJ, Natrajan R, Vatcheva R, Levine DA, Boyd J, Reis-Filho JS, Ashworth A. 2008. Resistance to therapy caused by intragenic deletion in BRCA2. *Nature* **451**: 1111-1115.
Erkko H, Xia B, Nikkila J, Schleutker J, Syrjakoski K, Mannermaa A, Kallioniemi A, Pylkas K, Karppinen SM, Rapakko K et al. 2007. A recurrent mutation in PALB2 in Finnish cancer families. *Nature* **446**: 316-319.
Esashi F, Christ N, Gannon J, Liu Y, Hunt T, Jasin M, West SC. 2005. CDK-dependent phosphorylation of BRCA2 as a regulatory mechanism for recombinational repair. *Nature* **434**: 598-604.
Esashi F, Galkin VE, Yu X, Egelman EH, West SC. 2007. Stabilization of RAD51 nucleoprotein filaments by the C-terminal region of BRCA2. *Nat Struct Mol Biol* **14**: 468-474.
Evers B, Jonkers J. 2006. Mouse models of BRCA1 and BRCA2 deficiency: past lessons, current understanding and future prospects. *Oncogene* **25**: 5885-5897.
Farmer H, McCabe N, Lord CJ, Tutt AN, Johnson DA, Richardson TB, Santarosa M, Dillon KJ, Hickson I, Knights C et al. 2005. Targeting the DNA repair defect in BRCA mutant cells as a therapeutic strategy. *Nature* **434**: 917-921.
Feng W, Jasin M. 2017. BRCA2 suppresses replication stress-induced mitotic and G1 abnormalities through homologous recombination. *Nat Commun* **8**: 525.
-. 2018. Homologous Recombination and Replication Fork Protection: BRCA2 and More! *Cold Spring Harb Symp Quant Biol*.
Feng Z, Scott SP, Bussen W, Sharma GG, Guo G, Pandita TK, Powell SN. 2011. Rad52 inactivation is synthetically lethal with BRCA2 deficiency. *Proc Natl Acad Sci U S A* **108**: 686-691.
Fishel R, Lescoe MK, Rao MR, Copeland NG, Jenkins NA, Garber J, Kane M, Kolodner R. 1993. The human mutator gene homolog MSH2 and its association with hereditary nonpolyposis colon cancer. *Cell* **75**: 1027-1038.
Fox EJ, Prindle MJ, Loeb LA. 2013. Do mutator mutations fuel tumorigenesis? *Cancer and Metastasis Reviews* **32**: 353-361.
Friedman LS, Thistlethwaite FC, Patel KJ, Yu VP, Lee H, Venkitaraman AR, Abel KJ, Carlton MB, Hunter SM, Colledge WH et al. 1998. Thymic lymphomas in mice with a truncating mutation in Brca2. *Cancer Res* **58**: 1338-1343.
Fu Y, Foden JA, Khayter C, Maeder ML, Reyon D, Joung JK, Sander JD. 2013. High-frequency off-target mutagenesis induced by CRISPR-Cas nucleases in human cells. *Nat Biotechnol* **31**: 822-826.
Fu Y, Sander JD, Reyon D, Cascio VM, Joung JK. 2014. Improving CRISPR-Cas nuclease specificity using truncated guide RNAs. *Nat Biotechnol* **32**: 279-284.
Funk LC, Zasadil LM, Weaver BA. 2016. Living in CIN: Mitotic Infidelity and Its Consequences for Tumor Promotion and Suppression. *Dev Cell* **39**: 638-652.
Galkin VE, Esashi F, Yu X, Yang S, West SC, Egelman EH. 2005. BRCA2 BRC motifs bind RAD51-DNA filaments. *Proceedings of the National Academy of Sciences of the United States of America* **102**: 8537-8542.

Ganem NJ, Cornils H, Chiu SY, O'Rourke KP, Arnaud J, Yimlamai D, Thery M, Camargo FD, Pellman D. 2014a. Cytokinesis failure triggers hippo tumor suppressor pathway activation. *Cell* **158**: 833-848.

-. 2014b. Cytokinesis failure triggers hippo tumor suppressor pathway activation. *Cell* **158**: 833-848.

Ganem NJ, Pellman D. 2007. Limiting the proliferation of polyploid cells. *Cell* **131**: 437-440.

-. 2012. Linking abnormal mitosis to the acquisition of DNA damage. *J Cell Biol* **199**: 871-881.

Gao X, Tao Y, Lamas V, Huang M, Yeh WH, Pan B, Hu YJ, Hu JH, Thompson DB, Shu Y et al. 2018. Treatment of autosomal dominant hearing loss by in vivo delivery of genome editing agents. *Nature* **553**: 217-221.

Garaycoechea JI, Crossan GP, Langevin F, Mulderrig L, Louzada S, Yang F, Guilbaud G, Park N, Roerink S, Nik-Zainal S et al. 2018. Alcohol and endogenous aldehydes damage chromosomes and mutate stem cells. *Nature* **553**: 171-177.

Garcia-Muse T, Aguilera A. 2016. Transcription-replication conflicts: how they occur and how they are resolved. *Nat Rev Mol Cell Biol* **17**: 553-563.

Gisselsson D. 2008. Classification of chromosome segregation errors in cancer. *Chromosoma* **117**: 511-519.

Glover TW, Berger C, Coyle J, Echo B. 1984. DNA polymerase alpha inhibition by aphidicolin induces gaps and breaks at common fragile sites in human chromosomes. *Hum Genet* **67**: 136-142.

Glover TW, Wilson TE, Arlt MF. 2017. Fragile sites in cancer: more than meets the eye. *Nat Rev Cancer* **17**: 489-501.

Gluck S, Guey B, Gulen MF, Wolter K, Kang TW, Schmacke NA, Bridgeman A, Rehwinkel J, Zender L, Ablasser A. 2017. Innate immune sensing of cytosolic chromatin fragments through cGAS promotes senescence. *Nat Cell Biol* **19**: 1061-1070.

Gorgoulis VG, Vassiliou LV, Karakaidos P, Zacharatos P, Kotsinas A, Liloglou T, Venere M, Ditullio RA, Jr., Kastrinakis NG, Levy B et al. 2005. Activation of the DNA damage checkpoint and genomic instability in human precancerous lesions. *Nature* **434**: 907-913.

Greaves M, Maley CC. 2012. Clonal evolution in cancer. *Nature* **481**: 306-313.

Greenblatt MS, Chappuis PO, Bond JP, Hamel N, Foulkes WD. 2001. TP53 mutations in breast cancer associated with BRCA1 or BRCA2 germ-line mutations: distinctive spectrum and structural distribution. *Cancer Res* **61**: 4092-4097.

Gudmundsdottir K, Lord CJ, Witt E, Tutt AN, Ashworth A. 2004. DSS1 is required for RAD51 focus formation and genomic stability in mammalian cells. *EMBO Rep* **5**: 989-993.

Gudmundsson J, Johannesdottir G, Bergthorsson JT, Arason A, Ingvarsson S, Egilsson V, Barkardottir RB. 1995. Different tumor types from BRCA2 carriers show wild-type chromosome deletions on 13q12-q13. *Cancer Res* **55**: 4830-4832.

Guillemette S, Serra RW, Peng M, Hayes JA, Konstantinopoulos PA, Green MR, Cantor SB. 2015. Resistance to therapy in BRCA2 mutant cells due to loss of the nucleosome remodeling factor CHD4. *Genes & development* **29**: 489-494.

Haas KT, Lee M, Esposito A, Venkitaraman AR. 2018. Single-molecule localization microscopy reveals molecular transactions during RAD51 filament assembly at cellular DNA damage sites. *Nucleic Acids Res* **46**: 2398-2416.
Halazonetis TD, Gorgoulis VG, Bartek J. 2008. An oncogene-induced DNA damage model for cancer development. *Science* **319**: 1352-1355.
Hanahan D, Weinberg RA. 2000. The hallmarks of cancer. *Cell* **100**: 57-70.
-. 2011. Hallmarks of cancer: the next generation. *Cell* **144**: 646-674.
Harding SM, Benci JL, Irianto J, Discher DE, Minn AJ, Greenberg RA. 2017. Mitotic progression following DNA damage enables pattern recognition within micronuclei. *Nature* **548**: 466-470.
Harrigan JA, Belotserkovskaya R, Coates J, Dimitrova DS, Polo SE, Bradshaw CR, Fraser P, Jackson SP. 2011. Replication stress induces 53BP1-containing OPT domains in G1 cells. *J Cell Biol* **193**: 97-108.
Harris SL, Levine AJ. 2005. The p53 pathway: positive and negative feedback loops. *Oncogene* **24**: 2899-2908.
Hashimoto Y, Ray Chaudhuri A, Lopes M, Costanzo V. 2010. Rad51 protects nascent DNA from Mre11-dependent degradation and promotes continuous DNA synthesis. *Nat Struct Mol Biol* **17**: 1305-1311.
Hatch EM, Fischer AH, Deerinck TJ, Hetzer MW. 2013. Catastrophic nuclear envelope collapse in cancer cell micronuclei. *Cell* **154**: 47-60.
Helmrich A, Ballarino M, Tora L. 2011. Collisions between replication and transcription complexes cause common fragile site instability at the longest human genes. *Mol Cell* **44**: 966-977.
Higgs MR, Reynolds JJ, Winczura A, Blackford AN, Borel V, Miller ES, Zlatanou A, Nieminuszczy J, Ryan EL, Davies NJ et al. 2015. BOD1L Is Required to Suppress Deleterious Resection of Stressed Replication Forks. *Mol Cell* **59**: 462-477.
Hockemeyer D, Wang H, Kiani S, Lai CS, Gao Q, Cassady JP, Cost GJ, Zhang L, Santiago Y, Miller JC et al. 2011. Genetic engineering of human pluripotent cells using TALE nucleases. *Nat Biotechnol* **29**: 731-734.
Holsclaw JK, Sekelsky J. 2017. Annealing of Complementary DNA Sequences During Double-Strand Break Repair in Drosophila Is Mediated by the Ortholog of SMARCAL1. *Genetics* **206**: 467-480.
Hsu PD, Scott DA, Weinstein JA, Ran FA, Konermann S, Agarwala V, Li Y, Fine EJ, Wu X, Shalem O et al. 2013. DNA targeting specificity of RNA-guided Cas9 nucleases. *Nat Biotechnol* **31**: 827-832.
Huang KL, Mashl RJ, Wu Y, Ritter DI, Wang J, Oh C, Paczkowska M, Reynolds S, Wyczalkowski MA, Oak N et al. 2018. Pathogenic Germline Variants in 10,389 Adult Cancers. *Cell* **173**: 355-370 e314.
Hucl T, Rago C, Gallmeier E, Brody JR, Gorospe M, Kern SE. 2008. A syngeneic variance library for functional annotation of human variation: application to BRCA2. *Cancer Res* **68**: 5023-5030.
Huo Y, Cai H, Teplova I, Bowman-Colin C, Chen G, Price S, Barnard N, Ganesan S, Karantza V, White E et al. 2013. Autophagy Opposes p53-Mediated Tumor Barrier to Facilitate Tumorigenesis in a Model of PALB2-Associated Hereditary Breast Cancer. *Cancer Discov*.

Iwabuchi K, Bartel PL, Li B, Marraccino R, Fields S. 1994. Two cellular proteins that bind to wild-type but not mutant p53. *Proc Natl Acad Sci U S A* **91**: 6098-6102.
Janssen A, van der Burg M, Szuhai K, Kops GJ, Medema RH. 2011. Chromosome segregation errors as a cause of DNA damage and structural chromosome aberrations. *Science* **333**: 1895-1898.
Jasin M, Rothstein R. 2013. Repair of strand breaks by homologous recombination. *Cold Spring Harb Perspect Biol* **5**: a012740.
Jensen RB, Carreira A, Kowalczykowski SC. 2010. Purified human BRCA2 stimulates RAD51-mediated recombination. *Nature* **467**: 678-683.
Jeyasekharan AD, Liu Y, Hattori H, Pisupati V, Jonsdottir AB, Rajendra E, Lee M, Sundaramoorthy E, Schlachter S, Kaminski CF et al. 2013. A cancer-associated BRCA2 mutation reveals masked nuclear export signals controlling localization. *Nat Struct Mol Biol* **20**: 1191-1198.
Jiricny J. 2006. The multifaceted mismatch-repair system. *Nat Rev Mol Cell Biol* **7**: 335-346.
Jones RM, Mortusewicz O, Afzal I, Lorvellec M, Garcia P, Helleday T, Petermann E. 2013. Increased replication initiation and conflicts with transcription underlie Cyclin E-induced replication stress. *Oncogene* **32**: 3744-3753.
Jones S, Hruban RH, Kamiyama M, Borges M, Zhang X, Parsons DW, Lin JC, Palmisano E, Brune K, Jaffee EM et al. 2009. Exomic sequencing identifies PALB2 as a pancreatic cancer susceptibility gene. *Science* **324**: 217.
Jonkers J, Meuwissen R, van der Gulden H, Peterse H, van der Valk M, Berns A. 2001. Synergistic tumor suppressor activity of BRCA2 and p53 in a conditional mouse model for breast cancer. *Nat Genet* **29**: 418-425.
Kanu N, Cerone MA, Goh G, Zalmas LP, Bartkova J, Dietzen M, McGranahan N, Rogers R, Law EK, Gromova I et al. 2016. DNA replication stress mediates APOBEC3 family mutagenesis in breast cancer. *Genome Biol* **17**: 185.
Kao J, Salari K, Bocanegra M, Choi YL, Girard L, Gandhi J, Kwei KA, Hernandez-Boussard T, Wang P, Gazdar AF et al. 2009. Molecular profiling of breast cancer cell lines defines relevant tumor models and provides a resource for cancer gene discovery. *PLoS One* **4**: e6146.
Kass EM, Lim PX, Helgadottir HR, Moynahan ME, Jasin M. 2016a. Robust homology-directed repair within mouse mammary tissue is not specifically affected by Brca2 mutation. *Nat Commun* **7**: 13241.
Kass EM, Moynahan ME, Jasin M. 2016b. When Genome Maintenance Goes Badly Awry. *Mol Cell* **62**: 777-787.
Kile AC, Chavez DA, Bacal J, Eldirany S, Korzhnev DM, Bezsonova I, Eichman BF, Cimprich KA. 2015. HLTF's Ancient HIRAN Domain Binds 3' DNA Ends to Drive Replication Fork Reversal. *Mol Cell* **58**: 1090-1100.
Kim C, Gao R, Sei E, Brandt R, Hartman J, Hatschek T, Crosetto N, Foukakis T, Navin NE. 2018. Chemoresistance Evolution in Triple-Negative Breast Cancer Delineated by Single-Cell Sequencing. *Cell* **173**: 879-893 e813.
Kim H, Zheng S, Amini SS, Virk SM, Mikkelsen T, Brat DJ, Grimsby J, Sougnez C, Muller F, Hu J et al. 2015. Whole-genome and multisector exome sequencing

of primary and post-treatment glioblastoma reveals patterns of tumor evolution. *Genome Res* **25**: 316-327.
King TA, Li W, Brogi E, Yee CJ, Gemignani ML, Olvera N, Levine DA, Norton L, Robson ME, Offit K et al. 2007. Heterogenic loss of the wild-type BRCA allele in human breast tumorigenesis. *Ann Surg Oncol* **14**: 2510-2518.
Kojic M, Yang H, Kostrub CF, Pavletich NP, Holloman WK. 2003. The BRCA2-interacting protein DSS1 is vital for DNA repair, recombination, and genome stability in Ustilago maydis. *Mol Cell* **12**: 1043-1049.
Kojic M, Zhou Q, Lisby M, Holloman WK. 2005. Brh2-Dss1 interplay enables properly controlled recombination in Ustilago maydis. *Mol Cell Biol* **25**: 2547-2557.
Kolinjivadi AM, Sannino V, De Antoni A, Zadorozhny K, Kilkenny M, Techer H, Baldi G, Shen R, Ciccia A, Pellegrini L et al. 2017. Smarcal1-Mediated Fork Reversal Triggers Mre11-Dependent Degradation of Nascent DNA in the Absence of Brca2 and Stable Rad51 Nucleofilaments. *Mol Cell*.
Kondrashova O, Nguyen M, Shield-Artin K, Tinker AV, Teng NNH, Harrell MI, Kuiper MJ, Ho GY, Barker H, Jasin M et al. 2017a. Secondary Somatic Mutations Restoring RAD51C and RAD51D Associated with Acquired Resistance to the PARP Inhibitor Rucaparib in High-Grade Ovarian Carcinoma. *Cancer Discov* **7**: 984-998.
Kondrashova O, Nguyen M, Shield-Artin K, Tinker AV, Teng NNH, Harrell MI, Kuiper MJ, Ho GY, Barker H, Jasin M et al. 2017b. Secondary Somatic Mutations Restoring RAD51C and RAD51D Associated with Acquired Resistance to the PARP Inhibitor Rucaparib in High-grade Ovarian Carcinoma. *Cancer Discov*.
Kristensen CN, Bystol KM, Li B, Serrano L, Brenneman MA. 2010. Depletion of DSS1 protein disables homologous recombinational repair in human cells. *Mutation research* **694**: 60-64.
Krogan NJ, Lam MH, Fillingham J, Keogh MC, Gebbia M, Li J, Datta N, Cagney G, Buratowski S, Emili A et al. 2004. Proteasome involvement in the repair of DNA double-strand breaks. *Mol Cell* **16**: 1027-1034.
Kuffer C, Kuznetsova AY, Storchova Z. 2013. Abnormal mitosis triggers p53-dependent cell cycle arrest in human tetraploid cells. *Chromosoma* **122**: 305-318.
Kurtova AV, Xiao J, Mo Q, Pazhanisamy S, Krasnow R, Lerner SP, Chen F, Roh TT, Lay E, Ho PL et al. 2015. Blocking PGE2-induced tumour repopulation abrogates bladder cancer chemoresistance. *Nature* **517**: 209-213.
Kuznetsov SG, Liu P, Sharan SK. 2008. Mouse embryonic stem cell-based functional assay to evaluate mutations in BRCA2. *Nat Med* **14**: 875-881.
Lai X, Broderick R, Bergoglio V, Zimmer J, Badie S, Niedzwiedz W, Hoffmann JS, Tarsounas M. 2017. MUS81 nuclease activity is essential for replication stress tolerance and chromosome segregation in BRCA2-deficient cells. *Nat Commun* **8**: 15983.
Langevin F, Crossan GP, Rosado IV, Arends MJ, Patel KJ. 2011. Fancd2 counteracts the toxic effects of naturally produced aldehydes in mice. *Nature* **475**: 53-58.
Laulier C, Cheng A, Stark JM. 2011. The relative efficiency of homology-directed repair has distinct effects on proper anaphase chromosome separation. *Nucleic Acids Res* **39**: 5935-5944.

Le Tallec B, Millot GA, Blin ME, Brison O, Dutrillaux B, Debatisse M. 2013. Common fragile site profiling in epithelial and erythroid cells reveals that most recurrent cancer deletions lie in fragile sites hosting large genes. *Cell Rep* **4**: 420-428.

Leach FS, Nicolaides NC, Papadopoulos N, Liu B, Jen J, Parsons R, Peltomaki P, Sistonen P, Aaltonen LA, Nystrom-Lahti M et al. 1993. Mutations of a mutS homolog in hereditary nonpolyposis colorectal cancer. *Cell* **75**: 1215-1225.

Lee H, Trainer AH, Friedman LS, Thistlethwaite FC, Evans MJ, Ponder BA, Venkitaraman AR. 1999. Mitotic checkpoint inactivation fosters transformation in cells lacking the breast cancer susceptibility gene, Brca2. *Mol Cell* **4**: 1-10.

Lemacon D, Jackson J, Quinet A, Brickner JR, Li S, Yazinski S, You Z, Ira G, Zou L, Mosammaparast N et al. 2017. MRE11 and EXO1 nucleases degrade reversed forks and elicit MUS81-dependent fork rescue in BRCA2-deficient cells. *Nat Commun* **8**: 860.

Letessier A, Millot GA, Koundrioukoff S, Lachages AM, Vogt N, Hansen RS, Malfoy B, Brison O, Debatisse M. 2011. Cell-type-specific replication initiation programs set fragility of the FRA3B fragile site. *Nature* **470**: 120-123.

Li J, Zou C, Bai Y, Wazer DE, Band V, Gao Q. 2006. DSS1 is required for the stability of BRCA2. *Oncogene* **25**: 1186-1194.

Lieber MR. 2010. The mechanism of double-strand DNA break repair by the nonhomologous DNA end-joining pathway. *Annu Rev Biochem* **79**: 181-211.

Lim DS, Hasty P. 1996. A mutation in mouse rad51 results in an early embryonic lethal that is suppressed by a mutation in p53. *Mol Cell Biol* **16**: 7133-7143.

Lindahl T, Barnes DE. 2000. Repair of endogenous DNA damage. *Cold Spring Harb Symp Quant Biol* **65**: 127-133.

Liu J, Doty T, Gibson B, Heyer WD. 2010. Human BRCA2 protein promotes RAD51 filament formation on RPA-covered single-stranded DNA. *Nat Struct Mol Biol* **17**: 1260-1262.

Lok BH, Carley AC, Tchang B, Powell SN. 2013. RAD52 inactivation is synthetically lethal with deficiencies in BRCA1 and PALB2 in addition to BRCA2 through RAD51-mediated homologous recombination. *Oncogene* **32**: 3552-3558.

Lomonosov M, Anand S, Sangrithi M, Davies R, Venkitaraman AR. 2003. Stabilization of stalled DNA replication forks by the BRCA2 breast cancer susceptibility protein. *Genes Dev* **17**: 3017-3022.

Lord CJ, Ashworth A. 2017. PARP inhibitors: Synthetic lethality in the clinic. *Science* **355**: 1152-1158.

Loveday C, Turnbull C, Ramsay E, Hughes D, Ruark E, Frankum JR, Bowden G, Kalmyrzaev B, Warren-Perry M, Snape K et al. 2011. Germline mutations in RAD51D confer susceptibility to ovarian cancer. *Nat Genet* **43**: 879-882.

Ludwig T, Chapman DL, Papaioannou VE, Efstratiadis A. 1997. Targeted mutations of breast cancer susceptibility gene homologs in mice: lethal phenotypes of Brca1, Brca2, Brca1/Brca2, Brca1/p53, and Brca2/p53 nullizygous embryos. *Genes Dev* **11**: 1226-1241.

Ludwig T, Fisher P, Murty V, Efstratiadis A. 2001. Development of mammary adenocarcinomas by tissue-specific knockout of Brca2 in mice. *Oncogene* **20**: 3937-3948.

Lukas C, Savic V, Bekker-Jensen S, Doil C, Neumann B, Pedersen RS, Grofte M, Chan KL, Hickson ID, Bartek J et al. 2011. 53BP1 nuclear bodies form around DNA lesions generated by mitotic transmission of chromosomes under replication stress. *Nat Cell Biol* **13**: 243-253.

Ly P, Teitz LS, Kim DH, Shoshani O, Skaletsky H, Fachinetti D, Page DC, Cleveland DW. 2017. Selective Y centromere inactivation triggers chromosome shattering in micronuclei and repair by non-homologous end joining. *Nat Cell Biol* **19**: 68-75.

Maass PG, Barutcu AR, Shechner DM, Weiner CL, Mele M, Rinn JL. 2018. Spatiotemporal allele organization by allele-specific CRISPR live-cell imaging (SNP-CLING). *Nat Struct Mol Biol* **25**: 176-184.

Macheret M, Halazonetis TD. 2015. DNA replication stress as a hallmark of cancer. *Annu Rev Pathol* **10**: 425-448.

-. 2018. Intragenic origins due to short G1 phases underlie oncogene-induced DNA replication stress. *Nature* **555**: 112-116.

Maciejowski J, de Lange T. 2017. Telomeres in cancer: tumour suppression and genome instability. *Nat Rev Mol Cell Biol* **18**: 175-186.

Maciejowski J, Li Y, Bosco N, Campbell PJ, de Lange T. 2015. Chromothripsis and Kataegis Induced by Telomere Crisis. *Cell* **163**: 1641-1654.

Mackenzie KJ, Carroll P, Martin CA, Murina O, Fluteau A, Simpson DJ, Olova N, Sutcliffe H, Rainger JK, Leitch A et al. 2017. cGAS surveillance of micronuclei links genome instability to innate immunity. *Nature* **548**: 461-465.

Mali P, Yang L, Esvelt KM, Aach J, Guell M, DiCarlo JE, Norville JE, Church GM. 2013. RNA-guided human genome engineering via Cas9. *Science* **339**: 823-826.

Mankouri HW, Huttner D, Hickson ID. 2013. How unfinished business from S-phase affects mitosis and beyond. *EMBO J* **32**: 2661-2671.

Marechal A, Zou L. 2013. DNA damage sensing by the ATM and ATR kinases. *Cold Spring Harb Perspect Biol* **5**.

Margalef P, Kotsantis P, Borel V, Bellelli R, Panier S, Boulton SJ. 2018. Stabilization of Reversed Replication Forks by Telomerase Drives Telomere Catastrophe. *Cell* **172**: 439-453 e414.

Marston NJ, Richards WJ, Hughes D, Bertwistle D, Marshall CJ, Ashworth A. 1999. Interaction between the product of the breast cancer susceptibility gene BRCA2 and DSS1, a protein functionally conserved from yeast to mammals. *Mol Cell Biol* **19**: 4633-4642.

Marteijn JA, Lans H, Vermeulen W, Hoeijmakers JH. 2014. Understanding nucleotide excision repair and its roles in cancer and ageing. *Nat Rev Mol Cell Biol* **15**: 465-481.

Mateos-Gomez PA, Gong F, Nair N, Miller KM, Lazzerini-Denchi E, Sfeir A. 2015. Mammalian polymerase theta promotes alternative NHEJ and suppresses recombination. *Nature* **518**: 254-257.

Maxwell KN, Wubbenhorst B, Wenz BM, De Sloover D, Pluta J, Emery L, Barrett A, Kraya AA, Anastopoulos IN, Yu S et al. 2017. BRCA locus-specific loss of heterozygosity in germline BRCA1 and BRCA2 carriers. *Nat Commun* **8**: 319.
McAllister KA, Bennett LM, Houle CD, Ward T, Malphurs J, Collins NK, Cachafeiro C, Haseman J, Goulding EH, Bunch D et al. 2002. Cancer susceptibility of mice with a homozygous deletion in the COOH-terminal domain of the Brca2 gene. *Cancer Res* **62**: 990-994.
Meacham CE, Morrison SJ. 2013. Tumour heterogeneity and cancer cell plasticity. *Nature* **501**: 328-337.
Meindl A, Hellebrand H, Wiek C, Erven V, Wappenschmidt B, Niederacher D, Freund M, Lichtner P, Hartmann L, Schaal H et al. 2010. Germline mutations in breast and ovarian cancer pedigrees establish RAD51C as a human cancer susceptibility gene. *Nat Genet* **42**: 410-414.
Menzel T, Nahse-Kumpf V, Kousholt AN, Klein DK, Lund-Andersen C, Lees M, Johansen JV, Syljuasen RG, Sorensen CS. 2011. A genetic screen identifies BRCA2 and PALB2 as key regulators of G2 checkpoint maintenance. *EMBO Rep* **12**: 705-712.
Michaloglou C, Vredeveld LC, Soengas MS, Denoyelle C, Kuilman T, van der Horst CM, Majoor DM, Shay JW, Mooi WJ, Peeper DS. 2005. BRAFE600-associated senescence-like cell cycle arrest of human naevi. *Nature* **436**: 720-724.
Mijic S, Zellweger R, Chappidi N, Berti M, Jacobs K, Mutreja K, Ursich S, Ray Chaudhuri A, Nussenzweig A, Janscak P et al. 2017. Replication fork reversal triggers fork degradation in BRCA2-defective cells. *Nat Commun* **8**: 859.
Minocherhomji S, Ying S, Bjerregaard VA, Bursomanno S, Aleliunaite A, Wu W, Mankouri HW, Shen H, Liu Y, Hickson ID. 2015. Replication stress activates DNA repair synthesis in mitosis. *Nature* **528**: 286-290.
Mizuta R, LaSalle JM, Cheng HL, Shinohara A, Ogawa H, Copeland N, Jenkins NA, Lalande M, Alt FW. 1997. RAB22 and RAB163/mouse BRCA2: proteins that specifically interact with the RAD51 protein. *Proceedings of the National Academy of Sciences of the United States of America* **94**: 6927-6932.
Mondal G, Rowley M, Guidugli L, Wu J, Pankratz VS, Couch FJ. 2012. BRCA2 localization to the midbody by filamin A regulates cep55 signaling and completion of cytokinesis. *Dev Cell* **23**: 137-152.
Moreno A, Carrington JT, Albergante L, Al Mamun M, Haagensen EJ, Komseli ES, Gorgoulis VG, Newman TJ, Blow JJ. 2016. Unreplicated DNA remaining from unperturbed S phases passes through mitosis for resolution in daughter cells. *Proc Natl Acad Sci U S A* **113**: E5757-5764.
Moynahan ME, Jasin M. 2010. Mitotic homologous recombination maintains genomic stability and suppresses tumorigenesis. *Nat Rev Mol Cell Biol* **11**: 196-207.
Moynahan ME, Pierce AJ, Jasin M. 2001. BRCA2 is required for homology-directed repair of chromosomal breaks. *Mol Cell* **7**: 263-272.
Musacchio A. 2015. The Molecular Biology of Spindle Assembly Checkpoint Signaling Dynamics. *Curr Biol* **25**: R1002-1018.
Muthuswamy SK, Li D, Lelievre S, Bissell MJ, Brugge JS. 2001. ErbB2, but not ErbB1, reinitiates proliferation and induces luminal repopulation in epithelial acini. *Nat Cell Biol* **3**: 785-792.

Naim V, Rosselli F. 2009. The FANC pathway and BLM collaborate during mitosis to prevent micro-nucleation and chromosome abnormalities. *Nat Cell Biol* **11**: 761-768.
Naim V, Wilhelm T, Debatisse M, Rosselli F. 2013. ERCC1 and MUS81-EME1 promote sister chromatid separation by processing late replication intermediates at common fragile sites during mitosis. *Nat Cell Biol* **15**: 1008-1015.
Nakanishi K, Cavallo F, Perrouault L, Giovannangeli C, Moynahan ME, Barchi M, Brunet E, Jasin M. 2011. Homology-directed Fanconi anemia pathway cross-link repair is dependent on DNA replication. *Nat Struct Mol Biol* **18**: 500-503.
Nakanishi K, Yang YG, Pierce AJ, Taniguchi T, Digweed M, D'Andrea AD, Wang ZQ, Jasin M. 2005. Human Fanconi anemia monoubiquitination pathway promotes homologous DNA repair. *Proc Natl Acad Sci U S A* **102**: 1110-1115.
Navin NE. 2015. The first five years of single-cell cancer genomics and beyond. *Genome Res* **25**: 1499-1507.
Neelsen KJ, Lopes M. 2015. Replication fork reversal in eukaryotes: from dead end to dynamic response. *Nat Rev Mol Cell Biol* **16**: 207-220.
Neelsen KJ, Zanini IM, Herrador R, Lopes M. 2013. Oncogenes induce genotoxic stress by mitotic processing of unusual replication intermediates. *J Cell Biol* **200**: 699-708.
Neve RM, Chin K, Fridlyand J, Yeh J, Baehner FL, Fevr T, Clark L, Bayani N, Coppe JP, Tong F et al. 2006. A collection of breast cancer cell lines for the study of functionally distinct cancer subtypes. *Cancer Cell* **10**: 515-527.
Nik-Zainal S, Davies H, Staaf J, Ramakrishna M, Glodzik D, Zou X, Martincorena I, Alexandrov LB, Martin S, Wedge DC et al. 2016. Landscape of somatic mutations in 560 breast cancer whole-genome sequences. *Nature* **534**: 47-54.
Nordling M, Karlsson P, Wahlstrom J, Engwall Y, Wallgren A, Martinsson T. 1998. A large deletion disrupts the exon 3 transcription activation domain of the BRCA2 gene in a breast/ovarian cancer family. *Cancer Res* **58**: 1372-1375.
Norquist B, Wurz KA, Pennil CC, Garcia R, Gross J, Sakai W, Karlan BY, Taniguchi T, Swisher EM. 2011. Secondary somatic mutations restoring BRCA1/2 predict chemotherapy resistance in hereditary ovarian carcinomas. *J Clin Oncol* **29**: 3008-3015.
Nowell PC. 1976. The clonal evolution of tumor cell populations. *Science* **194**: 23-28.
Oliver AW, Swift S, Lord CJ, Ashworth A, Pearl LH. 2009. Structural basis for recruitment of BRCA2 by PALB2. *EMBO Rep* **10**: 990-996.
Olson E, Nievera CJ, Liu E, Lee AY, Chen L, Wu X. 2007. The Mre11 complex mediates the S-phase checkpoint through an interaction with replication protein A. *Mol Cell Biol* **27**: 6053-6067.
Patch AM, Christie EL, Etemadmoghadam D, Garsed DW, George J, Fereday S, Nones K, Cowin P, Alsop K, Bailey PJ et al. 2015. Whole-genome characterization of chemoresistant ovarian cancer. *Nature* **521**: 489-494.
Patel KJ, Yu VP, Lee H, Corcoran A, Thistlethwaite FC, Evans MJ, Colledge WH, Friedman LS, Ponder BA, Venkitaraman AR. 1998. Involvement of Brca2 in DNA repair. *Mol Cell* **1**: 347-357.

Pattanayak V, Lin S, Guilinger JP, Ma E, Doudna JA, Liu DR. 2013. High-throughput profiling of off-target DNA cleavage reveals RNA-programmed Cas9 nuclease specificity. *Nat Biotechnol* **31**: 839-843.

Pedersen RS, Karemore G, Gudjonsson T, Rask MB, Neumann B, Heriche JK, Pepperkok R, Ellenberg J, Gerlich DW, Lukas J et al. 2016. Profiling DNA damage response following mitotic perturbations. *Nat Commun* **7**: 13887.

Pellegrini L, Yu DS, Lo T, Anand S, Lee M, Blundell TL, Venkitaraman AR. 2002. Insights into DNA recombination from the structure of a RAD51-BRCA2 complex. *Nature* **420**: 287-293.

Pennington KP, Walsh T, Harrell MI, Lee MK, Pennil CC, Rendi MH, Thornton A, Norquist BM, Casadei S, Nord AS et al. 2014. Germline and somatic mutations in homologous recombination genes predict platinum response and survival in ovarian, fallopian tube, and peritoneal carcinomas. *Clin Cancer Res* **20**: 764-775.

Petermann E, Orta ML, Issaeva N, Schultz N, Helleday T. 2010. Hydroxyurea-stalled replication forks become progressively inactivated and require two different RAD51-mediated pathways for restart and repair. *Mol Cell* **37**: 492-502.

Pfeifer A, Brandon EP, Kootstra N, Gage FH, Verma IM. 2001. Delivery of the Cre recombinase by a self-deleting lentiviral vector: efficient gene targeting in vivo. *Proc Natl Acad Sci U S A* **98**: 11450-11455.

Pierce AJ, Johnson RD, Thompson LH, Jasin M. 1999. XRCC3 promotes homology-directed repair of DNA damage in mammalian cells. *Genes Dev* **13**: 2633-2638.

Pingjuan L, P. KB, Y. LM, S. PM, Daniel N-G, H. GS, A. PE, Keith JJ, Qin L. 2018. Allele-Specific CRISPR-Cas9 Genome Editing of the Single-Base P23H Mutation for Rhodopsin-Associated Dominant Retinitis Pigmentosa. *The CRISPR Journal* **1**: 55-64.

Polak P, Kim J, Braunstein LZ, Karlic R, Haradhavala NJ, Tiao G, Rosebrock D, Livitz D, Kubler K, Mouw KW et al. 2017. A mutational signature reveals alterations underlying deficient homologous recombination repair in breast cancer. *Nat Genet*.

Pontel LB, Rosado IV, Burgos-Barragan G, Garaycoechea JI, Yu R, Arends MJ, Chandrasekaran G, Broecker V, Wei W, Liu L et al. 2015. Endogenous Formaldehyde Is a Hematopoietic Stem Cell Genotoxin and Metabolic Carcinogen. *Mol Cell* **60**: 177-188.

Prakash R, Zhang Y, Feng W, Jasin M. 2015. Homologous recombination and human health: the roles of BRCA1, BRCA2, and associated proteins. *Cold Spring Harb Perspect Biol* **7**: a016600.

Quigley D, Alumkal JJ, Wyatt AW, Kothari V, Foye A, Lloyd P, Aggarwal R, Kim W, Lu E, Schwartzman J et al. 2017. Analysis of Circulating Cell-Free DNA Identifies Multiclonal Heterogeneity of BRCA2 Reversion Mutations Associated with Resistance to PARP Inhibitors. *Cancer Discov* **7**: 999-1005.

Quinet A, Lemacon D, Vindigni A. 2017. Replication Fork Reversal: Players and Guardians. *Mol Cell* **68**: 830-833.

Rahman N, Seal S, Thompson D, Kelly P, Renwick A, Elliott A, Reid S, Spanova K, Barfoot R, Chagtai T et al. 2007a. PALB2, which encodes a BRCA2-interacting protein, is a breast cancer susceptibility gene. *Nat Genet* **39**: 165-167.

Rahman N, Seal S, Thompson D, Kelly P, Renwick A, Elliott A, Reid S, Spanova K, Barfoot R, Chagtai T et al. 2007b. PALB2, which encodes a BRCA2-interacting protein, is a breast cancer susceptibility gene. *Nat Genet* **39**: 165-167.

Ramus SJ, Bobrow LG, Pharoah PD, Finnigan DS, Fishman A, Altaras M, Harrington PA, Gayther SA, Ponder BA, Friedman LS. 1999. Increased frequency of TP53 mutations in BRCA1 and BRCA2 ovarian tumours. *Genes Chromosomes Cancer* **25**: 91-96.

Ran FA, Hsu PD, Lin CY, Gootenberg JS, Konermann S, Trevino AE, Scott DA, Inoue A, Matoba S, Zhang Y et al. 2013. Double nicking by RNA-guided CRISPR Cas9 for enhanced genome editing specificity. *Cell* **154**: 1380-1389.

Ray Chaudhuri A, Callen E, Ding X, Gogola E, Duarte AA, Lee JE, Wong N, Lafarga V, Calvo JA, Panzarino NJ et al. 2016. Replication fork stability confers chemoresistance in BRCA-deficient cells. *Nature* **535**: 382-387.

Reid S, Schindler D, Hanenberg H, Barker K, Hanks S, Kalb R, Neveling K, Kelly P, Seal S, Freund M et al. 2007. Biallelic mutations in PALB2 cause Fanconi anemia subtype FA-N and predispose to childhood cancer. *Nat Genet* **39**: 162-164.

Reuter M, Zelensky A, Smal I, Meijering E, van Cappellen WA, de Gruiter HM, van Belle GJ, van Royen ME, Houtsmuller AB, Essers J et al. 2014. BRCA2 diffuses as oligomeric clusters with RAD51 and changes mobility after DNA damage in live cells. *J Cell Biol* **207**: 599-613.

Robinson D, Van Allen EM, Wu YM, Schultz N, Lonigro RJ, Mosquera JM, Montgomery B, Taplin ME, Pritchard CC, Attard G et al. 2015a. Integrative Clinical Genomics of Advanced Prostate Cancer. *Cell* **162**: 454.

Robinson D, Van Allen EM, Wu YM, Schultz N, Lonigro RJ, Mosquera JM, Montgomery B, Taplin ME, Pritchard CC, Attard G et al. 2015b. Integrative clinical genomics of advanced prostate cancer. *Cell* **161**: 1215-1228.

Robinson DR, Wu YM, Lonigro RJ, Vats P, Cobain E, Everett J, Cao X, Rabban E, Kumar-Sinha C, Raymond V et al. 2017. Integrative clinical genomics of metastatic cancer. *Nature* **548**: 297-303.

Rondinelli B, Gogola E, Yucel H, Duarte AA, van de Ven M, van der Sluijs R, Konstantinopoulos PA, Jonkers J, Ceccaldi R, Rottenberg S et al. 2017. EZH2 promotes degradation of stalled replication forks by recruiting MUS81 through histone H3 trimethylation. *Nat Cell Biol* **19**: 1371-1378.

Roy R, Chun J, Powell SN. 2011. BRCA1 and BRCA2: different roles in a common pathway of genome protection. *Nat Rev Cancer* **12**: 68-78.

Sachs N, de Ligt J, Kopper O, Gogola E, Bounova G, Weeber F, Balgobind AV, Wind K, Gracanin A, Begthel H et al. 2018. A Living Biobank of Breast Cancer Organoids Captures Disease Heterogeneity. *Cell* **172**: 373-386 e310.

Saeki H, Siaud N, Christ N, Wiegant WW, van Buul PP, Han M, Zdzienicka MZ, Stark JM, Jasin M. 2006. Suppression of the DNA repair defects of BRCA2-deficient cells with heterologous protein fusions. *Proceedings of the National Academy of Sciences of the United States of America* **103**: 8768-8773.

Sakai W, Swisher EM, Karlan BY, Agarwal MK, Higgins J, Friedman C, Villegas E, Jacquemont C, Farrugia DJ, Couch FJ et al. 2008. Secondary mutations as a mechanism of cisplatin resistance in BRCA2-mutated cancers. *Nature* **451**: 1116-1120.

Saldivar JC, Cortez D, Cimprich KA. 2017. The essential kinase ATR: ensuring faithful duplication of a challenging genome. *Nat Rev Mol Cell Biol* **18**: 622-636.

Sanchez H, Paul MW, Grosbart M, van Rossum-Fikkert SE, Lebbink JHG, Kanaar R, Houtsmuller AB, Wyman C. 2017. Architectural plasticity of human BRCA2-RAD51 complexes in DNA break repair. *Nucleic Acids Res* **45**: 4507-4518.

Sanjana NE, Shalem O, Zhang F. 2014. Improved vectors and genome-wide libraries for CRISPR screening. *Nat Methods* **11**: 783-784.

Sansregret L, Vanhaesebroeck B, Swanton C. 2018. Determinants and clinical implications of chromosomal instability in cancer. *Nat Rev Clin Oncol* **15**: 139-150.

Santaguida S, Amon A. 2015. Short- and long-term effects of chromosome mis-segregation and aneuploidy. *Nat Rev Mol Cell Biol* **16**: 473-485.

Sarbassov DD, Guertin DA, Ali SM, Sabatini DM. 2005. Phosphorylation and regulation of Akt/PKB by the rictor-mTOR complex. *Science* **307**: 1098-1101.

Schlacher K, Christ N, Siaud N, Egashira A, Wu H, Jasin M. 2011. Double-strand break repair-independent role for BRCA2 in blocking stalled replication fork degradation by MRE11. *Cell* **145**: 529-542.

Schlacher K, Wu H, Jasin M. 2012. A distinct replication fork protection pathway connects Fanconi anemia tumor suppressors to RAD51-BRCA1/2. *Cancer Cell* **22**: 106-116.

Schoonen PM, Talens F, Stok C, Gogola E, Heijink AM, Bouwman P, Foijer F, Tarsounas M, Blatter S, Jonkers J et al. 2017. Progression through mitosis promotes PARP inhibitor-induced cytotoxicity in homologous recombination-deficient cancer cells. *Nat Commun* **8**: 15981.

Schwartz M, Zlotorynski E, Kerem B. 2006. The molecular basis of common and rare fragile sites. *Cancer Lett* **232**: 13-26.

Serrano M, Lin AW, McCurrach ME, Beach D, Lowe SW. 1997. Oncogenic ras provokes premature cell senescence associated with accumulation of p53 and p16INK4a. *Cell* **88**: 593-602.

Shahid T, Soroka J, Kong EH, Malivert L, McIlwraith MJ, Pape T, West SC, Zhang X. 2014. Structure and mechanism of action of the BRCA2 breast cancer tumor suppressor. *Nat Struct Mol Biol* **21**: 962-968.

Sharan SK, Morimatsu M, Albrecht U, Lim DS, Regel E, Dinh C, Sands A, Eichele G, Hasty P, Bradley A. 1997. Embryonic lethality and radiation hypersensitivity mediated by Rad51 in mice lacking Brca2. *Nature* **386**: 804-810.

Sheltzer JM, Ko JH, Replogle JM, Habibe Burgos NC, Chung ES, Meehl CM, Sayles NM, Passerini V, Storchova Z, Amon A. 2017. Single-chromosome Gains Commonly Function as Tumor Suppressors. *Cancer Cell* **31**: 240-255.

Shi Q, King RW. 2005. Chromosome nondisjunction yields tetraploid rather than aneuploid cells in human cell lines. *Nature* **437**: 1038-1042.

Shiloh Y, Ziv Y. 2013. The ATM protein kinase: regulating the cellular response to genotoxic stress, and more. *Nat Rev Mol Cell Biol* **14**: 197-210.

Shin JW, Kim KH, Chao MJ, Atwal RS, Gillis T, MacDonald ME, Gusella JF, Lee JM. 2016. Permanent inactivation of Huntington's disease mutation by personalized allele-specific CRISPR/Cas9. *Hum Mol Genet* **25**: 4566-4576.
Shivji MKK, Renaudin X, Williams CH, Venkitaraman AR. 2018. BRCA2 Regulates Transcription Elongation by RNA Polymerase II to Prevent R-Loop Accumulation. *Cell Rep* **22**: 1031-1039.
Siaud N, Barbera MA, Egashira A, Lam I, Christ N, Schlacher K, Xia B, Jasin M. 2011. Plasticity of BRCA2 function in homologous recombination: genetic interactions of the PALB2 and DNA binding domains. *PLoS Genet* **7**: e1002409.
Skoulidis F, Cassidy LD, Pisupati V, Jonasson JG, Bjarnason H, Eyfjord JE, Karreth FA, Lim M, Barber LM, Clatworthy SA et al. 2010. Germline Brca2 heterozygosity promotes Kras(G12D) -driven carcinogenesis in a murine model of familial pancreatic cancer. *Cancer Cell* **18**: 499-509.
Smith C, Abalde-Atristain L, He C, Brodsky BR, Braunstein EM, Chaudhari P, Jang YY, Cheng L, Ye Z. 2015. Efficient and allele-specific genome editing of disease loci in human iPSCs. *Mol Ther* **23**: 570-577.
Smith SA, Easton DF, Evans DG, Ponder BA. 1992. Allele losses in the region 17q12-21 in familial breast and ovarian cancer involve the wild-type chromosome. *Nat Genet* **2**: 128-131.
Somyajit K, Saxena S, Babu S, Mishra A, Nagaraju G. 2015. Mammalian RAD51 paralogs protect nascent DNA at stalled forks and mediate replication restart. *Nucleic Acids Res* **43**: 9835-9855.
Soule HD, Maloney TM, Wolman SR, Peterson WD, Jr., Brenz R, McGrath CM, Russo J, Pauley RJ, Jones RF, Brooks SC. 1990. Isolation and characterization of a spontaneously immortalized human breast epithelial cell line, MCF-10. *Cancer Res* **50**: 6075-6086.
Srinivasan SV, Dominguez-Sola D, Wang LC, Hyrien O, Gautier J. 2013. Cdc45 is a critical effector of myc-dependent DNA replication stress. *Cell Rep* **3**: 1629-1639.
Stark JM, Hu P, Pierce AJ, Moynahan ME, Ellis N, Jasin M. 2002. ATP hydrolysis by mammalian RAD51 has a key role during homology-directed DNA repair. *J Biol Chem* **277**: 20185-20194.
Suzuki A, de la Pompa JL, Hakem R, Elia A, Yoshida R, Mo R, Nishina H, Chuang T, Wakeham A, Itie A et al. 1997. Brca2 is required for embryonic cellular proliferation in the mouse. *Genes Dev* **11**: 1242-1252.
Sy SM, Huen MS, Chen J. 2009. PALB2 is an integral component of the BRCA complex required for homologous recombination repair. *Proceedings of the National Academy of Sciences of the United States of America* **106**: 7155-7160.
Taglialatela A, Alvarez S, Leuzzi G, Sannino V, Ranjha L, Huang JW, Madubata C, Anand R, Levy B, Rabadan R et al. 2017. Restoration of Replication Fork Stability in BRCA1- and BRCA2-Deficient Cells by Inactivation of SNF2-Family Fork Remodelers. *Mol Cell* **68**: 414-430 e418.
Tan SLW, Chadha S, Liu Y, Gabasova E, Perera D, Ahmed K, Constantinou S, Renaudin X, Lee M, Aebersold R et al. 2017. A Class of Environmental and Endogenous

Toxins Induces BRCA2 Haploinsufficiency and Genome Instability. *Cell* **169**: 1105-1118 e1115.
Tarsounas M, Davies D, West SC. 2003. BRCA2-dependent and independent formation of RAD51 nuclear foci. *Oncogene* **22**: 1115-1123.
Taylor AM, Shih J, Ha G, Gao GF, Zhang X, Berger AC, Schumacher SE, Wang C, Hu H, Liu J et al. 2018. Genomic and Functional Approaches to Understanding Cancer Aneuploidy. *Cancer Cell* **33**: 676-689 e673.
Thangavel S, Berti M, Levikova M, Pinto C, Gomathinayagam S, Vujanovic M, Zellweger R, Moore H, Lee EH, Hendrickson EA et al. 2015. DNA2 drives processing and restart of reversed replication forks in human cells. *J Cell Biol* **208**: 545-562.
Thorslund T, Esashi F, West SC. 2007. Interactions between human BRCA2 protein and the meiosis-specific recombinase DMC1. *EMBO J* **26**: 2915-2922.
Thorslund T, McIlwraith MJ, Compton SA, Lekomtsev S, Petronczki M, Griffith JD, West SC. 2010. The breast cancer tumor suppressor BRCA2 promotes the specific targeting of RAD51 to single-stranded DNA. *Nat Struct Mol Biol* **17**: 1263-1265.
Tischkowitz M, Xia B. 2010. PALB2/FANCN: recombining cancer and Fanconi anemia. *Cancer Res* **70**: 7353-7359.
Tischkowitz M, Xia B, Sabbaghian N, Reis-Filho JS, Hamel N, Li G, van Beers EH, Li L, Khalil T, Quenneville LA et al. 2007a. Analysis of PALB2/FANCN-associated breast cancer families. *Proc Natl Acad Sci USA* **104**: 6788-6793.
-. 2007b. Analysis of PALB2/FANCN-associated breast cancer families. *Proc Natl Acad Sci U S A* **104**: 6788-6793.
Tiwari A, Addis Jones O, Chan KL. 2018. 53BP1 can limit sister-chromatid rupture and rearrangements driven by a distinct ultrafine DNA bridging-breakage process. *Nat Commun* **9**: 677.
Toledo LI, Altmeyer M, Rask MB, Lukas C, Larsen DH, Povlsen LK, Bekker-Jensen S, Mailand N, Bartek J, Lukas J. 2013. ATR prohibits replication catastrophe by preventing global exhaustion of RPA. *Cell* **155**: 1088-1103.
Tsuzuki T, Fujii Y, Sakumi K, Tominaga Y, Nakao K, Sekiguchi M, Matsushiro A, Yoshimura Y, MoritaT. 1996. Targeted disruption of the Rad51 gene leads to lethality in embryonic mice. *Proceedings of the National Academy of Sciences of the United States of America* **93**: 6236-6240.
Tutt A, Gabriel A, Bertwistle D, Connor F, Paterson H, Peacock J, Ross G, Ashworth A. 1999. Absence of Brca2 causes genome instability by chromosome breakage and loss associated with centrosome amplification. *Curr Biol* **9**: 1107-1110.
Vassilev LT, Tovar C, Chen S, Knezevic D, Zhao X, Sun H, Heimbrook DC, Chen L. 2006. Selective small-molecule inhibitor reveals critical mitotic functions of human CDK1. *Proc Natl Acad Sci U S A* **103**: 10660-10665.
Vilar E, Gruber SB. 2010. Microsatellite instability in colorectal cancer-the stable evidence. *Nat Rev Clin Oncol* **7**: 153-162.
Vitolo MI, Weiss MB, Szmacinski M, Tahir K, Waldman T, Park BH, Martin SS, Weber DJ, Bachman KE. 2009. Deletion of PTEN promotes tumorigenic signaling, resistance to anoikis, and altered response to chemotherapeutic agents in human mammary epithelial cells. *Cancer Res* **69**: 8275-8283.

Vogelstein B, Kinzler KW. 1993. The multistep nature of cancer. *Trends Genet* **9**: 138-141.

Vriend LE, Jasin M, Krawczyk PM. 2014. Assaying break and nick-induced homologous recombination in mammalian cells using the DR-GFP reporter and Cas9 nucleases. *Methods Enzymol* **546**: 175-191.

Walsh T, Casadei S, Lee MK, Pennil CC, Nord AS, Thornton AM, Roeb W, Agnew KJ, Stray SM, Wickramanayake A et al. 2011. Mutations in 12 genes for inherited ovarian, fallopian tube, and peritoneal carcinoma identified by massively parallel sequencing. *Proceedings of the National Academy of Sciences of the United States of America* **108**: 18032-18037.

Wang AT, Kim T, Wagner JE, Conti BA, Lach FP, Huang AL, Molina H, Sanborn EM, Zierhut H, Cornes BK et al. 2015. A Dominant Mutation in Human RAD51 Reveals Its Function in DNA Interstrand Crosslink Repair Independent of Homologous Recombination. *Mol Cell* **59**: 478-490.

Wang Q, Zou Y, Nowotschin S, Kim SY, Li QV, Soh CL, Su J, Zhang C, Shu W, Xi Q et al. 2017. The p53 Family Coordinates Wnt and Nodal Inputs in Mesendodermal Differentiation of Embryonic Stem Cells. *Cell Stem Cell* **20**: 70-86.

Willis NA, Chandramouly G, Huang B, Kwok A, Follonier C, Deng C, Scully R. 2014. BRCA1 controls homologous recombination at Tus/Ter-stalled mammalian replication forks. *Nature* **510**: 556-559.

Wong AK, Pero R, Ormonde PA, Tavtigian SV, Bartel PL. 1997. RAD51 interacts with the evolutionarily conserved BRC motifs in the human breast cancer susceptibility gene brca2. *J Biol Chem* **272**: 31941-31944.

Wooster R, Bignell G, Lancaster J, Swift S, Seal S, Mangion J, Collins N, Gregory S, Gumbs C, Micklem G. 1995. Identification of the breast cancer susceptibility gene BRCA2. *Nature* **378**: 789-792.

Xia B, Dorsman JC, Ameziane N, de Vries Y, Rooimans MA, Sheng Q, Pals G, Errami A, Gluckman E, Llera J et al. 2007. Fanconi anemia is associated with a defect in the BRCA2 partner PALB2. *Nat Genet* **39**: 159-161.

Xia B, Sheng Q, Nakanishi K, Ohashi A, Wu J, Christ N, Liu X, Jasin M, Couch FJ, Livingston DM. 2006. Control of BRCA2 cellular and clinical functions by a nuclear partner, PALB2. *Mol Cell* **22**: 719-729.

Xia F, Taghian DG, DeFrank JS, Zeng ZC, Willers H, Iliakis G, Powell SN. 2001a. Deficiency of human BRCA2 leads to impaired homologous recombination but maintains normal nonhomologous end joining. *Proc Natl Acad Sci U S A* **98**: 8644-8649.

-. 2001b. Deficiency of human BRCA2 leads to impaired homologous recombination but maintains normal nonhomologous end joining. *Proc Natl Acad Sci USA* **98**: 8644-8649.

Xu G, Chapman JR, Brandsma I, Yuan J, Mistrik M, Bouwman P, Bartkova J, Gogola E, Warmerdam D, Barazas M et al. 2015. REV7 counteracts DNA double-strand break resection and affects PARP inhibition. *Nature* **521**: 541-544.

Xu S, Wu X, Wu L, Castillo A, Liu J, Atkinson E, Paul A, Su D, Schlacher K, Komatsu Y et al. 2017a. Abro1 maintains genome stability and limits replication stress by protecting replication fork stability. *Genes Dev* **31**: 1469-1482.

Xu Y, Ning S, Wei Z, Xu R, Xu X, Xing M, Guo R, Xu D. 2017b. 53BP1 and BRCA1 control pathway choice for stalled replication restart. *Elife* **6**.
Yang H, Jeffrey PD, Miller J, Kinnucan E, Sun Y, Thoma NH, Zheng N, Chen PL, Lee WH, Pavletich NP. 2002. BRCA2 function in DNA binding and recombination from a BRCA2-DSS1-ssDNA structure. *Science* **297**: 1837-1848.
Yang H, Wang H, Ren J, Chen Q, Chen ZJ. 2017. cGAS is essential for cellular senescence. *Proc Natl Acad Sci U S A* **114**: E4612-E4620.
Yata K, Bleuyard JY, Nakato R, Ralf C, Katou Y, Schwab RA, Niedzwiedz W, Shirahige K, Esashi F. 2014. BRCA2 coordinates the activities of cell-cycle kinases to promote genome stability. *Cell Rep* **7**: 1547-1559.
Yates LR, Campbell PJ. 2012. Evolution of the cancer genome. *Nat Rev Genet* **13**: 795-806.
Ying S, Hamdy FC, Helleday T. 2012. Mre11-dependent degradation of stalled DNA replication forks is prevented by BRCA2 and PARP1. *Cancer Res* **72**: 2814-2821.
Ying S, Minocherhomji S, Chan KL, Palmai-Pallag T, Chu WK, Wass T, Mankouri HW, Liu Y, Hickson ID. 2013. MUS81 promotes common fragile site expression. *Nat Cell Biol* **15**: 1001-1007.
Yoshimi K, Kaneko T, Voigt B, Mashimo T. 2014. Allele-specific genome editing and correction of disease-associated phenotypes in rats using the CRISPR-Cas platform. *Nat Commun* **5**: 4240.
Yu DS, Sonoda E, Takeda S, Huang CL, Pellegrini L, Blundell TL, Venkitaraman AR. 2003. Dynamic control of Rad51 recombinase by self-association and interaction with BRCA2. *Mol Cell* **12**: 1029-1041.
Yuan SS, Lee SY, Chen G, Song M, Tomlinson GE, Lee EY. 1999. BRCA2 is required for ionizing radiation-induced assembly of Rad51 complex in vivo. *Cancer Res* **59**: 3547-3551.
Zack TI, Schumacher SE, Carter SL, Cherniack AD, Saksena G, Tabak B, Lawrence MS, Zhsng CZ, Wala J, Mermel CH et al. 2013. Pan-cancer patterns of somatic copy number alteration. *Nat Genet* **45**: 1134-1140.
Zellweger R, Dalcher D, Mutreja K, Berti M, Schmid JA, Herrador R, Vindigni A, Lopes M. 2015. Rad51-mediated replication fork reversal is a global response to genotoxic treatments in human cells. *J Cell Biol* **208**: 563-579.
Zhang CZ, Spektor A, Cornils H, Francis JM, Jackson EK, Liu S, Meyerson M, Pellman D. 2015. Chromothripsis from DNA damage in micronuclei. *Nature* **522**: 179-184.
Zhang F, Fan Q, Ren K, Andreassen PR. 2009a. PALB2 functionally connects the breast cancer susceptibility proteins BRCA1 and BRCA2. *Molecular cancer research : MCR* **7**: 1110-1118.
Zhang F, Ma J, Wu J, Ye L, Cai H, Xia B, Yu X. 2009b. PALB2 links BRCA1 and BRCA2 in the DNA-damage response. *Curr Biol* **19**: 524-529.
Zhang Y, Vanoli F, LaRocque JR, Krawczyk PM, Jasin M. 2014. Biallelic targeting of expressed genes in mouse embryonic stem cells using the Cas9 system. *Methods* **69**: 171-178.
Zhao W, Vaithiyalingam S, San Filippo J, Maranon DG, Jimenez-Sainz J, Fontenay GV, Kwon Y, Leung SG, Lu L, Jensen RB et al. 2015. Promotion of BRCA2-

Dependent Homologous Recombination by DSS1 via RPA Targeting and DNA Mimicry. *Mol Cell* **59**: 176-187.

Zimmer J, Tacconi EM, Folio C, Badie S, Porru M, Klare K, Tumiati M, Markkanen E, Halder S, Ryan A et al. 2016. Targeting BRCA1 and BRCA2 Deficiencies with G-Quadruplex-Interacting Compounds. *Mol Cell* **61**: 449-460.

Zimmermann M, Lottersberger F, Buonomo SB, Sfeir A, de Lange T. 2013. 53BP1 regulates DSB repair using Rif1 to control 5' end resection. *Science* **339**: 700-704.